

Electronic Thesis and Dissertation Repository

7-29-2024 1:00 PM

Paracrine factors regulate glucagon trafficking through the Stmn2-mediated lysosomal network

Nelson Chang, *Western University*

Supervisor: Dhanvantari, Savita, *The University of Western Ontario*

A thesis submitted in partial fulfillment of the requirements for the Master of Science degree in Pathology and Laboratory Medicine

© Nelson Chang 2024

Follow this and additional works at: <https://ir.lib.uwo.ca/etd>



Part of the [Medical Cell Biology Commons](#)

Recommended Citation

Chang, Nelson, "Paracrine factors regulate glucagon trafficking through the Stmn2-mediated lysosomal network" (2024). *Electronic Thesis and Dissertation Repository*. 10226.

<https://ir.lib.uwo.ca/etd/10226>

This Dissertation/Thesis is brought to you for free and open access by Scholarship@Western. It has been accepted for inclusion in Electronic Thesis and Dissertation Repository by an authorized administrator of Scholarship@Western. For more information, please contact wlsadmin@uwo.ca.

Abstract

In diabetes, excess glucagon secretion and insulin deficiency contribute to disease progression and hyperglycemia. Understanding the intracellular trafficking of glucagon in alpha cells can reveal potential therapeutic targets to alleviate hyperglycemia. Stathmin-2 (Stmn2) was previously found in the secretory granules of α TC1-6 cells and was hypothesized to direct glucagon to lysosomes for degradation. My work aims to investigate whether paracrine inhibition of glucagon secretion operates through the Stmn2-mediated lysosomal pathway.

I manipulated Stmn2 levels and applied paracrine treatment to observe glucagon and lysosome distribution using microscopy. I found that Stmn2 was essential in mediating paracrine redistribution of glucagon and lysosomes. Microscopy also showed strong colocalization and similar distribution of Stmn2 and lysosomes in both mouse and human alpha cells, while qPCR analysis showed that Stmn2 upregulated autophagy genes.

In summary, my thesis describes a potential regulator of glucagon secretion with therapeutic potential for hyperglucagonemia and hyperglycemia of diabetes.

Keywords: glucagon, glucagon secretion, Stathmin-2, diabetes, lysosomes, exocytosis, degradation, paracrine inhibition, hyperglucagonemia

Lay Summary

Diabetes is a condition of high blood sugar caused by abnormally high levels of a hormone called “glucagon”, vital in regulating physiological processes, such as sugar and fat metabolism. Cells that secrete hormones are called endocrine cells, and we wish to study the cellular mechanisms of how endocrine cells secrete hormones to maintain body balance and how this process can go wrong. Our research focuses on glucagon, secreted from endocrine alpha cells in the pancreas, to increase blood sugar levels. Inside the alpha cell, glucagon is contained in tiny specialized packages called “granules” which move to different destinations. Within these granules are important molecules that may affect whether glucagon is released or degraded for an optimal level, with one candidate being stathmin-2. We know these granules must be in particular locations within the cell for glucagon to be released or degraded in response to signals like other pancreatic hormones (insulin and somatostatin). However, how they get to these locations is unclear. This is an important question because it explains how abnormally high glucagon secretion can be controlled in diabetes. To find out how other pancreatic hormones can potentially direct glucagon towards sites of degradation(lysosomes) via stathmin-2, we used state-of-the-art technologies in advanced microscopy to visualize the movement of glucagon in mouse alpha cells. We found that insulin and somatostatin both moved glucagon towards degradation. In addition, Stmn2 and lysosomes overlapped strongly in their locations, suggesting a link between them. So, I followed up with a genetic analysis and found that stathmin-2 increased genes that produce more lysosomes. To determine stathmin-2’s role in trafficking glucagon, I removed Stmn2 from alpha cells and found that glucagon no longer moved towards lysosomes even in the presence of insulin and somatostatin, which confirms that trafficking of glucagon by other endocrine hormones requires Stmn2. Therefore, Stmn2 is a molecule that can control glucagon secretion and can be used to decrease high blood sugar in people with diabetes.

Co-Authorship Statement

Hakam Madahey generated Stmn2-GFP, Stmn2-tdTomato and LAMP1-RFP plasmids for overexpression and live-cell imaging experiments. Dr. Danielle Dean from Vanderbilt University provided human pancreatic alpha-like cells while Dr. Madushika Wimalarathne, Anna Marie R. Schornack, and Tyler Rodgers from Dr. Dean's lab helped maintain the human alpha-like cell line, optimize our transfection protocol and image the human cell samples with the Zeiss LSM710 confocal microscope at Vanderbilt.

Acknowledgments

I would first like to express my heartfelt appreciation to my supervisor, Dr. Savita Dhanvantari, for allowing me to work in such a supportive and cohesive lab environment. She is not only an inspiring role model and leader but also a great mentor who supported me through some of the most challenging times in my life: overcoming a major surgery and the loss of loved ones during my degree. Being part of Savita's lab is one of the most unforgettable experiences in my life, and her kindness shows through her advocacy, life lessons, and care for her students. Savita is also patient and always sets time aside to provide critical and constructive feedback for my work, which has largely contributed to many of the recognitions I have received. These are only few of the many ways she has helped and inspired me to become a better person, scientist, and future physician. I am genuinely grateful for everything I have learned and experienced during my two years with Savita; this work is dedicated to her.

I want to thank my external mentor Dr. Jonathan Rocheleau, from the CIRTN program and my advisory committee members, Dr. Reninan Wang and Dr. Van Lu, for providing regular feedback on my work, and showing me their systems that helped me overcome a very challenging part of my live-cell imaging experiments.

I want to thank Dr. Danielle Dean for her full support while hosting me at her lab at Vanderbilt University in Nashville, Tennessee. I would also like to thank Dr. Dean's lab members, Dr. Madushika Wimalarathne, Anna Marie R. Schornack and Tyler Rodgers, for all their help with the human alpha-like cell line. They made me feel welcome and a sense of belonging in a foreign city.

I want to thank Wongsakorn Kiattiburut, Daisy Sun, and Juan Fernández for training me on epifluorescence and confocal microscopy, a huge part of my project and a precious lifelong skill to acquire.

I want to express my sincere gratitude to my sister, Justine Chang, who has always been there during my toughest struggles and my happiest and proudest moments. I could not have achieved what I have today without her, and I aspire to continue making her proud.

Table of Contents

Abstract	ii
Lay Summary	iii
Co-Authorship Statement.....	iv
Acknowledgments.....	v
Table of Contents	vi
List of Tables	x
List of Figures	xi
List of Abbreviations	xiii
List of Appendices	xvi
Chapter 1	1
1 Introduction	1
1.1 Significance of the study	1
1.2 The clinical problem: glucagonocentric hypothesis of diabetes	2
1.2 Islet architecture and paracrine interactions reflect islet function	4
1.3 Regulation of glucagon secretion in α cells	5
1.4 Secretory pathway within the pancreatic alpha cells	9
1.5 The lysosome: a novel compartment for glucagon trafficking	10
1.6 Stathmin-2 directs glucagon towards the lysosome	11
1.7 Central hypothesis	12
Chapter 2.....	13
2 Material and Methods	13
2.1 Cell Type.....	13
2.1.1 Alpha TC1-6 cells	13
2.1.2 Human pancreatic alpha-like cells	13

2.2 Cell culture	13
2.3 Transient transfection.....	14
2.4 Glucagon secretion experiments	15
2.4.1 Glucagon secretion in the presence of paracrine factors.....	15
2.4.2 Glucagon secretion inhibition by insulin post-Stmn2- transfection.....	16
2.5 Immunofluorescence microscopy	17
2.5.1 Immunostaining	17
2.5.2 Antibodies	17
2.5.3 Confocal microscopy	19
2.5.3.1 Image acquisition	19
2.5.3.2 Image analysis.....	20
2.5.4 Paracrine inhibition of glucagon exocytosis	21
2.5.5 Lysosomal dynamics mediated by Stmn2.....	21
2.5.5.1 Stmn2 and LAMP1 co-expression in human pancreatic alpha-like cells	22
2.5.6 Glucagon distribution mediated by Stmn2.....	22
2.5.7 Paracrine inhibition of glucagon exocytosis mediated by Stmn2	22
2.5.8 Nuclear translocation of TFEB mediated by Stmn2	23
2.6 Gene expression of MCOLN1 in Stmn2-overexpression	23
2.6.1 Primer design	23
2.6.2 Treatment, RNA Extraction and cDNA Synthesis.....	24
2.6.3 qPCR	24
2.7 Statistical analysis	25
Chapter 3.....	26
3 Results	26
3.1 Regulation of glucagon secretion.....	26
3.1.1 Regulation of basal and stimulated glucagon secretion by glucose and insulin .	26

3.1.2 Regulation of basal and stimulated glucagon secretion by glucose and co-secreted β cell effectors.....	27
3.1.3 Regulation of basal glucagon secretion by Stmn2	28
3.2 Paracrine factors regulate intracellular glucagon trafficking	29
3.3 New analysis tool defining cellular regions as “Intracellular” or “Cell periphery”.....	30
3.4 Microscopy shows paracrine redistribution of colocalized vesicles	33
3.4.1 Paracrine factors redistribute glucagon and Stmn2 towards the intracellular region	33
3.4.2 Paracrine factors redistribute glucagon and LAMP1 towards the intracellular region	35
3.4.3 Paracrine factors redistribute glucagon and Syntaxin1A towards the intracellular region	37
3.5 Stmn2 induces nuclear translocation of TFEB.....	39
3.5.1 Stmn2 upregulates MCOLN1, upstream of TFEB.....	40
3.6 Stmn2 regulates lysosomal dynamics	42
3.6.1 Stmn2-mediated lysosomal network is sensitive to paracrine factors	45
3.7 Stmn2 mediates the intracellular trafficking of glucagon	52
3.7.1 Insulin directs lysosomal trafficking of glucagon in a Stmn2-dependent manner	55
3.7.2 Somatostatin directs lysosomal trafficking of glucagon in a Stmn2-dependent manner.....	58
3.8 A novel human alpha-like cell line expresses Stmn2-GFP and LAMP1-RFP similarly to mouse pancreatic α TC1-6 cells	61
Chapter 4.....	64
4 Discussions and Future Direction.....	64
4.1 Measurement of overall glucagon levels masked treatment effects due to heterogeneity in cell circadian phase, secretion capacity and inhibition	65
4.2 Paracrine factors affect glucagon trafficking to lysosomes via Stmn2	67
4.3 Alpha cell membrane protrusions similar to filopodia and neuronal axon	68
4.4 Stmn2 levels alter lysosomal distribution	69

4.5 Stmn2 induces nuclear translocation of TFEB.....	71
4.6 Novel proposed mechanism of insulin and somatostatin resistance of α cells in diabetes	72
4.7 Future directions.....	74
4.8 Concluding remarks	75
References or Bibliography	76
Appendices.....	86
Curriculum Vitae	92

List of Tables

Appendix Table 1. α TC1-6 cell viability assay post-transfection.	87
Appendix Table 2. Raw MCOLN1 and beta-actin C_q values after Stmn2-OE and KD in α TC1-6 cells cultured in regular growth media.	90

List of Figures

Figure 1. Paracrine regulation of glucagon secretion under various glucose concentrations...	8
Figure 2. Basal and K ⁺ -stimulated glucagon secretion in response to insulin under either high (25 mM) or low (5.5) glucose.....	26
Figure 3. Basal and K ⁺ -stimulated glucagon secretion in response to insulin and GABA under either high (25 mM) or low (5.5) glucose.....	27
Figure 4. Basal glucagon secretion post-Stmn2 knockdown (KD), overexpression (OE), before and after 1 nM insulin treatment.....	28
Figure 5. Colocalization between glucagon and Stmn2, Syntaxin1A and LAMP1 treated with 1 nM insulin/25 μM GABA cultured under high glucose (25 mM) media..	29
Figure 6. Immunofluorescence and average plot profile of the general lysosomal marker, LAMP1, cultured under high glucose (25 mM) media.....	31
Figure 7. Immunofluorescence and average plot profile of the exocytosis marker, Syntaxin1A, cultured under high glucose (25 mM) media.....	32
Figure 8. Redistribution of colocalized glucagon and Stmn2 upon 1 nM insulin/25 μM GABA or 400 nM somatostatin treatment.....	34
Figure 9. Redistribution of colocalized glucagon and LAMP1 upon 1 nM insulin/25 μM GABA or 400 nM somatostatin treatment.....	36
Figure 10. Redistribution of colocalized glucagon and Syntaxin1A upon 1 nM insulin/25 μM GABA or 400 nM somatostatin treatment.....	38
Figure 11. Nuclear translocation of transcription factor EB (TFEB, white) upon overexpressing Stmn2 with Stmn2-GFP.....	39
Figure 12. Relative gene expression of MCOLN1 upon Stmn2 overexpression (OE) and knockdown (KD) to the control normalized to beta-actin..	41

Figure 13. Live imaging of LAMP1-RFP in response to Stmn2 overexpression (OE) or knockdown (KD).	44
Figure 14. Live imaging of LAMP1-RFP in response to 1 nM insulin in cells with Stmn2 overexpression (OE) or knockdown (KD)..	48
Figure 15. Temporal changes in lysosomal dynamics upon 1 nM insulin treatment. s).....	48
Figure 16. Live imaging of LAMP1-RFP in response to somatostatin in cells with Stmn2 overexpression (OE) or knockdown (KD)..	51
Figure 17. Fixed-cell immunostaining showing glucagon distribution changes in response to Stmn2-GFP (OE) and Stmn2 siRNAs (KD).	54
Figure 18. Fixed-cell immunostaining showing glucagon distribution changes in the presence of 1 nM insulin in cells with Stmn2-GFP (OE) and Stmn2 siRNAs(KD)..	57
Figure 19. Fixed-cell immunostaining showing glucagon distribution changes in the presence of 400 nM somatostatin in cells with Stmn2-GFP (OE) and Stmn2 siRNAs(KD).	60
Figure 20. Human pancreatic alpha-like cells express LAMP1-RFP and Stmn2-GFP in patterns similar to α TC1-6 cells.	62
Figure 21. Types of glucagon secretion and the proposed mechanism of Stmn2-mediated crinophagy in α cells.	73

List of Abbreviations

2D	Two-Dimensional
ANOVA	Analysis of variance
ATP	Adenosine triphosphate
BCA	Bicinchoninic acid assay
BSA	Bovine serum albumin
cDNA	Complementary deoxyribonucleic acid
cAMP	Cyclic adenosine monophosphate
Cy5	Cyanine-5
DAPI	4', 6-diamidino-2-phenylindole
DM	Diabetes mellitus
DMEM	Dulbecco's modified eagle medium
EDTA	Ethylenediaminetetraacetic acid
ELISA	Enzyme-linked immunosorbent assay
FBS	Fetal bovine serum
FITC	Fluorescein isothiocyanate
GABA	Gamma amino butyric acid
GCG	Glucagon
GcgR	Glucagon receptor
GFP	Green fluorescent protein
GLUT1	Glucose transporter 1
GPCR	G-protein-coupled-receptor
HG	High glucose

HS	Horse serum
INS	Insulin
ISG	Immature secretory granule
KD	Knockdown
LG	Low glucose
MCOLN1	Mucolipin 1
mRNA	Messenger Ribonucleic Acid
MSG	Mature secretory granule
mTORC1	Mammalian Target of Rapamycin-1
OE	Overexpression
PBS	Phosphate buffered saline
PCC	Pearson's correlation coefficient
PI3K	Phosphoinositide 3 kinases
PKA	Protein kinase A
qPCR	Quantitative polymerase chain reaction
RFP	Red fluorescent protein
RILP	Rab-interacting lysosomal protein
RIPA	Radioimmunoprecipitation assay buffer
RRP	Readily-releasable pool
RP	Reserve pool
SCG10	Superior cervical ganglion-10 protein
SEM	Standard error of the mean
siRNA	Small interfering ribonucleic acid

SNAP 25	Synaptosome associated protein 25
SNARE	Soluble N-ethylmaleimide-sensitive factor Activating Protein Receptor
SST	Somatostatin
SSTR	Somatostatin receptor
Stmn2	Stathmin-2
SV40	Simian virus 40 (oncogenic DNA virus)
TFEB	Transcription factor EB
TGN	Trans-Golgi network
tM	Melting temperature
TRITC	Tetramethylrhodamine-isothiocyanate
T1DM	Type 1 diabetes mellitus
T2DM	Type 2 diabetes mellitus
VAMP 2	Vesicle-associated membrane protein 2

List of Appendices

Appendix Figure 1. 40 nM GFP-alone and Stmn2-GFP localization and efficiency in α TC1-6 cells.	86
Appendix Figure 2. MCOLN1 and beta-actin amplicons post-qPCR, and their specificity, purity and size in α TC1-6 cells cultured in regular 25 mM glucose growth media..	89
Appendix Figure 3. Live imaging of LAMP1-RFP treated with 10 nM insulin receptor antagonist in response to 1 nM insulin.	91

Chapter 1

1 Introduction

1.1 Significance of the study

Diabetes mellitus (DM) is a metabolic condition characterized by chronic hyperglycemia resulting from impaired synthesis, release, regulation, and actions of hormones secreted from the pancreas, projected to affect 10.2% of the global population or an equivalence of 643 million by 2030. The human pancreas is primarily comprised of exocrine cells that secrete digestive enzymes. About 1% of the pancreas is comprised of the islets of Langerhans, which contain a mixed population of functionally heterogenic endocrine cells such as the insulin-producing β cells, glucagon-producing α cells, somatostatin-producing δ cells, γ cells, and ϵ cells. Most commonly, dysfunctions of α and β cells result in the combination of excess glucagon secretion and insulin deficiency, which impair blood glucose homeostasis and ultimately present clinically as diabetes mellitus. With increasing evidence suggesting the dominant role of dysfunctional α cells contributing to the disease progression and the harmful effects of glucagon receptor blockers, an alternative to regulate excess glucagon secretion is urgently needed. To address this need, our lab is investigating the intracellular trafficking of glucagon in mouse pancreatic α cells to understand the regulators involved in resorting glucagon for secretion or degradation physiologically and pathologically. We have identified a neuronal protein, stathmin-2 (Stmn2 or SCG10), known to be involved in microtubule dynamics and hormone transport in neurons, to play a role in directing glucagon toward the lysosomal network of mouse pancreatic α cells. Our lab utilizes a combination of protein markers and fluorescence microscopy to visualize the presence of glucagon in subcellular compartments such as lysosomes and secretory granules and their dynamics in response to paracrine factors and in pathological conditions such as when Stmn2 is knocked down, disabling the lysosomal network important for glucagon regulation. The work described in this thesis aims to connect the role of Stmn2's roles in overlapping domains of functions, including trafficking glucagon, the lysosomal network, and

paracrine inhibition of glucagon secretion to understand how glucagon secretion can be regulated to alleviate hyperglucagonemia of diabetes.

1.2 The clinical problem: glucagonocentric hypothesis of diabetes

Diabetes mellitus (DM) comprises many subclassifications, including type 1 (T1DM) and type 2 (T2DM) as the main subtypes¹. T1DM is typically characterized by an autoimmune destruction of beta cells in the pancreas, resulting in insulin depletion with an early onset. In contrast, T2DM is generally characterized by insulin resistance or its functional deficit, typically developed from aging and obesity¹. Nevertheless, it was not until decades after the discovery of insulin that the bihormonal hypothesis and, more recently, the glucagonocentric hypothesis started ascribing the significant contribution of alpha cell dysfunction to chronic hyperglycemia in diabetes^{2,3}. Specifically, the bi-hormonal hypothesis first proposed by Roger Unger and Lelio Orci in 1975 suggested that excessive glucagon secretion, in addition to insulin deficiency, contributes to hyperglycemia in diabetes mellitus². Following the first proposal of the theory, studies have found that blocking glucagon actions in diabetic mice resulted in reduced plasma glucose levels and improved glucose tolerance despite beta-cell deficiency, suggesting glucagon-secreting alpha cells may play a primary role in the development of diabetic hyperglycemia⁴⁻⁶.

Functionally, α cells secrete glucagon as the major glucose counterregulatory hormone, which increases blood glucose by stimulating hepatic glycogenolysis and gluconeogenesis in fasted states to prevent hypoglycemia^{7,8}. Glucagon acts on its target organs through the signalling of the glucagon receptor (GcgR). This seven-transmembrane G-protein receptor is expressed in the liver, other endocrine cells of the pancreas, kidney, small intestine, regions of the brain and heart⁹. Binding to GcgR on hepatocytes results in adenylate cyclase activation and cAMP formation, which activates protein kinase A (PKA), phosphorylating the transcription factor cAMP-response-element-binding (CREB) protein. CREB then induces the transcription of glucose 6-phosphatase and phosphoenolpyruvate carboxykinase (PEPCK), which are key enzymes

involved in gluconeogenesis. PKA activation can also activate phosphorylase kinase to induce glycogenolysis and lower substrates involved in glycolysis for suppression¹⁰. In general, though, glucagon actions include but are not limited to increasing hepatic glucose production, fatty acids and amino acids breakdown, energy expenditure, and potentially increasing heart rate and cardiac contractility¹¹.

Hyperglucagonemia or excess glucagon secretion is observed in diabetes¹². Specifically, alpha cell pathophysiology presents commonly in T2DM, such that glucose and paracrine-induced glucagon suppression is impaired^{11,13}. The importance of the interplay of paracrine factors and the contribution of dysfunctional α cells to diabetes has been demonstrated by blocking insulin actions on the α cells in mice, resulting in glucose intolerance, hyperglucagonemia and hyperglycemia¹⁴. Nevertheless, although blocking glucagon actions through knocking down glucagon receptors(GcgR) has been found to improve glucose levels and glucose tolerance, GcgR knock-out mice, humans with dysfunctional GcgR mutations, and genetic deletion of proglucagon-processing genes in mice have been shown to result in with α cell hyperplasia and hyperaminoacidemia^{4,5,15-18}. Blocking glucagon actions disrupts the hepatic- α cell axis, specifically the catabolism of amino acids in the liver to maintain appropriate amino acid homeostasis, which regulates α cell proliferation and mass through nutrient-sensing pathways^{19,20}.

As a result, understanding that glucagon-secreting alpha cells play a significant role in diabetes hyperglycemia and that blocking glucagon actions disrupts with the hepatic- α cell axis, studying the intracellular trafficking of glucagon from the secretion standpoint is much more cell-specific and may be a more attractive approach to finding a therapeutic target for the hyperglycemia of diabetes.

1.2 Islet architecture and paracrine interactions reflect islet function

The human pancreas secretes digestive enzymes (exocrine) and hormones (endocrine) to maintain optimal glucose control, metabolism and feeding behaviour⁷. In particular, the islets of Langerhans, the endocrine compartment of the pancreas, consists of a mixed population of highly vascularized endocrine cells that secrete counter-regulatory hormones in coordination to achieve glucose homeostasis, including glucagon secreted by α cells, insulin secreted by β cells and somatostatin secreted by δ cells^{8,21}. Glucagon, insulin and somatostatin are released in response to various glucose concentrations such that glucagon is secreted in a feed-forward manner under low glucose (1-3 mM), insulin is secreted in high glucose (> 7mM), and somatostatin is secreted when glucose concentrations are higher than 3 mM²². Specifically, insulin is a known inhibitor of glucagon secretion during hyperglycemia, while somatostatin is known to inhibit both glucagon and insulin secretion at different glycemic states, as shown in **Figure 1**^{23,24}.

Islet architecture has also been found to reflect islet function and intricate paracrine interactions²⁵⁻²⁷. While the typical composition of human islets is around 60% β cells, 30% α cells, and the remainder is made up of δ and pp cells, a study conducted by Over Cabrera in 2005 showed that human islets contain significantly more glucagon-positive α cells and less insulin-positive β cells than mouse islets^{8,25}. In addition, α -cell mass has been shown to increase in both T1D and T2D²⁸. This further ascribed the potential importance of α cells in human glucose metabolism, which may often be overlooked in mouse models due to the difference in islet cytoarchitecture. Nevertheless, endocrine cells are arranged within the islet such that direct heterotypic contacts between endocrine cells and islet blood vessels reflect the significance of paracrine interactions for fine-tuning hormonal secretions to optimize glucose levels^{25,27,29}. Specifically, 71% of β cells and more than 90% of α cells in human islets are in direct contact with other endocrine cell types²⁵.

Islets make up only 1-2% of the pancreas but receive up to 20% of pancreatic blood flow^{30,31}. Islet vasculature plays a crucial role in adequate glucose sensing and efficient insulin and glucagon release into the circulation in response to different glycemic states,

and disrupted islet vasculature is found in diabetes^{26,32–34}. Specifically, contractile pericytes covering islet capillaries innervated by the sympathetic nervous system contract during hypoglycemia to limit the diffusion of circulating glucose to endocrine parenchyma^{26,34}. This glucose-dependent decrease in islet blood flow during hypoglycemia also increases nitric oxide levels, an established effector in decreasing insulin and increasing glucagon secretion to induce hyperglycemic effects^{34,35}. In summary, islet vasculature dictates communication between endocrine cells and regulates the glucose-dependent secretion of endocrine hormones via the dynamics of intra-islet blood flow.

From clinical manifestations of hyperglucagonemia in diabetes, to unwanted side effects of targeting glucagon actions, the importance of paracrine interplay in glucose homeostasis, islet architecture and vasculature reflecting islet function and secretion, I have compiled evidence supporting why understanding the regulation of glucagon secretion in its physiological states and during paracrine inhibition may reveal better therapeutic targets than glucagon action blockers, for alleviating hyperglucagonemia and in turn hyperglycemia of diabetes.

1.3 Regulation of glucagon secretion in α cells

Glucagon secretion falls into two major categories: constitutive basal secretion through a rapid transfer of proteins in small vesicles from the trans-Golgi network (TGN) to the plasma membrane and regulated glucagon secretion, which is a more specialized process involving dynamic processing, sorting and maturing of selective proteins within the secretory granules in response to a stimulus³⁶.

Regulated glucagon exocytosis responds to several factors, including glucose, paracrine factors, neurotransmitters, and amino acids. These factors are currently known to alter voltage-gated ion channel activity, which in turn changes the overall α cell membrane electrical activity and regulates calcium (Ca^{2+})—dependent exocytosis^{37,38}.

In regulated secretion, glucagon is stored within the secretory granules of α cells until a stimulus triggers Ca^{2+} -SNARE protein-dependent exocytosis, where glucagon-containing granules fuse with the plasma membrane and release their content. α cells contain different pools of secretory granules such that there is a reserve pool (RP), and around 1% of granules make up a readily-releasable pool (RRP) primed to be exocytosed near the plasma membrane^{39,40}. Precisely, the release of Ca^{2+} activates synaptosome-associated protein 25 (SNAP-25), which helps transport the granules and mediate the interactions between granular SNARE proteins like vesicle-associated membrane protein 2 (VAMP 2) and plasma membrane SNARE proteins like Syntaxin1A to form the SNARE complex for exocytosis³⁹. Interestingly, expressions of genes encoding SNARE proteins and ion channels are also found to be disrupted in α cells of patients with T1DM⁴¹.

The alpha cell membrane is electrically excitable, and exocytosis regulated by glucose occurs at the level of receptor-mediated changes to K_{ATP} activities, which in turn alter the α cell membrane potential where Ca^{2+} channels can directly stimulate the release of glucagon⁴². Specifically, glucose uptake is mediated by glucose transporter 1 (GLUT1) in the cell membrane, and glucose undergoes subsequent glycolysis¹¹. Low glycolysis-generated adenosine triphosphate (ATP) levels in the mitochondria within the α cell directly reflect low glucose concentration. In response, ATP-sensitive potassium (K^+) channels close, leading to the build-up of intracellular K^+ , depolarizing the membrane and activating the P/Q type voltage-gated calcium (Ca^{2+}) channels, resulting in a Ca^{2+} influx and ultimately depolarization-evoked glucagon exocytosis¹¹.

Insulin inhibition of glucagon secretion occurs through the insulin receptor-activated phosphoinositide 3-kinases (PI3K) pathway, which results in the efflux of positively-charged K^+ ions and membrane hyperpolarization^{22,42}. Insulin has also been found to significantly reduce K_{ATP} channel sensitivity to ATP in α cells to maintain K^+ efflux, which in turn reduces depolarization-evoked glucagon exocytosis⁴³. Gamma amino butyric acid (GABA) is another potent glucagon secretion suppressor that is co-secreted with insulin by β cells. GABA binds to GABA_A receptors to the membranes of α cells, which results in α cell membrane hyperpolarization via Cl^- influx and insulin has been

shown to increase the translocation of GABA_A receptors as an indirect mechanism to inhibit glucagon secretion^{22,44}. In addition, insulin has been shown to inhibit glucagon secretion by another indirect mechanism, through stimulating the intra-islet release of somatostatin, which is also known to inhibit glucagon secretion⁴⁵. In the context of diabetes, destroyed or dysfunctional β cells do not secrete sufficient amounts of insulin, GABA, and ultimately somatostatin to appropriately inhibit glucagon secretion, which may partially contribute to excess glucagon secretion or hyperglucagonemia, further worsening the disease progression of diabetes. Alpha-cell insulin resistance also contributes to impaired inhibition of glucagon secretion in T2DM, such that membrane potential and exocytosis do not reduce in response to insulin^{40,46}.

Somatostatin secreted by δ cells binds to the somatostatin receptor 2 (SSTR2) on α cells to inhibit glucagon secretion^{38,45}. Specifically, SSTR2 is a G_{ai}-coupled receptor, which, upon binding somatostatin, inhibits adenylyl cyclase and decreases cytoplasmic cAMP levels, directly decreasing calcium entry through voltage-gated calcium channels^{24,47}. This then, in turn, reduces SNARE complex formation and results in a decrease in exocytosis. In addition, somatostatin has also been found to inhibit glucagon secretion by de-priming the RRP of glucagon granules away from the plasma membrane via activating phosphatase calcineurin, which inactivates ATP-dependent exocytotic proteins⁴⁸. Similarly, the expression of SSTR2 on α cell membrane is reduced in T2D, suggesting α cell insensitivity to paracrine inhibition contributes to elevated glucagon secretion in human T2D⁴⁰. Interestingly, δ cells exhibit neuron-like morphology, with well-defined cell soma and filopodia-like extensions that allows them to reach several cell layers and exert islet-wide paracrine regulation at a low population (~10% of islet cells)^{28,38,49,50}.

Interestingly, α cells' morphological features have also been found to affect their electrophysiologic properties, which ultimately give its unique secretion capacity compared to β cells. Specifically, α cells' smaller membrane area, spherical morphology, lower membrane capacitance, and high granule density enable much faster, transient, and robust electrical exocytosis in response to a considerably more dangerous state of hypoglycemia, as opposed to hyperglycemia^{38,51,52}.

In this section, I have discussed regulated glucagon secretion by external effectors like glucose and paracrine factors, which are currently known to primarily act by altering α cell excitability at the plasma membrane level. However, this is only one part of the glucagon secretory pathway; the regulation of secretion begins with glucagon granule biogenesis, trafficking of granules along the TGN, maturation of secretory granules, and finally, the trafficking of granules from the RP to the RRP at the membrane. As a result, understanding glucagon trafficking in the secretory pathway could reveal more clues about alpha cell resistance to paracrine inhibition in diabetes.

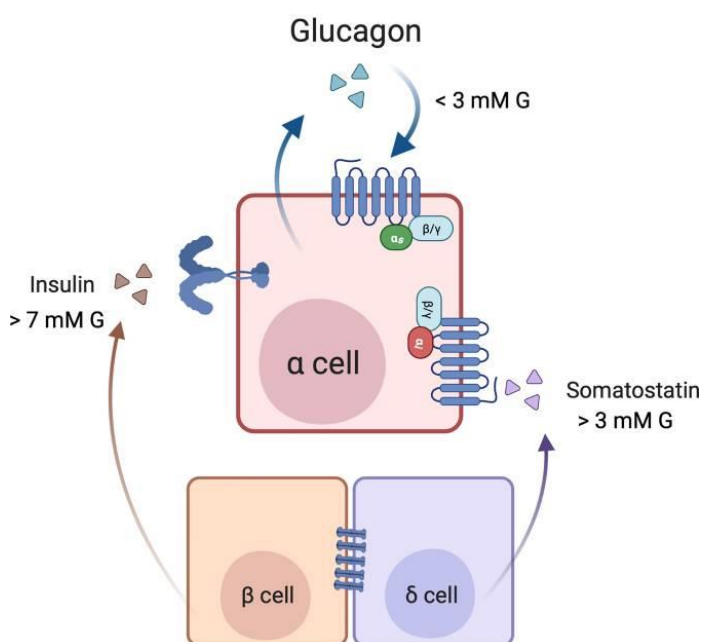


Figure 1. Paracrine regulation of glucagon secretion under various glucose concentrations.

Under low glucose conditions (1-3 mM), glucagon acts in an autocrine feed-forward manner. Under high glucose conditions (> 7 mM), insulin releases from β cells, inhibits glucagon secretion through receptors on α cells and stimulates somatostatin release from δ cells through gap junctions. Somatostatin also secretes independently of insulin when glucose concentrations are > 3 mM and inhibits glucagon secretion through receptor-mediated actions. From “Pathways of Glucagon Secretion and Trafficking in the Pancreatic Alpha Cell: Novel Pathways, Proteins, and Targets for Hyperglucagonemia”. by Asadi, Farzad, 2021, *Frontiers in Endocrinology*, 12: 726368.

1.4 Secretory pathway within the pancreatic alpha cells

Glucagon synthesis begins with its precursor proglucagon, which is synthesized in the endoplasmic reticulum and transported through the Golgi to the TGN^{22,53}. The formation of secretory granules begins with packaging and sorting secretory proteins such as proglucagon, its processing enzymes and other proteins into the granules from the TGN. The maturation process of the granules involves altering the composition of contents within the granule, removing constitutively-secreted proteins for basal secretion, retaining mature hormones, acidification, and removing water to condense the intragranular environment^{22,36}. Specifically, post-translational processing of proglucagon to mature glucagon is mediated by prohormone convertase 2 (PC2) in which its activity is found to be optimal within the granules due to optimal acidity and calcium levels⁵⁴⁻⁵⁷. As a result, proteins incorporated into secretory granules and their interactions are potentially the key to understanding the mechanisms that underlie the granule's ultimate fate along the secretory pathway. For example, in trying to find a sorting receptor that directs proglucagon to secretory granules, previous work from the Dhanvantari lab has found that upon knocking down a membrane-bound form of the processing enzyme carboxypeptidase E (CPE), stimulated glucagon secretion was inhibited, suggesting CPE's role in sorting proglucagon into the secretory granules^{54,58}. Interestingly, newly synthesized lysosomal enzymes from TGN, such as cathepsin B, have also been found inside the immature secretory granules of β cells and proinsulin, which gets removed during the granule maturation process, providing an additional regulated secretion capacity^{53,59,60}. Subsequently, upon normal granule maturation, external stimuli can then act on a receptor-mediated change in ion-channel activity, which alters the membrane potential and triggers the fusion of the granule membrane and plasma membrane for the stimulated-release of glucagon. This model predicts that dysfunctional proteins incorporated within the secretory granules may ultimately impact the protein interactions and their maturation process, leading to unregulated secretion.

Other cellular compartments may also be involved in the secretory pathway, such as the endo-lysosomal system involved in constitutive basal secretion. Specifically, basal secretion of glucagon begins with small vesicles being removed from the immature

secretory granule and directed towards the early endosomes and, ultimately, recycled to the plasma membrane for basal secretion or towards lysosomes for degradation³⁶. In addition, this alternative trafficking pathway involving the endo-lysosomal system has been shown to regulate insulin secretion, suggesting that understanding glucagon trafficking in the endo-lysosomal system is also crucial in fully understanding glucagon secretion⁶¹.

1.5 The lysosome: a novel compartment for glucagon trafficking

In addition to regulating hormone synthesis and secretion to govern hormone actions, trafficking hormone-containing granules towards degradative lysosomes adds another layer of regulation on secretion⁶². This direct fusion of secretory granules with late endo-lysosomes as a means of rapid elimination or regulation is known as crinophagy, the most unique and least known subtype of autophagy^{62,63}. Importantly, crinophagy maintains the intracellular pool of secretory granules and the granule maturation process.⁶⁴ Specifically, inhibiting the activity of a lysosomal nutrient sensor, mechanistic target of rapamycin complex 1 (mTORC1) induces crinophagy in the mouse α TC9 cells and has been shown to increase the localization of glucagon into lysosomal compartments, marked by lysosomal-associated membrane protein 1 (LAMP1), and reduce glucagon secretion effectively⁶². Interestingly, insulin secretion has also been shown to be tightly regulated by endocytic trafficking proteins like the Rab7 and Rab-interacting lysosomal protein (RILP)⁶¹. It was found that RILP overexpression not only promoted decreased biogenesis and increased degradation of pro-insulin-containing granules, but it also induced retrograde movement and clustering of mature-insulin-containing granules in the perinuclear region of rat insulinoma INS-1 cells⁶¹. Another study has also shown that metabolic stress can result in excess proinsulin trafficked towards the degradative lysosomes, exacerbating insulin deficiency in addition to the already reduced insulin synthesis seen in T2DM⁶⁵. Nevertheless, impaired autophagy can mean either excess or too little autophagy, which are both harmful⁶⁶⁻⁶⁸. Given that β cell lysosomal functions are impaired in diabetes, excess glucagon levels in diabetes may likely also occur at the level of crinophagy, where there is an insufficient degradation of glucagon-containing

granules. In addition, insulin and somatostatin resistance of α cells contributing to dysregulated glucagon secretion in diabetes suggests a potential link between paracrine resistance of α cells and impaired lysosomal functions in α cells. To investigate this proposed mechanism, proteins incorporated into the secretory granules of endocrine cells need to be investigated to understand their roles not just in the synthesis and secretory process but also in the crinophagy process, trafficking of granules towards the appropriate cellular compartment and the overall lysosomal network in maintaining an optimal level of secretory hormones.

1.6 Stathmin-2 directs glucagon towards the lysosome

Our lab previously investigated the dynamic glucagon interactome and searched for a modulator of glucagon secretion within the secretory granule of α TC1-6 cells⁶⁹. Upon conducting secretory granule proteomics on the glucagon interactome, stathmin-2 (Stmn2 or SCG10), a neuronal protein involved in microtubule dynamics and hormone transport, was identified under conditions that inhibit glucagon secretion⁷⁰⁻⁷². Stmn2 is a phosphoprotein of the stathmin family that binds tubulin dimers and alters microtubule stability for intracellular transport, essential in enhancing neurite growth. Its loss of function was found to be associated with motor neuropathy in amyotrophic lateral sclerosis (ALS)⁷³⁻⁷⁶. Stmn2 is also involved in regulating secretory granule formation or maturation in the TGN, such that its ablation decreases chromogranin A secretion in neuroendocrine cells⁷⁷. Given the similarity between neurons and endocrine cells, Stmn2 being important in neuronal maintenance and regulating secretory granules in neuroendocrine cells may imply its potential regulatory role in glucagon secretion of α cells. In addition, microtubule dynamics have also been shown to mediate insulin-containing vesicle movements and, in turn, mediate glucose-stimulated insulin secretion (GSIS) in β cells⁷⁸. Specifically, the movement of insulin granules from the RP to the RRP is regulated by microtubules⁷⁹⁻⁸¹. As a result, Stmn2, as a microtubule regulator, is a desirable target for investigating the intracellular trafficking of glucagon and changes to secretion in physiological conditions, during paracrine inhibition, and pathological states.

Previous work from the Dhanvantari lab showed that overexpression of stathmin-2 abolished both basal and K^+ -stimulated glucagon secretion in α TC1-6 cells. In addition, overexpression of Stmn2 also increased the localization of glucagon in the endosomal-lysosomal compartment⁶⁹. In addition, previous work has shown Stmn2 to be downregulated in diabetic mice and potentially humans and that Stmn2-mediated trafficking of glucagon to lysosomes was disrupted in a mouse model of diabetes with hyperglucagonemia^{22,71,82}. Nevertheless, the role of Stmn2-mediated lysosomal trafficking of glucagon as a normal physiological mechanism of controlling glucagon secretion needs to be investigated, and I will answer these questions in my thesis.

1.7 Central hypothesis

My studies focus on understanding how paracrine factors like insulin and somatostatin interact with Stmn2-mediated lysosomal trafficking of glucagon and if this is a possible mechanism of paracrine inhibition of glucagon secretion.

Hypothesis: I hypothesize that paracrine factors inhibit glucagon secretion through Stmn2-mediated lysosomal trafficking and biogenesis.

The aims of this project are:

1. To investigate paracrine regulation of glucagon secretion in relation to Stmn2 and cellular compartment markers in α TC1-6 cells by immunofluorescence microscopy.
2. To determine how Stmn2 affects lysosomal biogenesis in α TC1-6 cells using immunofluorescence microscopy and qPCR.
3. To determine if paracrine factors inhibit glucagon secretion by Stmn2-dependent lysosomal trafficking using live-cell imaging.

Chapter 2

2 Material and Methods

2.1 Cell Type

2.1.1 Alpha TC1-6 cells

Alpha TC1 clone 6 (α TC1-6) cells (a kind gift from C. Bruce Verchere, University of British Columbia, Vancouver, BC, Canada) are a glucagon-secreting cell line derived from an adenoma created in transgenic mice expressing the simian virus 40 (SV40) large T antigen under the control of the mouse preproglucagon promoter. This cell line has previously been used in our lab for studies involving intracellular trafficking of glucagon, the glucagon interactome, and glucagon processing along the secretory pathway^{54,57,69,70,82}.

2.1.2 Human pancreatic alpha-like cells

Experiments involving human pancreatic alpha-like cells (Celprogen, cat#35002-05) were provided by our collaborator, Dr. Danielle Dean, and conducted with the help of Dr. Madushika Wimalaratne at Vanderbilt University Medical Center. This cell line is SV40 negative and derived from transplant rejects from cadaveric adult donors. All other information about the cell line is proprietary.

2.2 Cell culture

For all α TC1-6 cells experiments, cells were maintained in 25 mM glucose Dulbecco's modified eagle medium (DMEM) (Gibco™, cat#11995073) supplemented with 15% horse serum (HS), 2.5% fetal bovine serum (FBS), and 100 units/mL penicillin-streptomycin (Life Technologies, cat#15070063) at 37°C and 5% CO₂. When α TC1-6 cells reached 80% confluency, cells were washed with phosphate-buffered saline (PBS), lifted using 0.25% trypsin/EDTA (Thermo Fisher Scientific, cat#25200072), and

resuspended with DMEM. Cells were seeded on 6-well plates for all experiments and 10-centimeter plates for passage continuation. New cells were thawed every three months and propagated until passage 12. For the human pancreatic alpha-like cell experiment, cells were maintained in 13 mM glucose human pancreatic alpha cell culture with complete growth media (Celprogen, cat#M35002-05).

2.3 Transient transfection

LAMP1-RFP was a gift from Walther Mothes (Addgene plasmid#1817; http://n2t.net/addgene:1817;RRID:Addgene_1817)⁸³. Stmn2-GFP fusion protein was obtained as the Stmn2 mouse tagged ORF clone (OriGene, cat#NM_025285) and pcDNA3-eGFP was used as the empty vector. Cells were transiently transfected at 60-70% confluency in 6-well plates. For overexpression experiments, around 7-10 ng of plasmid DNA (Stmn2-GFP, LAMP1-RFP, or GFP-alone) were diluted in Opti-MEM reduced serum medium (Thermo Fisher Scientific, cat#31985062) and combined with Lipofectamine 2000 (Invitrogen, cat#1168019) in Opti-MEM medium for 5 minutes at room temperature before the addition to serum-free media (Gibco™, cat#11960044) supplemented with sodium pyruvate to induce uptake of plasmids. For gene silencing experiments, 40 nM pooled siRNAs targeting Stmn2 were used (Thermo Fisher Scientific, cat#4390771; s73354, s73355, s73356) in addition to the siRNA negative control (Thermo Fisher Scientific, cat#4390846) with scrambled sequences that do not target any gene product, as done previously with some modifications^{57,69}. Cells were incubated with transfection reagents for 6 h before replacement to normal growth DMEM for cell recovery. The transfection efficiency and localization of Stmn2-GFP were compared to GFP-alone in **Appendix Figure 1**. Cell viability in various transfection conditions is shown in **Appendix Table 1**.

2.4 Glucagon secretion experiments

Glucagon secretion experiments aimed to detect quantifiable changes in glucagon release by detecting glucagon levels in media using ELISA and normalizing secretion to total cell protein concentration. Treatments included paracrine factors in order to confirm the physiological inhibition of glucagon secretion by paracrine factors in the cell line. Also, as done previously, Stmn2-GFP(OE) or Stmn2 siRNAs (KD) were transfected to reveal the protein's direct influence on glucagon secretion.

2.4.1 Glucagon secretion in the presence of paracrine factors

α TC1-6 cells under passage 6 were grown to 70-80% confluency in six biological replicates. 25 mM glucose DMEM was replaced with serum-free media (supplemented with sodium pyruvate) containing 25 mM glucose and 100 pM insulin (Sigma-Aldrich, cat#I0516) or 1 nM insulin plus 25 μ M GABA (Sigma-Aldrich, cat#A2129) for 24 h. The experiments were repeated with media containing 5.5 mM glucose (GibcoTM, cat#11885084). Media were removed and replaced with serum-free media containing treatments, and cells were incubated for 2 h for basal secretion. Media were collected, and cells were sequentially treated for 2 x 15 min periods without and with 55 mM potassium chloride (KCl) to induce exocytosis, after which media were collected for measuring regulated glucagon secretion. Cell protein was extracted using Radioimmunoprecipitation Assay (RIPA) buffer (PierceTM, cat#89900) for Bicinchoninic Acid Assay (BCA) (PierceTM, cat#23225) to measure total protein concentration. Secreted glucagon in the media was quantified using the glucagon ELISA kit (Thermo Fisher Scientific, cat#37072423) and normalized to the total protein concentration.

2.4.2 Glucagon secretion inhibition by insulin post-Stmn2-transfection

The glucagon sequential secretion experiment aimed to determine the functionality of our Stmn2-GFP and siRNAs targeting Stmn2 in altering glucagon secretion in α TC1-6 cells. Cells were transfected for 6 h with either Stmn2 siRNAs (KD), Stmn2-GFP (OE), scrambled siRNA or GFP alone. Twenty-four hours post-transfection, media was replaced with serum-free media for 2 h, and subsequently with media containing 1 nM insulin for 2 h, and these media were collected to measure glucagon secretion. Collected media was analyzed using the glucagon ELISA kit and normalized to the total protein concentration measured by BCA as previously done.

2.5 Immunofluorescence microscopy

2.5.1 Immunostaining

Coverslips were coated with sterile collagen as the extracellular matrix (ECM) for cell adherence and dried overnight. 100,000 cells per well were seeded on coverslips and allowed for adherence overnight. Treatments were applied accordingly for different experiments described below. Cells were fixed with 2% paraformaldehyde for 30 min and permeabilized with 0.1% Triton X-100 for 5 min. Background was blocked by blocking buffer (2% BSA in PBS and 0.05% Tween 20) for 2 h at room temperature (RT). Primary antibodies were diluted in blocking buffer as described below and added to cells overnight at 4°C. Cells were then washed with PBS and incubated in the appropriate secondary antibodies as described below at RT for 90 min. DAPI (1:1000 in PBS) was added, coverslips were mounted on microscope slides with anti-fade medium (Invitrogen, cat#2527959), sealed with nail polish, and stored at 4°C until analysis.

2.5.2 Antibodies

Secondary fluorophore-conjugated antibodies were chosen based on matching primary antibodies and avoiding emission overlap.

A) Glucagon (mouse anti-glucagon antibody, cat#10988, Abcam; 1:250): This primary antibody targeting glucagon was used in combination with either B), C), or D) to visualize glucagon distribution in various cellular compartments and its association with the protein of interest, Stmn2.

B) Stmn2 (goat anti-SCG10 antibody, cat#115513, Abcam; 1:250): This primary antibody targeting Stmn2 was combined with A) to visualize its association with glucagon. In addition, its immunofluorescence intensity was used to confirm Stmn2-KD and OE upon transfection.

C) LAMP1 (rabbit anti-LAMP1 antibody, cat#208943, Abcam; 1:100): A general lysosomal marker targeting dynamic components of the lysosomes, endosomes and the plasma membrane⁸⁴. This primary antibody targeting LAMP1 was combined with B) to visualize glucagon inside lysosomes. In addition, its immunofluorescence was used to define the intracellular region as the relation of its fluorescence intensity to the position of the signal within a cell.

D) Syntaxin1A (rabbit anti-Syntaxin1A antibody, cat#272736, Abcam; 1:50): This primary antibody targeting Syntaxin1A was used in combination with B) to visualize glucagon inside of secretory granules ready for exocytosis. In addition, its immunofluorescence was used to define the cell periphery region as the relation of its fluorescence intensity to the position of the signal within a cell.

E) Transcription Factor EB (TFEB) (rabbit anti-TFEB antibody, cat#264421, Abcam; 1:50): This primary antibody targeting TFEB was used to detect its nuclear translocation from the cytoplasm, which indicates upregulation of genes involved in lysosomal biogenesis and autophagy.

F) Alexa Fluor™ 594 donkey anti-mouse IgG antibody, cat#A21203, Thermo Fisher Scientific; 1:500): This long-wavelength secondary antibody was used in conjugation with A) to stain for glucagon due to its higher abundance compared to other proteins of interest. Immunofluorescence signals in this wavelength were visualized on the TRITC channel on the confocal microscopy and displayed in red.

G) Alexa Fluor™ 488 donkey anti-goat IgG antibody, cat#A11055, Thermo Fisher Scientific; 1:500): This short-wavelength secondary antibody was used in conjugation with B) to stain for Stmn2 due to its lower abundance compared glucagon. Immunofluorescence signals in this wavelength were visualized on the FITC channel on the confocal microscopy and displayed in green.

H) Alexa Fluor™ 488 donkey anti-rabbit IgG antibody, cat#A21206, Thermo Fisher Scientific; 1:500): This short-wavelength secondary antibody was used in conjugation with C), D) or E) to stain for LAMP1, Syntaxin1A, and TFEB due to their natural lower abundance compared glucagon. Immunofluorescence signals in this wavelength were visualized on the FITC channel on the confocal microscopy and displayed in green.

2.5.3 Confocal microscopy

2.5.3.1 Image acquisition

For fixed cells, imaging was done on the Nikon A1R confocal microscope (Canada), equipped with NIS-Elements AR 5.41.01 software, using 60X oil-immersed objective with Galvano laser, at 1024 x 1024, pinhole size (1), average (16), and dwell time (2.4). The microscope was equipped with four lasers, including DAPI (405 nm), FITC (490 nm-519 nm), TRITC (561-594 nm), and Cy5 (633-647 nm). Images were processed using the AI algorithm (restore.ai) to restore lost signals and then 2D deconvolution for maximum contrast and brightness. For live-cell imaging, parameters remained the same except for average (1) and dwell time (1.1), sacrificing resolution in exchange for minimal rendering delays and real-time capture of signals over time.

Zeiss LSM710 (Vanderbilt University Medical Center, Nashville) was used to capture images of human primary pancreatic alpha-like cells using the same parameters.

2.5.3.2 Image analysis

A) Cellular region definition: Pearson Correlation Coefficient (PCC) was used initially to measure colocalization between protein markers at the whole cell level; however, this method does not account for the change in the distribution pattern and the intensity of the signals. In addition, the distribution of intracellular vesicles reveals important information about cellular trafficking and secretion⁸⁵. As a result, inspired by how do Couto et al. (2020) measured intracellular vesicle density and dispersion using plot profiles, cellular regions α TC1-6 cells were defined using the fluorescence intensity of different known cellular region markers along a distance from the center of the nucleus to the end of the cell periphery⁸⁵. Specifically, DAPI, LAMP1 and Syntaxin1A fluorescence were used to define the nuclear region, the intracellular region containing lysosomes and the cell periphery where exocytosis occurs, respectively. Lines were drawn from the center of the nucleus to the cell membrane and were drawn to include signals from all regions. The intensity of signals was quantified along the distance on ImageJ Fiji. Therefore, using plot profile quantification of ImageJ allowed for quantification of immunofluorescence as a function of distance from the nucleus. The intensity across the distance was then normalized to the individual cell's nuclear radius for cell shape and size differences. Across multiple cells, an average plot profile was created for LAMP1, a general lysosomal marker, and its distance range was defined as the "intracellular region". The average plot profile generated for Syntaxin1A, an exocytosis marker, marked the range of distance was defined as the "cell periphery" region.

C) Co-localization of proteins and re-distribution analysis: Images from individual channels were processed using the "Image Calculator" function on ImageJ Fiji under the "AND" operation so that only the pixels containing two wavelengths would be captured with adjusted intensity. Plot profiles of the co-localized pixels were generated, and the re-distribution of the co-localized signals was quantified and categorized to the "intracellular region" or the "cell periphery" region, as described above.

2.5.4 Paracrine inhibition of glucagon exocytosis

This experiment aimed to visualize how paracrine factors such as insulin and somatostatin altered glucagon trafficking towards the lysosomes. α TC1-6 cells under passage six were grown to 60 to 70% confluency in 6-well plates and treated in various conditions in triplicates. Specifically, cells were treated overnight with vehicle alone in 25 mM glucose DMEM, 1 nM insulin plus 25 μ M GABA to mimic β -cell co-secretion, or 400 nM somatostatin (Sigma-Aldrich, cat#S1763) to mimic δ -cell secretion. Glucagon (mouse anti-glucagon, 1:250, cat#ab10988) was co-stained with Stmn2 (goat anti-SCG10, 1:250, cat#ab115513), LAMP1A (1:100, cat#ab208943), and Syntaxin1A (1:50, cat#ab272736). The intensity of colocalized signals was compared across different cellular regions and treatment groups. Four to five fields of view were captured per biological replicate, and data was analyzed with 2-way ANOVA with post-hoc tests.

2.5.5 Lysosomal dynamics mediated by Stmn2

This live-cell imaging experiment aimed to investigate the role of Stmn2 in changing lysosomal dynamics and if paracrine factors inhibited glucagon secretion through Stmn2-mediated change in lysosomal trafficking. α TC1-6 cells were transfected with GFP-alone or scrambled siRNA as negative controls for Stmn2-GFP (OE) and Stmn2 siRNAs (KD), respectively. LAMP1-RFP was co-transfected across all four groups to detect changes in intensity and distribution of lysosomal signal with Stmn2 (OE) and (KD). Upon 24 h post-transfection, lysosomal dynamics in real-time were captured before, during and five minutes after 1 nM insulin or 400 nM somatostatin treatment. A follow-up experiment examining lysosomal dynamics with 1 nM insulin was repeated in the presence of 10 nM insulin receptor tyrosine kinase inhibitor (Abcam, cat#ab141566) to test the receptor-mediated effect of insulin on the lysosomal network.

2.5.5.1 Stmn2 and LAMP1 co-expression in human pancreatic alpha-like cells

This live timepoint experiment aimed to investigate the role of Stmn2 in changing lysosomal distribution in a human pancreatic alpha-like cell line. I conducted these experiments in the lab of our collaborators, Dr. Danielle Dean and Dr. Madushika Wimalaratne, at Vanderbilt University. This preliminary experiment was conducted to compare the human alpha-like cells to the mouse pancreatic α TC1-6 cells in terms of cell morphology, lysosomal, and Stmn2 distribution.

2.5.6 Glucagon distribution mediated by Stmn2

This fixed-cell experiment aimed to connect Stmn2's role in the lysosomal dynamics and its role in changing glucagon distribution. α TC1-6 cells were transfected with GFP-alone as a negative control for Stmn2-GFP (OE) and Stmn2 siRNAs (KD). Anti-Stmn2 antibody was used to confirm Stmn2-OE and KD using fluorescence intensity, while glucagon was stained to visualize changes in its distribution pattern.

2.5.7 Paracrine inhibition of glucagon exocytosis mediated by Stmn2

This fixed-cell experiment aimed to determine if paracrine factors inhibit glucagon secretion via the Stmn2-mediated lysosomal pathway. α TC1-6 cells were transfected with GFP-alone, Stmn2-GFP (OE) and Stmn2 siRNAs (KD), followed by a 24-hour incubation with 1 nM insulin or 400 nM somatostatin. Stmn2 and glucagon were co-stained as done previously, and changes in glucagon distribution patterns were analyzed.

2.5.8 Nuclear translocation of TFEB mediated by Stmn2

Transcription Factor EB (TFEB), a transcription factor involved in lysosomal biogenesis, was stained (Abcam, 1:50, #ab264421, anti-rabbit) along with DAPI (1:1000 in PBS) (Thermo Fisher Scientific, cat#62248) upon transfection with GFP-alone or Stmn2-GFP (OE). The nuclear translocation of TFEB was calculated as the fluorescence intensity of TFEB within the nucleus stained by DAPI, normalized to the cytoplasmic fluorescence intensity of TFEB. This analysis method was used by Wessel & Hanson (2015) to detect the nuclear translocation of p65⁸⁶.

2.6 Gene expression of MCOLN1 in Stmn2-overexpression

Quantitative polymerase chain reaction (qPCR) was conducted to evaluate and quantify the relative expression of genes involved in lysosomal biogenesis with Stmn2-OE and KD. By performing a qPCR on mucolipin 1 (MCOLN1), a known gene target upstream of TFEB, findings from the nuclear translocation of TFEB by immunohistochemistry and Stmn2's transcriptional role can be validated.

2.6.1 Primer design

β -actin was used as the housekeeping gene to analyze MCOLN1 expression in Stmn2-KD and OE models. The primer for β -actin (NM_007393.3, Gene ID: 11461) had the forward sequence of 5'-CCACCATGTACCCAGGCATT-3' (tM 66.80) and the reverse sequence of 5'-AGGGTGTAAAACGCAGCTCA-3' (tM 64.6) (product length 253 bps) as previously used⁸⁷. Primers for mouse MCOLN1 (NM_053177.1, Gene ID:94178) had the forward sequence 5'TGACGTGCTCACCATCTCGG-3' (tM 62.21) and reverse sequence of 5'-CACTCGCAACGTGGCAATCA-3' (tM 61.84) (product length 178 bps), designed using Primer-BLAST. An end-point PCR was run and visualized on a 2% agarose gel to confirm primer specificity and verify the product length of the amplicons. **(Appendix Figure 2 a).**

2.6.2 Treatment, RNA Extraction and cDNA Synthesis

α TC1-6 were grown to 60-70% confluency in regular 25 mM glucose media in 6-well plates. Cells were transiently transfected with either 40 nM GFP-alone, scrambled siRNA, Stmn2-GFP or siRNAs targeting Stmn2 in six biological replicates. RNA was then extracted using the PureLink™ RNA Mini Kit (Thermo Fisher Scientific, cat#12183018A), and cDNA was generated using the iScript™ Reverse Transcription Supermix from the extracted RNA (BIO-RAD, cat#1708840). The 5x iScript No-Reverse Transcription Control Supermix was used for the qPCR no-enzyme control (NEC).

2.6.3 qPCR

qPCR was used to amplify cDNA with primers targeting the MCOLN1 sequence as the gene of interest and beta-actin as the housekeeper to quantify the relative gene expression of MCOLN1 upon overexpressing Stmn2. SSoAdvanced universal SYBR® Green Supermix (BIO-RAD, cat#1725270) was used to amplify targeted sequences with the annealing temperature of 58 °C using the built-in thermocycler set-up cycles in the QuantStudio™ 5 Real-Time PCR System. Primer efficiency was assumed, the $2^{-\Delta\Delta CT}$ quantification method was used to calculate relative fold changes in various treatment groups, and a one-way ANOVA was conducted, followed by a t-test.

2.7 Statistical analysis

Individual wells of a plate were considered biological replicates for all experiments. Technical replicates for microscopy included multiple fields of view per coverslip (3-4). Secretion experiments consisted of three treatment variables, including differential glucose concentration, paracrine factors, and potassium stimulation, and analysis was conducted using a three-way ANOVA, followed by a Tukey post-hoc test. The *Stmn2*-manipulated secretion experiment with two treatment variables was analyzed using a two-way ANOVA, followed by a Tukey post-hoc test. As for microscopy, plot profiles were used to quantify the fluorescence intensity of different proteins along a distance within an individual cell, then a two-way ANOVA analysis was conducted with variables including paracrine treatment and protein localization. A direct comparison of transcription factor EB fluorescence intensity was conducted using a two-sample t-test. Significance for all statistical analyses was set at $\alpha \leq 0.05$.

Chapter 3

3 Results

3.1 Regulation of glucagon secretion

3.1.1 Regulation of basal and stimulated glucagon secretion by glucose and insulin

This secretion experiment aimed to examine the physiological regulation of glucagon exocytosis through glucose-induced, paracrine and membrane-depolarizing (55 mM K⁺) mechanisms. Glucagon secretion was significantly increased by 55 mM K⁺ at 25 mM glucose condition, both in the absence (p<0.001) and presence (p<0.01) of 100 pM insulin, respectively (**Figure 2**). At 5.5 mM glucose, there was no K⁺-stimulated secretion, either in the absence or presence of 100 pM insulin; however, insulin caused a decrease in basal (p<0.001) and K⁺-stimulated secretion (p<0.05). Lastly, lowering glucose concentration without insulin or K⁺ significantly increased basal glucagon secretion from (p<0.001) (**Figure 2**).

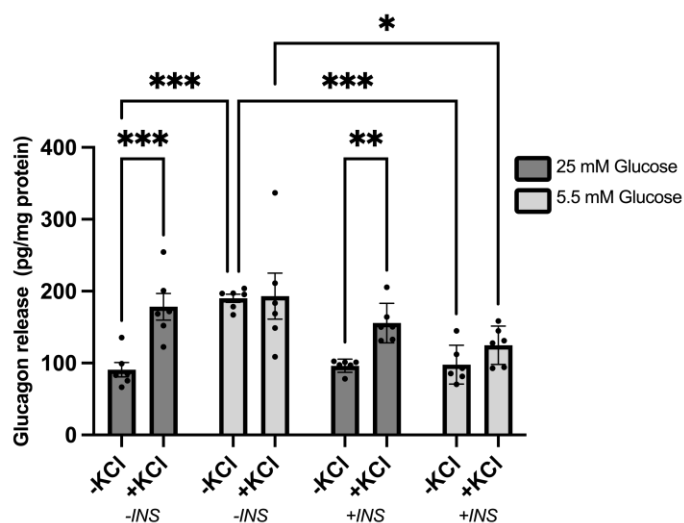


Figure 2. Basal and K⁺-stimulated glucagon secretion in response to insulin under either high (25 mM) or low (5.5) glucose. Alpha TC1-6 cells were incubated for 24 h in media containing 25 mM or 5.5 mM glucose in the absence or presence of 100 pM insulin. Cells were then treated with or without 55 mM KCl for 15 min. Glucagon in the media was measured by

ELISA and normalized to total protein. Values were expressed as mean \pm SEM (n=6) and compared among groups using a three-way ANOVA, followed by a post-hoc test ($\alpha = 0.05$). *p<0.05. **p<0.01, ***p<0.001.

3.1.2 Regulation of basal and stimulated glucagon secretion by glucose and co-secreted β cell effectors

This secretion experiment was a follow-up experiment of the previous with minor changes, including an increased insulin concentration from 100 pM to 1 nM with 25 μ M GABA to mimic the co-secretion of these effectors by β cells. Under high and low glucose conditions, 1 nM insulin and 25 μ M GABA did not inhibit glucagon secretion. In addition, the glucose concentration also did not inhibit glucagon secretion. In addition, the glucose concentration also did not affect glucagon secretion in this experiment. Nevertheless, 55 mM K^+ significantly (p<0.001) stimulated glucagon secretion across all four groups (**Figure 3**).

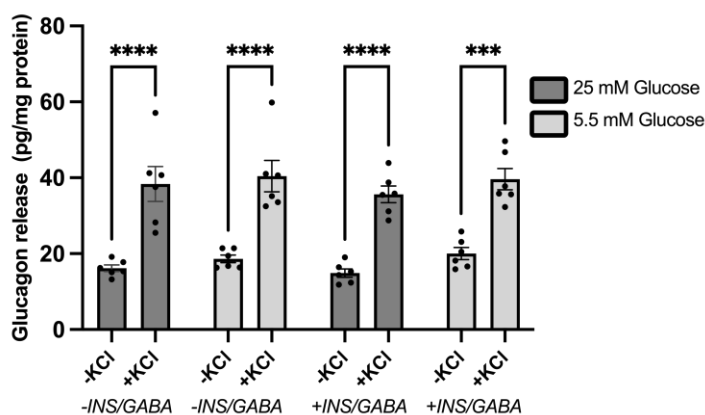


Figure 3. Basal and K^+ -stimulated glucagon secretion in response to insulin and GABA under either high (25 mM) or low (5.5) glucose. Alpha TC1-6 cells were incubated for 24 h in media containing 25 mM or 5.5 mM glucose in the absence or presence of 1 nM insulin and 25 μ M GABA. Cells were then treated with or without 55 mM KCl for 15 min. Glucagon in the media was measured by ELISA and normalized to total protein. Values were expressed as mean \pm SEM (n=6) and compared among groups using a three-way ANOVA, followed by a post-hoc test ($\alpha = 0.05$). ***p<0.001, ****p<0.0001.

3.1.3 Regulation of basal glucagon secretion by Stmn2

This experiment aimed to quantify changes in glucagon secretion in response to 1 nM insulin inhibition upon overexpressing or knocking down Stmn2. This experiment reveals the role of Stmn2 in the paracrine inhibition of glucagon secretion. In **Figure 4**, glucagon secretion was significantly lower ($p < 0.05$) in Stmn2-KD compared to Stmn2-OE.

Treatment with 1 nM insulin post-transfection did not result in any significant changes.

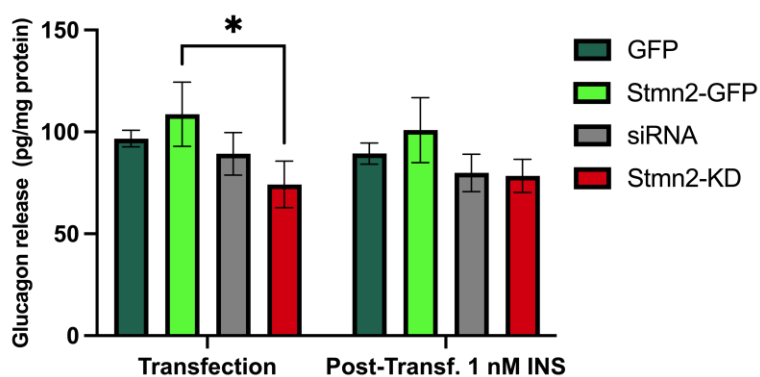


Figure 4. Basal glucagon secretion post-Stmn2 knockdown (KD), overexpression (OE), before and after 1 nM insulin treatment. Glucagon in the media was determined using ELISA and normalized to total protein concentration. Values were expressed as mean \pm SEM ($n=3$) and compared among groups using a two-way ANOVA, followed by a post-hoc test ($\alpha = 0.05$).

* $p < 0.05$.

3.2 Paracrine factors regulate intracellular glucagon trafficking

At first, colocalization analysis between protein markers was conducted using the Pearson Correlation Coefficient (PCC) with the Costes auto-threshold by ImageJ Fiji. Upon treatment of α TC1-6 cells with 1 nM insulin and 25 μ M GABA, the colocalization between glucagon and Syntaxin1A decreased significantly ($p < 0.01$), while there were no significant changes in the colocalization between glucagon/Stmn2, and glucagon/LAMP1 (Figure 5).

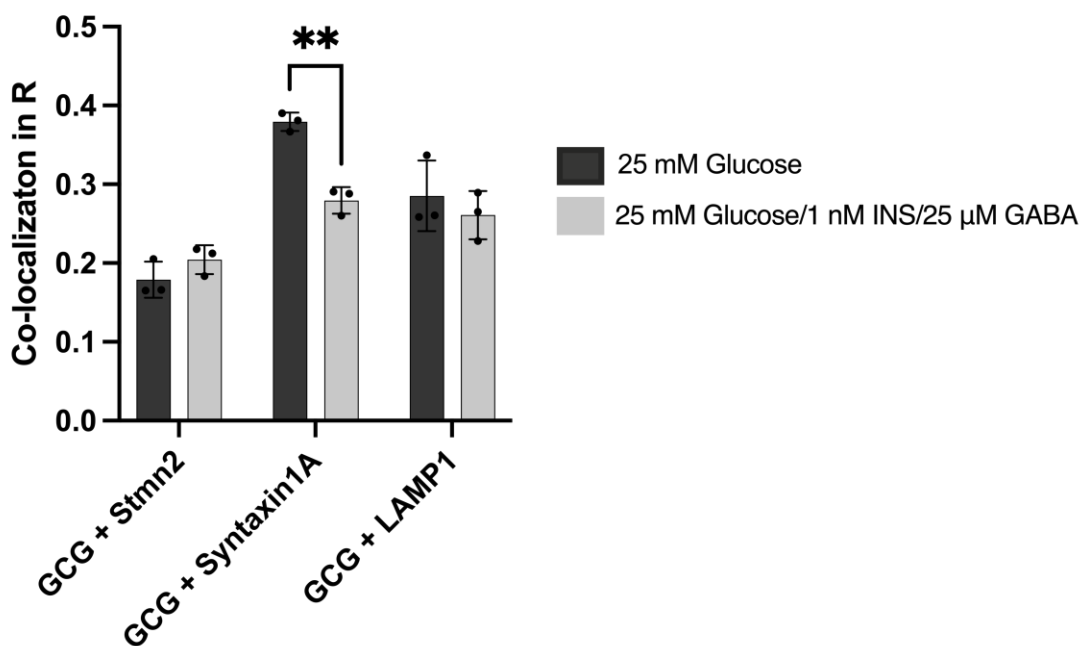
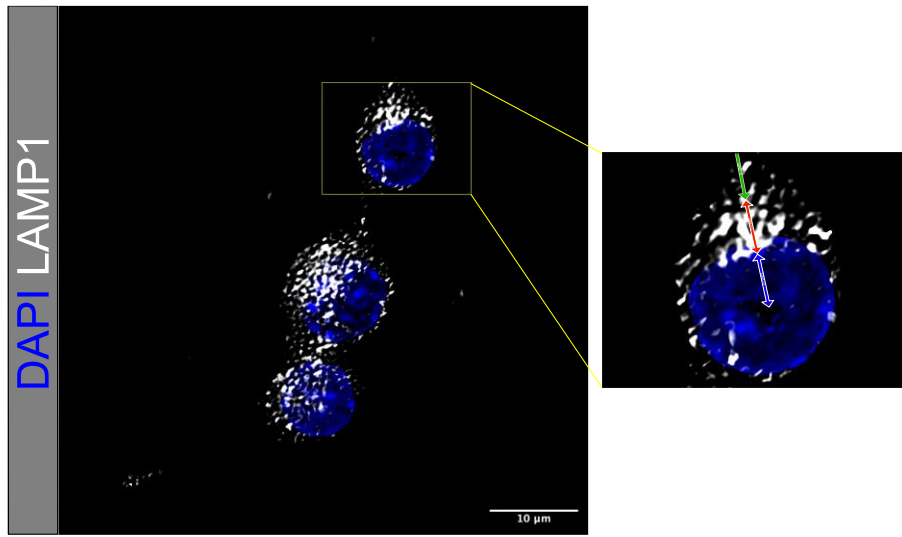


Figure 5. Colocalization between glucagon and Stmn2, Syntaxin1A and LAMP1 treated with 1 nM insulin/25 μ M GABA cultured under high glucose (25 mM) media. Regions of interest were drawn around individual cells and analyzed by ImageJ Fiji using Pearson Correlation Coefficient (PCC) at Costes auto-thresholds (BIOP JaCOP plugin). Values were expressed as mean \pm SEM (n=3) and compared among groups using a two-way ANOVA, followed by a post-hoc test ($\alpha = 0.05$). ** $p < 0.01$.

3.3 New analysis tool defining cellular regions as “Intracellular” or “Cell periphery”

Upon developing the new analysis tool, average plot profiles for cellular region markers were generated, as seen in **Figures 6** and **7**. LAMP1 was used to detect lysosomes, which are generally localized to the intracellular region, while Syntaxin1A was used to detect secretory granules ready for exocytosis, typically docked at the plasma membrane. In **Figure 6 a)**, LAMP1 displayed higher intensity in a region right next to the nucleus, and the intensity decreased when moving towards the cell periphery. On average, 0-1 times the distance of the nuclear radius from the center of cells contained minimal fluorescence signal, while 1-2 times the distance of the nuclear radius from the center of the cell, the LAMP1 fluorescence signal was the strongest, which defines this region as the “intracellular region” or where the lysosomes typically reside, as shown in **Figure 6 b)**. In contrast, the immunofluorescence image of Syntaxin1A showed signals aligning at the plasma membrane (**Figure 7 a)**, and this distribution pattern was reflected by the high fluorescence intensity in the region that was 2-3 times nuclear radius away from the center **Figure 7 b)**. This region was defined as the “cell periphery” region near the cell plasma membrane, where exocytosis typically occurs.

a)



b)

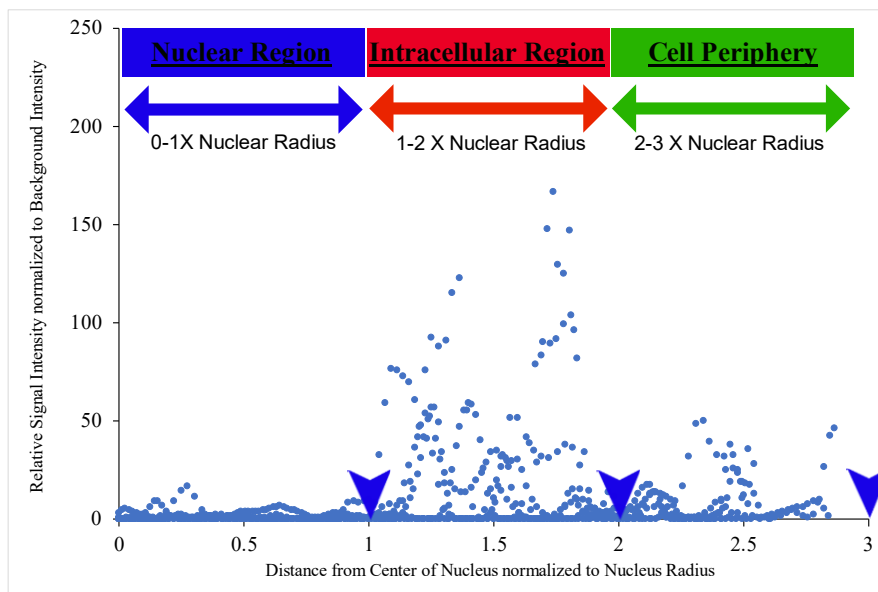
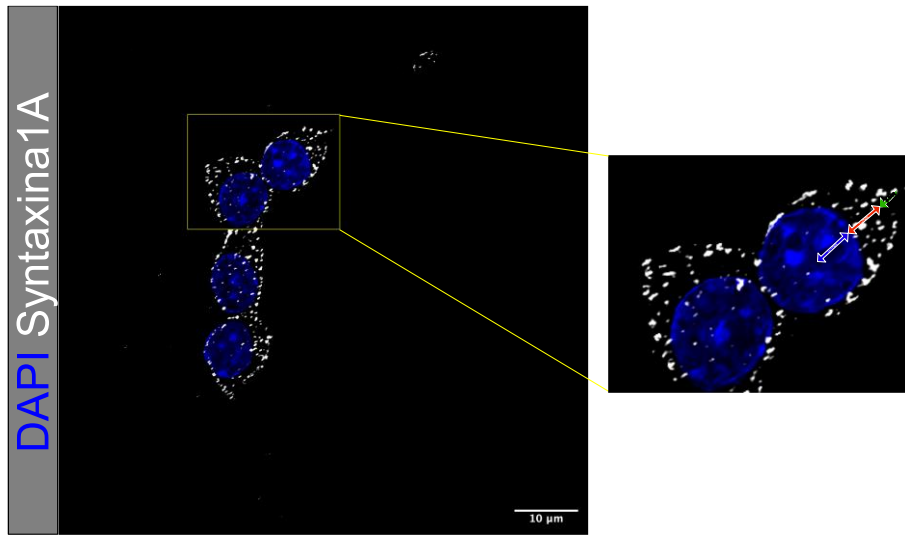


Figure 6. Immunofluorescence and average plot profile of the general lysosomal marker, LAMP1, cultured under high glucose (25 mM) media. Straight lines were drawn across multiple cells (n=6) from the center of the nucleus to the plasma membrane, and LAMP1 immunofluorescence intensity was measured along the line, with the distance normalized to the individual cell's nuclear radius to account for differences in cell shapes and sizes. Each data point represents the fluorescence intensity of an individual pixel with its relative distance to the cell nucleus.

a)



b)

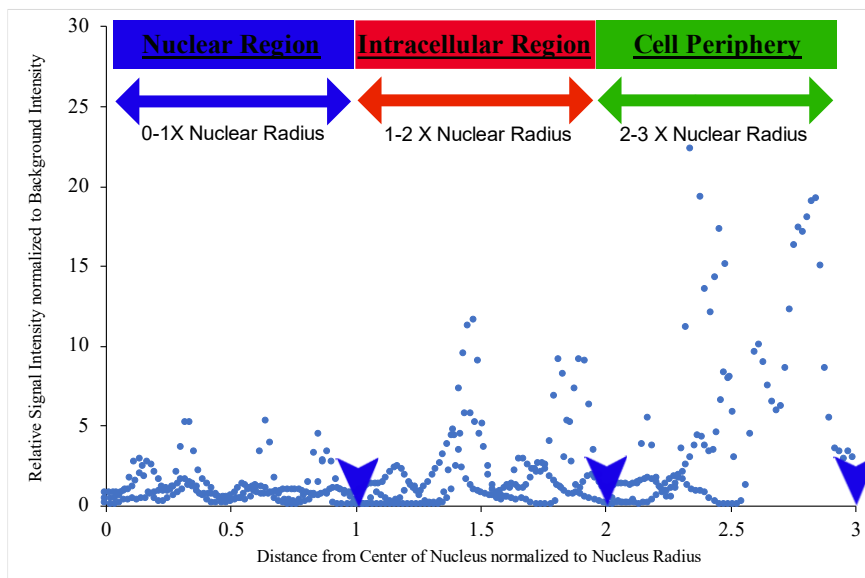


Figure 7. Immunofluorescence and average plot profile of the exocytosis marker, Syntaxin1A, cultured under high glucose (25 mM) media. Straight lines were drawn across multiple cells ($n=6$) from the center of the nucleus to the plasma membrane, and Syntaxin1A immunofluorescence intensity was measured along the line, with the distance normalized to the individual cell's nuclear radius to account for differences in cell shapes and sizes. Each data point represents the fluorescence intensity of an individual pixel with its relative distance to the cell nucleus.

3.4 Microscopy shows paracrine redistribution of colocalized vesicles

3.4.1 Paracrine factors redistribute glucagon and Stmn2 towards the intracellular region

Alpha TC1-6 cells were treated with 1 nM insulin/25 μ M GABA or 400 nM SST, and the intensities of the colocalized glucagon/Stmn2, glucagon/LAMP1 or glucagon/Syntaxin1A were analyzed by plot profiles. In **Figure 8 a**), the immunofluorescence images of the colocalized signal between glucagon and Stmn2 showed the strongest signal intensity near the plasma membrane in the control media containing regular 25 mM high glucose. Upon treatment with 1 nM insulin/25 μ M GABA or 400 nM SST, the co-localized signals redistributed intracellularly, and the signals in the periphery were no longer as prominent. This distribution pattern was reflected in the plot profile analysis (**Figure 8b**). There was a significant reduction in colocalized fluorescence intensity in the cell periphery upon treatment with either insulin/GABA ($p < 0.0001$) or somatostatin ($p < 0.0001$) (**Figure 8 b**). In addition, there were around 2.3 folds of more colocalized glucagon and Stmn2 in the cell periphery in the 25 mM glucose condition compared to the intracellular region. In contrast, the opposite distribution pattern was observed upon treatment with paracrine factors. Specifically, insulin and GABA induced around 2.5 folds and somatostatin 2.2 folds more colocalized glucagon and Stmn2 in the intracellular region than the cell periphery.

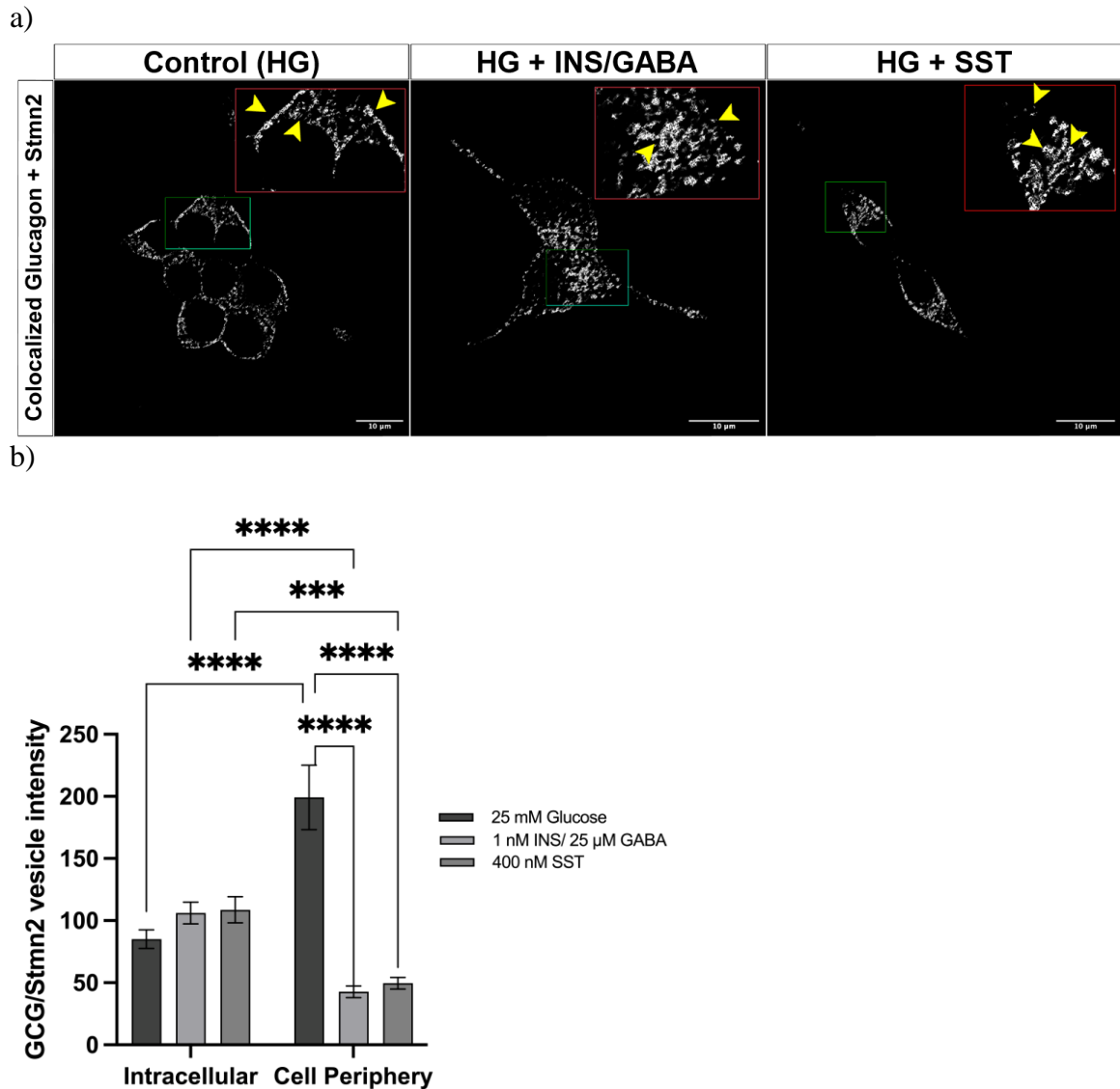


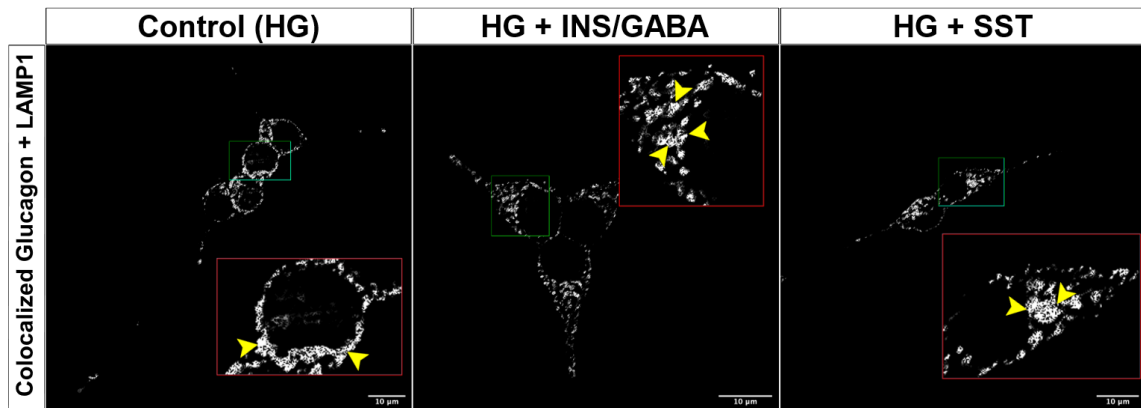
Figure 8. Redistribution of colocalized glucagon and Stmn2 upon 1 nM insulin/25 μM

GABA or 400 nM somatostatin treatment. a) Merged immunofluorescence images of glucagon and Stmn2 in the presence of insulin/GABA and SST, showing only the colocalized pixels processed by the “AND” operator with the image calculator plug-in by ImageJ Fiji. b) Plot profile analysis of colocalized signals across different cell regions in the presence of paracrine factors. Values were expressed as an average colocalized fluorescence intensity \pm SEM (n=3) and compared among groups and cellular regions using a two-way ANOVA, followed by a post-hoc test ($\alpha = 0.05$). ***p<0.001, ****p<0.0001.

3.4.2 Paracrine factors redistribute glucagon and LAMP1 towards the intracellular region

The colocalized signal between glucagon and LAMP1 in the presence of 1 nM insulin/25 μ M GABA or 400 nM SST reveals the paracrine-induced distribution of glucagon contained in lysosomes. In **Figure 9 a**), the colocalized signal was the most prominent near the plasma membrane in the 25 mM glucose condition and redistributed significantly to the intracellular region upon treatment of insulin/GABA and somatostatin. Plot profile analysis showed the colocalized signal between glucagon and LAMP1 increased significantly ($p < 0.0001$) in the intracellular region in response to 1 nM insulin/25 μ M GABA or 400 nM somatostatin (**Figure 9 b**). In addition, the colocalized signal between glucagon and LAMP1 in the intracellular region was around 2.4 folds of those in the periphery upon treatment of insulin and GABA and around 2.6 folds with the treatment of somatostatin.

a)



b)

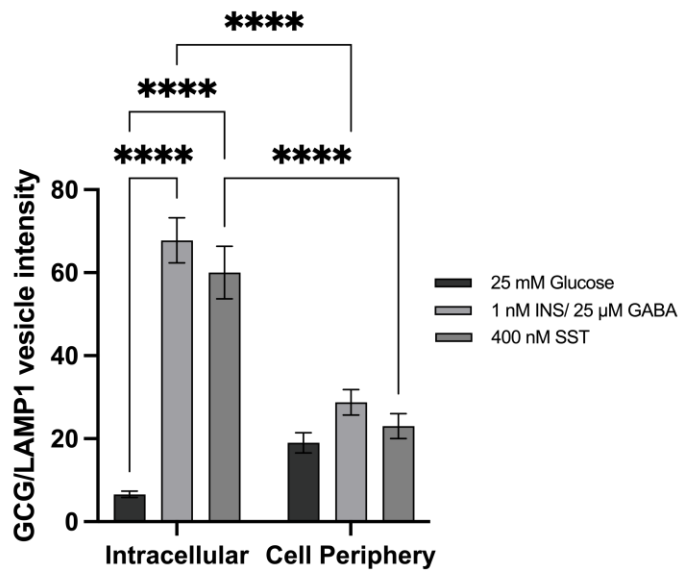
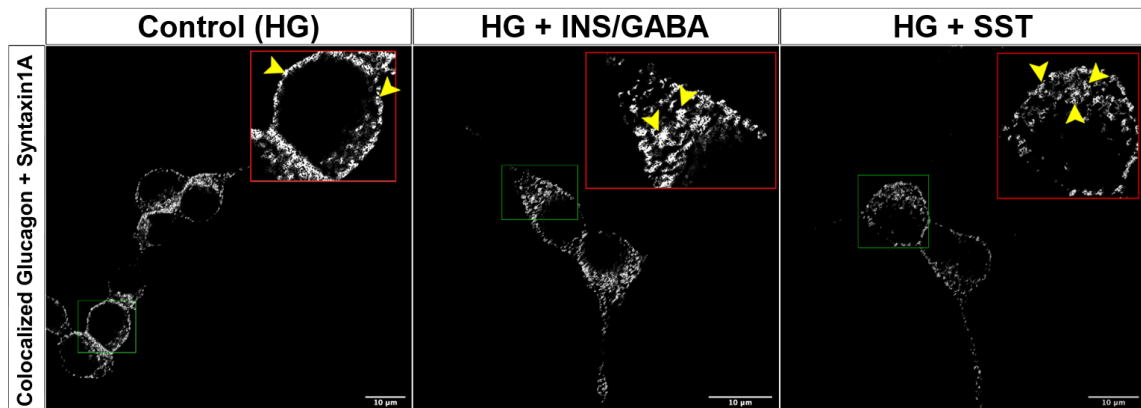


Figure 9. Redistribution of colocalized glucagon and LAMP1 upon 1 nM insulin/25 μM GABA or 400 nM somatostatin treatment. a) Merged immunofluorescence images of glucagon and LAMP1 in the presence of insulin/GABA or SST, showing only the colocalized pixels processed by the “AND” operator with the image calculator plug-in by ImageJ Fiji. b) Plot profile analysis of colocalized signals across different cell regions in the presence of paracrine factors. Values were expressed as an average colocalized fluorescence intensity \pm SEM (n=3) and compared among groups and cellular regions using a two-way ANOVA, followed by a post-hoc test ($\alpha = 0.05$). ****p<0.0001.

3.4.3 Paracrine factors redistribute glucagon and Syntaxin1A towards the intracellular region

The colocalized signal between glucagon and Syntaxin1A in the presence of 1 nM insulin/25 μ M GABA or 400 nM SST reveals the paracrine-induced distribution of glucagon inside secretory granules. In **Figure 10 a**), the colocalized signal was the most prominent near the plasma membrane in the 25 mM glucose condition and redistributed significantly to the intracellular region upon treatment of insulin/GABA and somatostatin. Plot profile analysis showed the colocalized signal between glucagon and Syntaxin1A increased significantly ($p < 0.0001$) in response to either 1 nM insulin/25 μ M GABA or 400 nM somatostatin (**Figure 10 b**). In addition, 400 nM somatostatin significantly reduced ($p < 0.001$) the peripheral colocalized signal by approximately 42%.

a)



b)

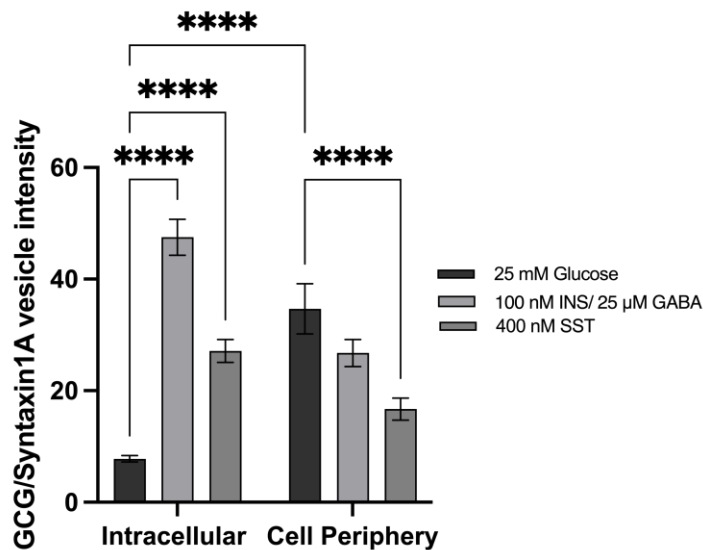


Figure 10. Redistribution of colocalized glucagon and Syntaxin1A upon 1 nM insulin/25 μM GABA or 400 nM somatostatin treatment. a) Merged immunofluorescence images of glucagon and Syntaxin1A in the presence of insulin/GABA or SST, showing only the colocalized pixels processed by the “AND” operator with the image calculator plug-in by ImageJ Fiji. b) Plot profile analysis of colocalized signals across different cell regions in the presence of paracrine factors. Values were expressed as an average colocalized fluorescence intensity \pm SEM (n=3) and compared among groups and cellular regions using a two-way ANOVA, followed by a post-hoc test ($\alpha = 0.05$). ****p<0.0001.

3.5 Stmn2 induces nuclear translocation of TFEB

In order to determine if Stmn2 had an effect on transcriptional regulation of lysosomal biogenesis, nuclear translocation of transcription factor EB (TFEB), a master regulator of lysosomal gene transcription, was measured upon overexpression of Stmn2.

Quantification of the nuclear translocation of TFEB was calculated by the fluorescence intensity of TFEB within the nucleus normalized to the fluorescence intensity of TFEB in the cytoplasm. In **Figure 11 a)**, TFEB (white) redistributed from the cytoplasm in the GFP-transfected (control) condition to the nucleus after Stmn2-GFP overexpression. The nuclear translocation of TFEB was quantified in **Figure 11 b)**, and showed that overexpression of Stmn2 significantly increased the nuclear TFEB intensity ($p < 0.0001$). Transfection distribution differentiation and efficiency are shown in **Appendix Figure 1**.

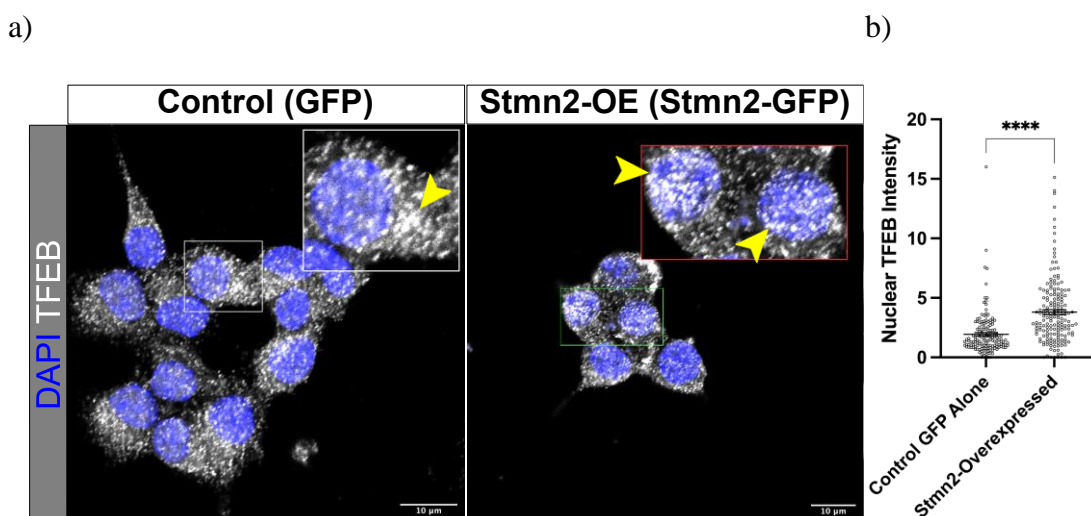


Figure 11. Nuclear translocation of transcription factor EB (TFEB, white) upon overexpressing Stmn2 with Stmn2-GFP. Cells were transfected with either GFP-alone or Stmn2-GFP plasmids, then immunostained using primary antibodies against TFEB. (A) Merged immunofluorescence images of TFEB (white) and cell nuclei (blue). (B) Values were expressed as the average nuclear TFEB intensity \pm SEM ($n=6$) normalized to the average cytoplasmic TFEB intensity analyzed by ImageJ Fiji, followed by a two-sample t-test ($\alpha = 0.05$). **** $p < 0.0001$.

3.5.1 Stmn2 upregulates MCOLN1, upstream of TFEB

Mucolipin 1 (MCOLN1) is an ion channel that releases lysosomal Ca^{2+} , activating calcineurin phosphatase that dephosphorylates TFEB into its active state⁸⁸. The relative gene expression of MCOLN1 in the Stmn2-overexpressed model was significantly higher ($p < 0.05$) than the knockdown model (**Figure 12**). Two specific amplicons are represented by beta-actin and MCOLN1 on the amplification plot in **Appendix Figure 2 c**). The amplicon sizes were also verified on a 2% agarose gel. Specifically, beta-actin amplicons were above the 200-bps ladder mark, comparable to the theoretical yield of 253 bps, while MCOLN1 amplicons were below the 200-bps ladder mark, comparable to the theoretical yield of 187 bps (**Appendix Figure 2 a**). Lastly, melt curve analysis post qPCR further validated the production of two specific amplicons with two peaks, one representing the melting temperature (t_m) of MCOLN1 primers at (84.10 ± 0.02 °C) and another representing beta-actin primers at (87.14 ± 0.01 °C) (**Appendix Figure 2 b**).

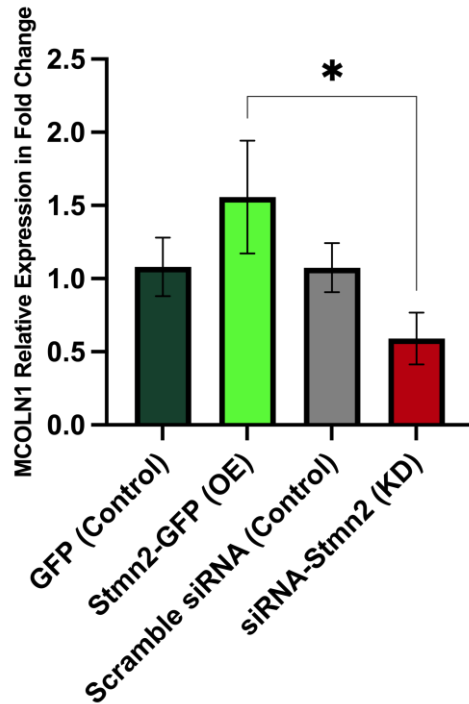
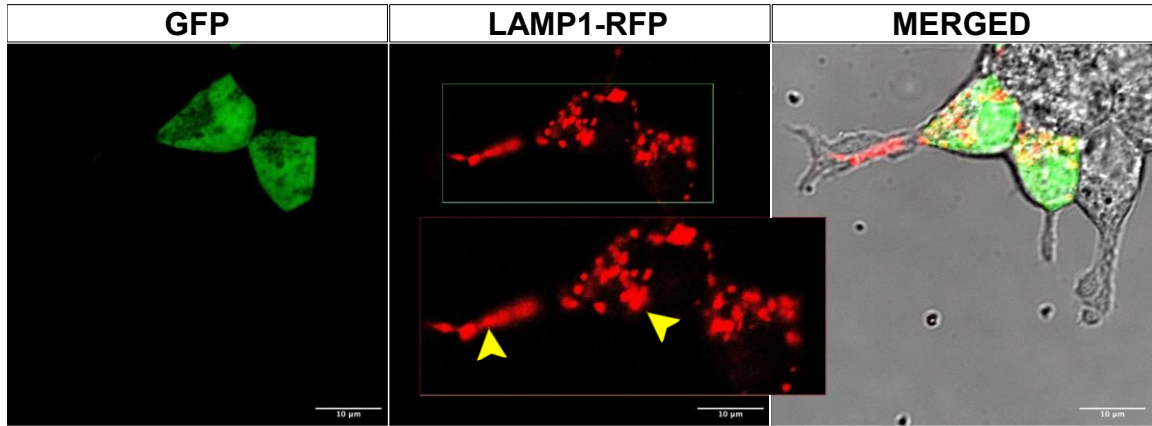


Figure 12. Relative gene expression of MCOLN1 upon Stmn2 overexpression (OE) and knockdown (KD) to the control normalized to beta-actin. Cells were transfected with GFP-alone, Stmn2-GFP, scrambled siRNA, or Stmn2 siRNAs (KD). Relative changes in MCOLN mRNA transcripts were quantified by its C_q values normalized to beta-actin compared to the control, calculated by the $2^{-\Delta\Delta CT}$ method. Values were expressed as the average fold change \pm SEM (n=6) of MCOLN1 and compared by one-way ANOVA, followed by post-hoc test ($\alpha = 0.05$). * $p < 0.05$.

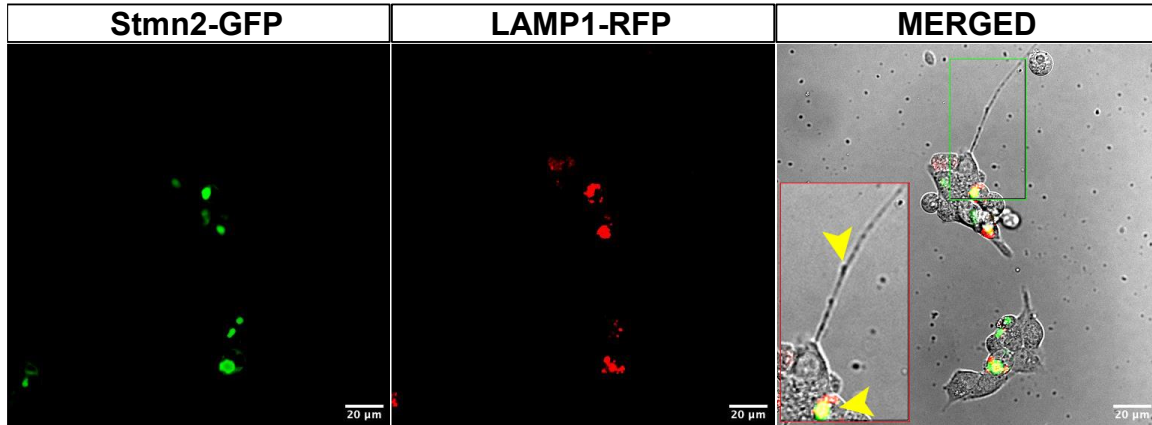
3.6 Stmn2 regulates lysosomal dynamics

The fluorescent reporters Stmn2-GFP and LAMP1-RFP allowed for visualization of the temporal and spatial dynamics of Stmn2 and its association with lysosomes. Negative controls were GFP-alone for Stmn2-overexpression and scrambled siRNA sequences for Stmn2-knockdown. As shown in **Figure 13 a**), the fluorescence signal from GFP-alone diffused across the entirety of the transfected cell, and LAMP1-RFP displayed some fluorescence signals in the cell periphery and some in the intracellular region. Stmn2-GFP overexpression caused almost complete colocalization with LAMP1-RFP in the intracellular region, with almost no fluorescence in the cell periphery (**Figure 13 b**). After transfection with scrambled siRNA-transfected cells, LAMP1-RFP displayed some fluorescence signals in the cell periphery and some in the intracellular region (**Figure 13 c**). In contrast, Stmn2-knockdown resulted in LAMP1-RFP exclusively in the cell periphery (**Figure 13 d**).

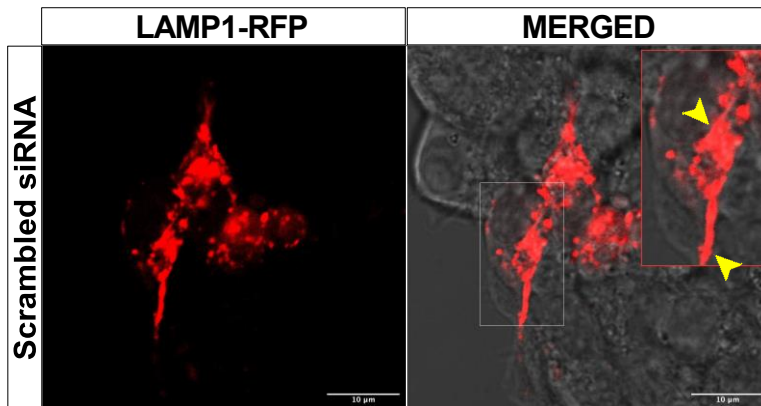
a)



b)



c)



d)

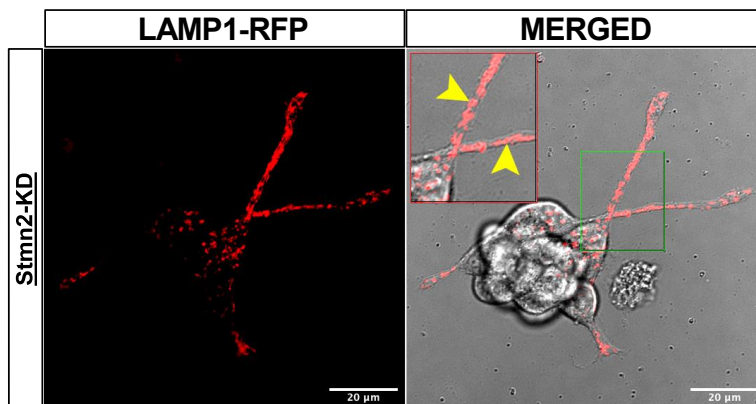
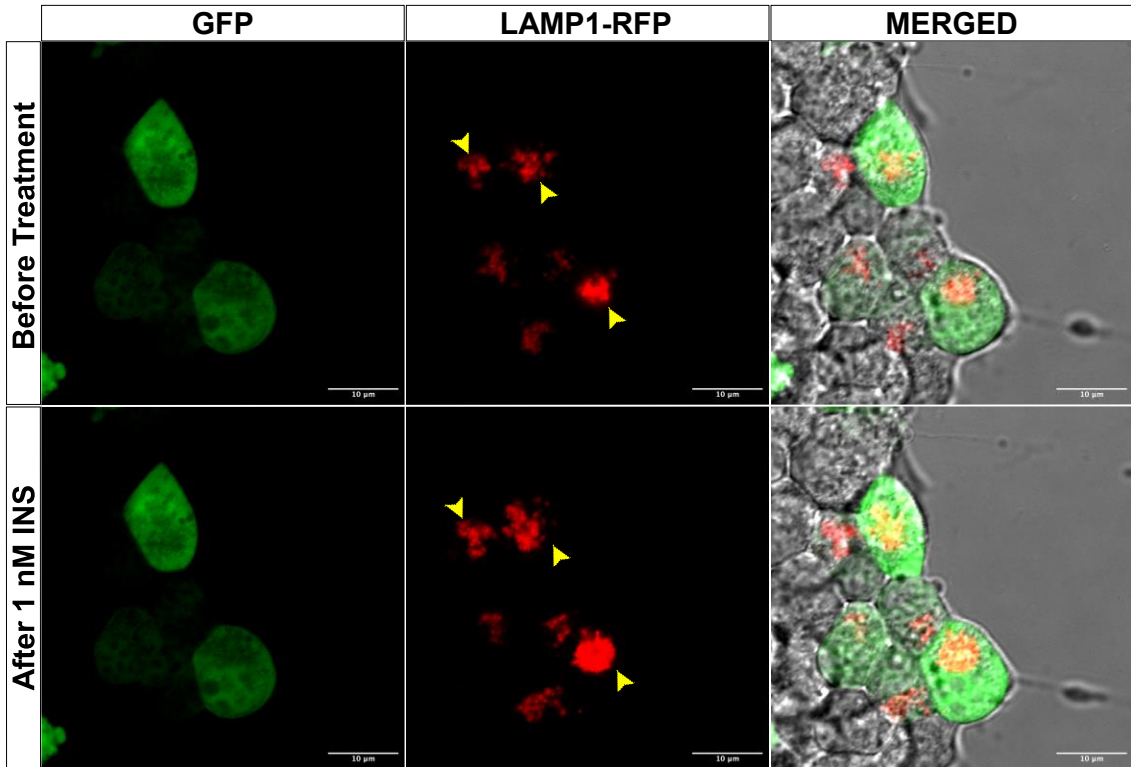


Figure 13. Live imaging of LAMP1-RFP in response to *Stmn2* overexpression (OE) or knockdown (KD). Cells (n=3) were transfected with 40 nM plasmids or siRNAs overnight, and live images were captured 24 hours post-transfection. a) LAMP1-RFP is present in the cell periphery and the intracellular region (yellow arrowheads) after co-transfection with GFP-alone as a negative control for *Stmn2*-overexpression (OE). b) After co-transfection with *Stmn2*-GFP (OE), LAMP1-RFP appears exclusively in the intracellular region (yellow arrowheads). c) LAMP1-RFP is present in the cell periphery and the intracellular region (yellow arrowheads) after co-transfection with scrambled siRNA sequences as a negative control for *Stmn2*-KD. d) *Stmn2* siRNAs (KD) resulted in LAMP1-RFP exclusively in the cell periphery (yellow arrowheads).

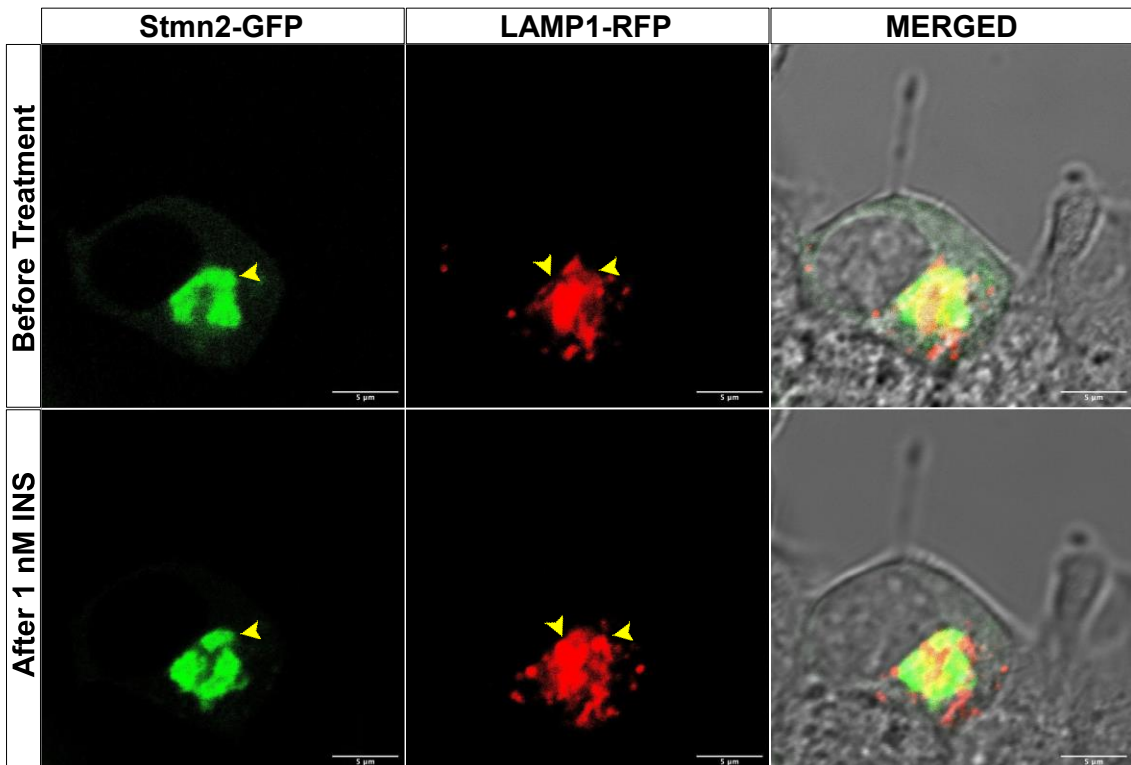
3.6.1 Stmn2-mediated lysosomal network is sensitive to paracrine factors

Upon observing the change in lysosomal distribution after knockdown or overexpression of Stmn2, I investigated the effects of insulin and somatostatin on lysosomal dynamics after Stmn2 knockdown or overexpression to determine the role of Stmn2 in paracrine inhibition of glucagon trafficking via the lysosomal network. As previously, negative controls were GFP-alone for Stmn2-overexpression and scrambled siRNA sequences for Stmn2-knockdown. In **Figure 14 a**), the fluorescence intensity of LAMP1-RFP in the intracellular region increased in response to 1 nM insulin treatment after the co-transfection with GFP-alone. Stmn2-GFP overexpression caused almost complete colocalization with LAMP1-RFP in the intracellular region and did not redistribute in response to 1 nM insulin (**Figure 14 b**). In **Figure 14 c**), LAMP1-RFP fluorescence in the cell periphery reduced while the fluorescence in the intracellular region increased in response to 1 nM insulin after the co-transfection with scrambled siRNA sequences. This change in the lysosomal redistribution in response to 1 nM insulin was captured frame-by-frame over the span of 15 seconds post-treatment (**Figure 15**). In contrast, Stmn2-knockdown resulted in LAMP1-RFP exclusively in the cell periphery, and there was no redistribution in response to 1 nM insulin treatment (**Figure 14 d**). Lastly, the co-transfection of GFP-alone and LAMP-RFP was repeated in the presence of 10 nM insulin receptor antagonist, and there was no redistribution of lysosomes in response to 1 nM insulin (**Appendix Figure 3**).

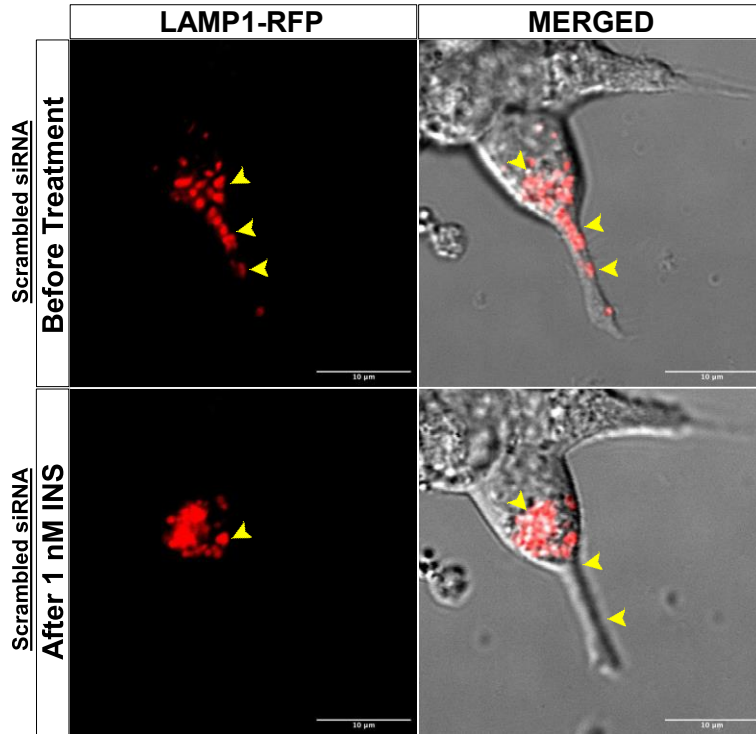
a)



b)



c)



d)

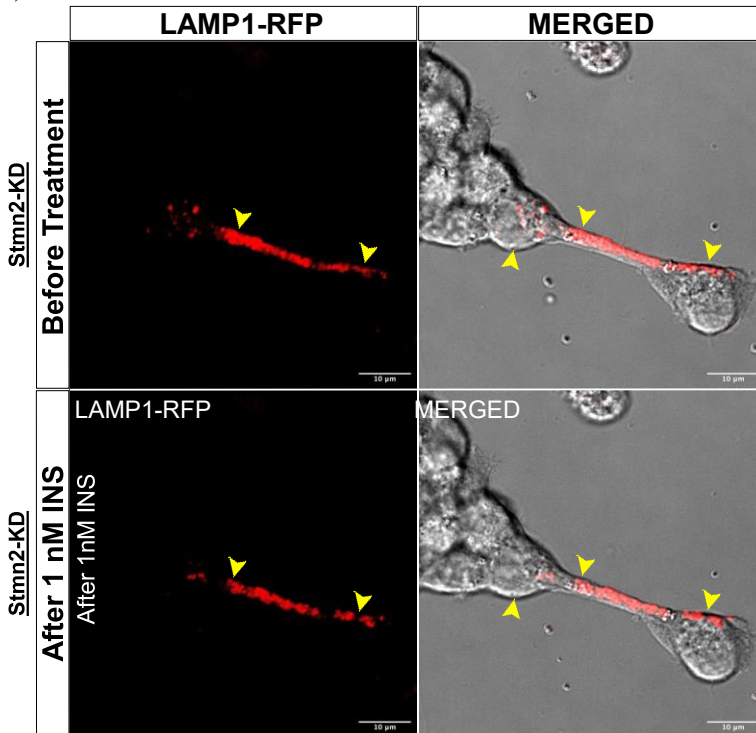


Figure 14. Live imaging of LAMP1-RFP in response to 1 nM insulin in cells with *Stmn2* overexpression (OE) or knockdown (KD). Cells (n=1) were transfected overnight, and live cell images were captured 24 hours post-transfection. Images were captured in the same cell before, during, and five minutes after treatment with 1 nM insulin. a) LAMP1-RFP intensity increased intracellularly in response to 1 nM insulin treatment after co-transfection with GFP-alone, as the negative control for *Stmn2*-overexpression (OE) (yellow arrowheads). b) *Stmn2*-GFP(OE) colocalized with LAMP1-RFP exclusively in the intracellular region before and after 1 nM insulin treatment (yellow arrowheads). c) LAMP1-RFP redistributed intracellularly in response to 1 nM insulin treatment after co-transfection with scrambled siRNA sequences, as a negative control for *Stmn2*-KD (yellow arrowheads). d) *Stmn2* siRNAs (KD) resulted in LAMP1-RFP exclusively in the cell periphery before and after 1 nM insulin treatment (yellow arrowheads).

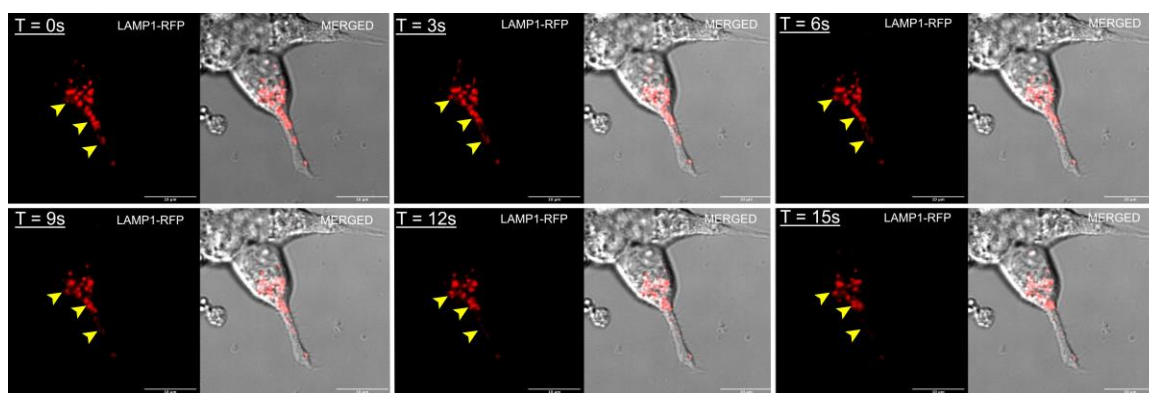
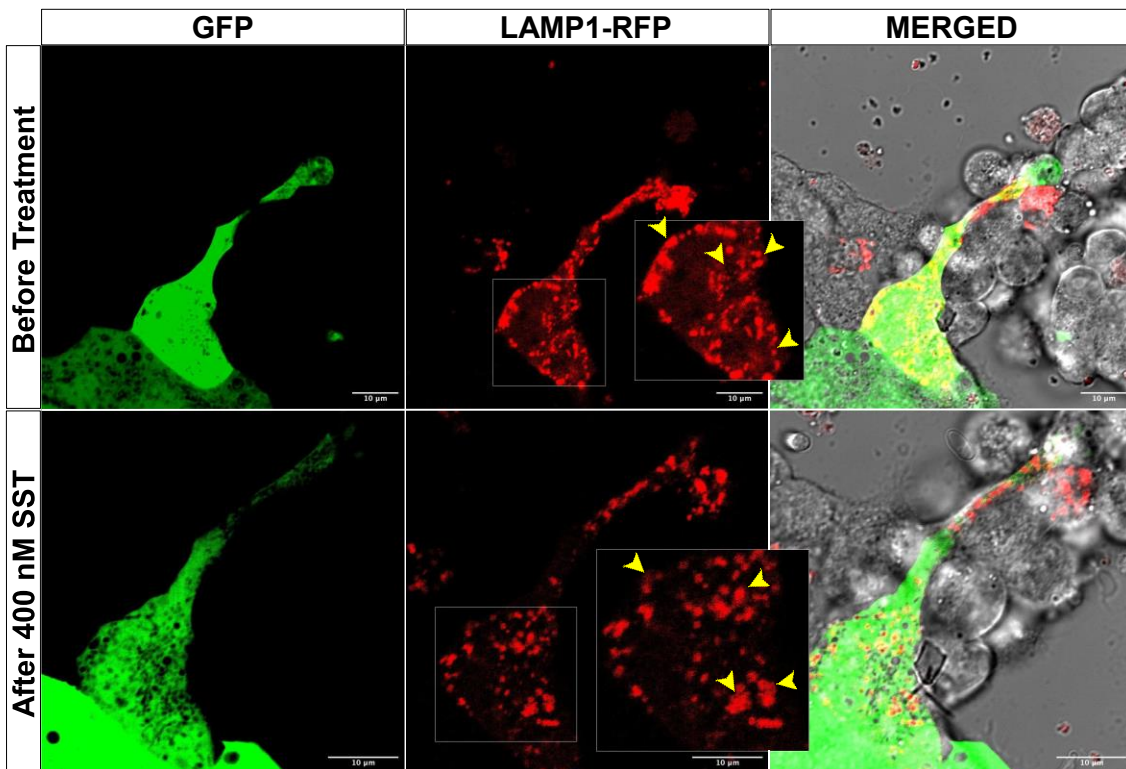


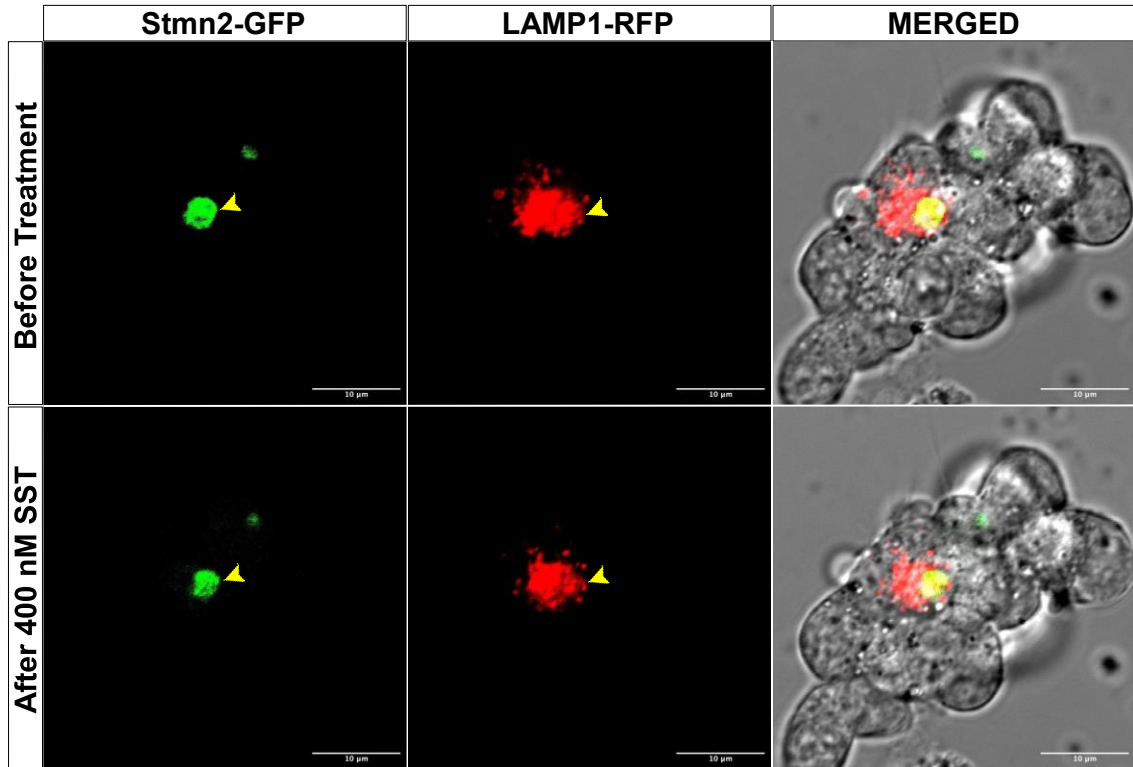
Figure 15. Temporal changes in lysosomal dynamics upon 1 nM insulin treatment. Frame-by-frame capture (3s/ frame for 15s) of image in Figure 14 c) illustrates the immediate response of lysosomal redistribution in response to insulin (yellow arrowheads).

Likewise, treatment of alpha TC1-6 cells with 400 nM somatostatin elicited similar responses of lysosomal trafficking (**Figure 16**). LAMP1-RFP redistributed towards the intracellular region upon treatment with somatostatin (**Figure 16 a**). Upon overexpressing *Stmn2* (**Figure 16 b**), the LAMP1-RFP fluorescence signal remained in the intracellular region and did not change upon treatment with 400 nM somatostatin. In **Figure 16 c**), the co-transfection of scrambled siRNA sequences and LAMP1-RFP showed LAMP1-RFP redistribution intracellularly upon 400 nM somatostatin treatment. Lastly, upon knocking down *Stmn2* (**Figure 16 d**), LAMP1-RFP was exclusively in the cell periphery, and no change in distribution pattern was observed after 400 nM somatostatin treatment.

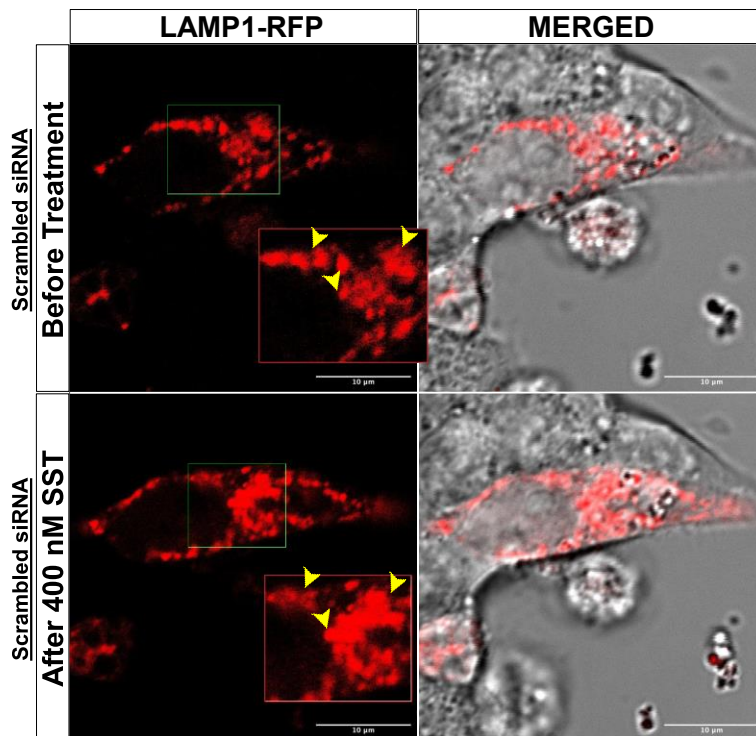
a)



b)



c)



d)

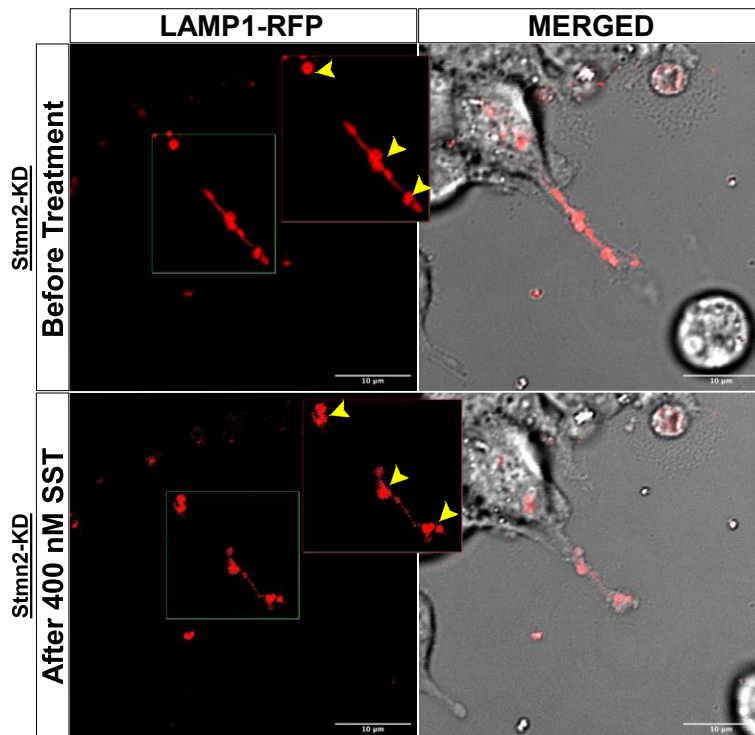
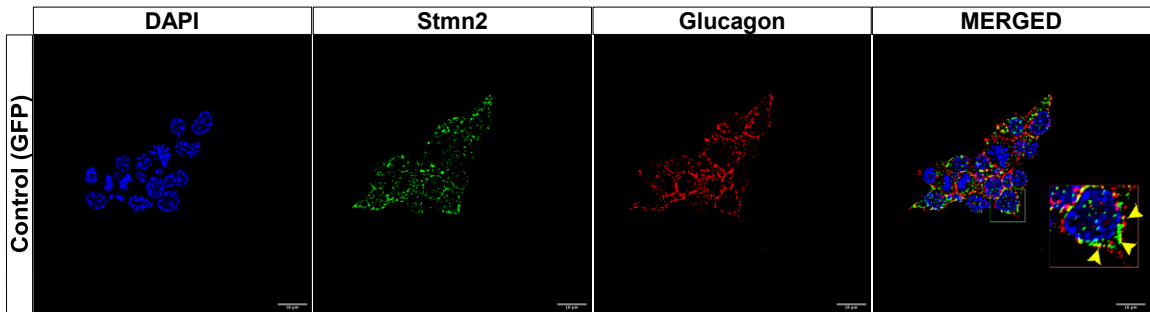


Figure 16. Live imaging of LAMP1-RFP in response to somatostatin in cells with *Stmn2* overexpression (OE) or knockdown (KD). Cells (n=1) were transfected overnight, and live cell images were captured 24 hours post-transfection. Images were captured in the same cell before, during, and five minutes after treatment with 400 nM somatostatin. a) LAMP1-RFP redistributed intracellularly in response to 400 nM somatostatin after co-transfection with GFP-alone, as the negative control for *Stmn2*-overexpression (OE) (yellow arrowheads). b) *Stmn2*-GFP(OE) colocalized with LAMP1-RFP exclusively in the intracellular region before and after 400 nM somatostatin (yellow arrowheads). c) LAMP1-RFP redistributed intracellularly in response to 400 nM somatostatin after co-transfection with scrambled siRNA sequences, as a negative control for *Stmn2*-KD (yellow arrowheads). d) *Stmn2* siRNAs (KD) resulted in LAMP1-RFP exclusively in the cell periphery before and after 400 nM somatostatin (yellow arrowheads).

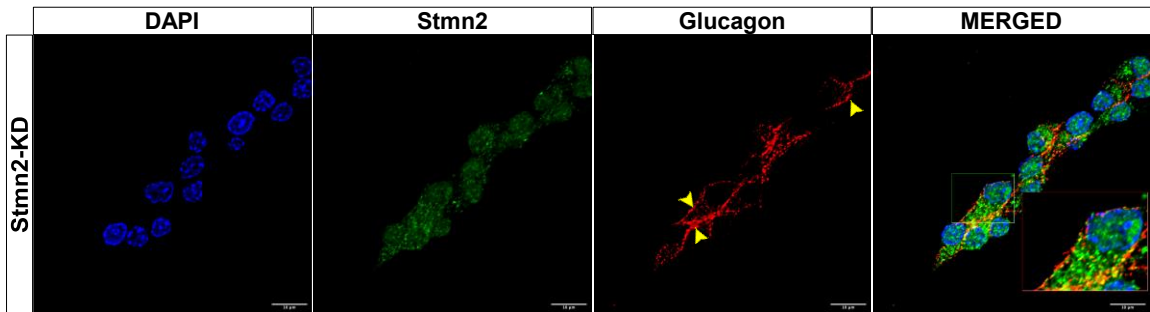
3.7 Stmn2 mediates the intracellular trafficking of glucagon

This fixed-cell experiment quantified the intracellular distribution of glucagon in response to Stmn2 overexpression or knockdown. GFP-alone transfection was the negative control for Stmn2-GFP(OE) and Stmn2 siRNAs (KD). Across **Figure 17 a), b), and c)**, the channels showed the relative fluorescence intensity of Stmn2 across treatments, with Stmn2-KD showing the least amount of fluorescence signal. In contrast, Stmn2-OE showed the strongest signal while distributing mainly in the intracellular region. Glucagon remained mostly in the cell periphery in the control (**Figure 17 a)** and the Stmn2-KD model (**Figure 17 b)**. In the Stmn2-OE model, glucagon was localized to the intracellular region with Stmn2 (**Figure 17 c)**. Quantitatively, the integrated fluorescence intensity of the knockdown model was significantly lower than the control ($p < 0.0001$). In contrast, Stmn2-GFP fluorescence in the overexpression model was significantly higher than the control ($p < 0.01$) (**Figure 17 d)**. In **Figure 17 e)**, plot profile analysis showed that in control cells, most glucagon was in the periphery, around 2.7 times the amount of glucagon in the intracellular region ($p < 0.0001$). Upon Stmn2-knockdown, the fluorescence intensity of glucagon in the intracellular region decreased significantly ($p < 0.05$) compared to the control, by approximately 64%. Upon Stmn2 overexpression, glucagon fluorescence intensity was about 2.1 folds higher in the intracellular region than in the cell periphery ($p < 0.0001$).

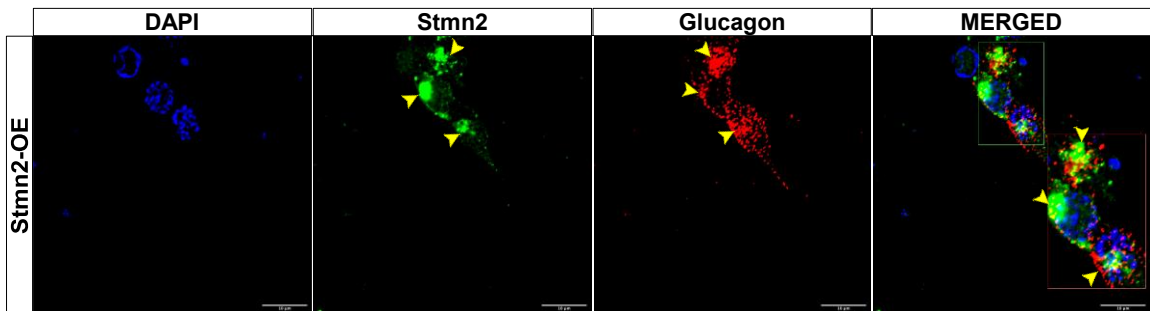
a)



b)



c)



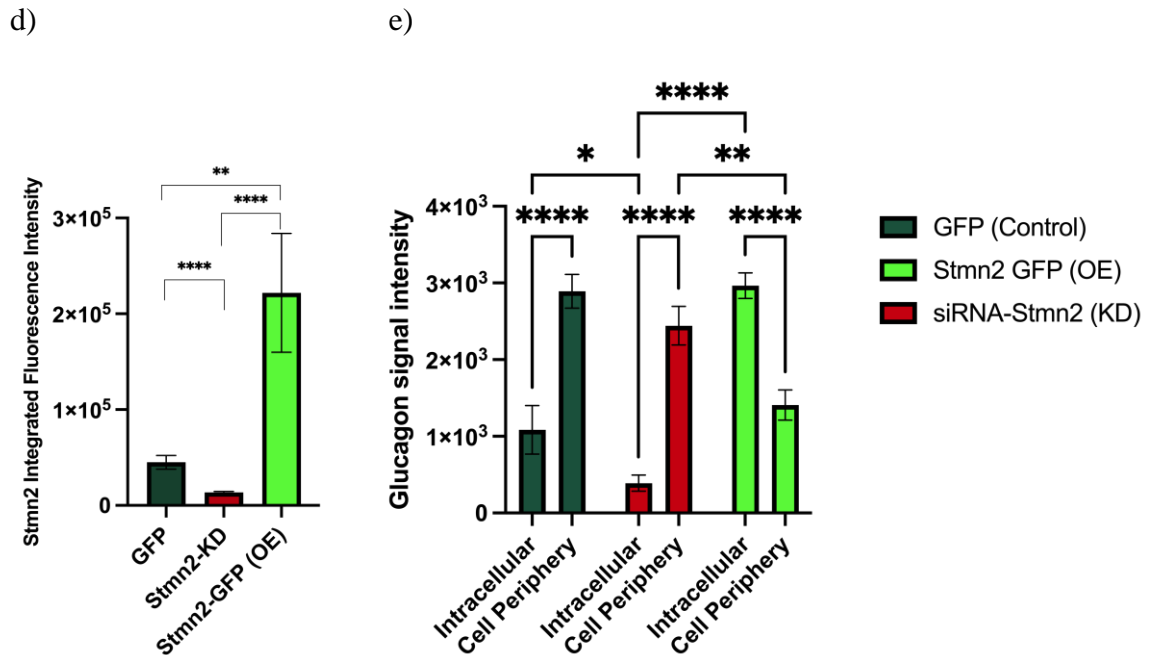
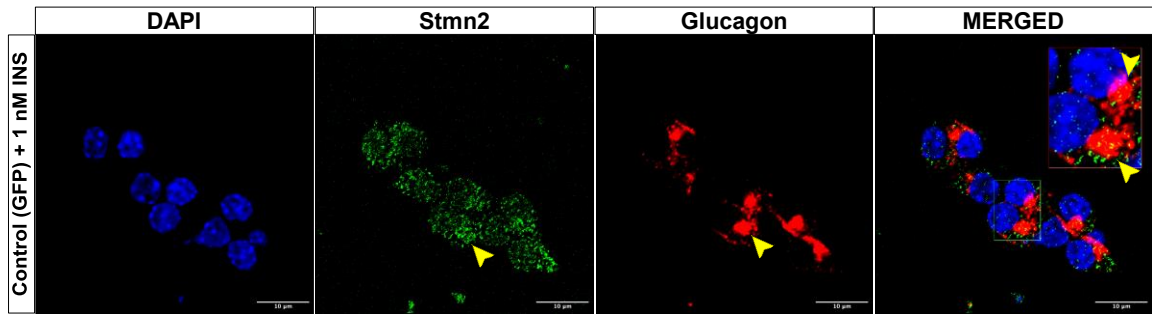


Figure 17. Fixed-cell immunostaining showing glucagon distribution changes in response to Stmn2-GFP (OE) and Stmn2 siRNAs (KD). Cells were transfected overnight and cultured in 25 mM glucose media, with GFP-alone as the visible negative control. Cells were then immunostained using primary antibodies against Stmn2 and glucagon. a) Cells transfected with just GFP resulted in a normal Stmn2 (green) distribution pattern with a majority of glucagon (red) in the cell periphery. b) The Stmn2-KD model diminished Stmn2 fluorescence and resulted in most glucagon in the periphery. c) The Stmn2-OE model increased Stmn2 fluorescence intensity while colocalizing strongly with glucagon in the intracellular region. d) Changes in integrated Stmn2 fluorescence intensity in the Stmn2-KD and OE compared to the control (GFP-alone). Values were expressed as average integrated fluorescence intensity \pm SEM (n=6) and compared among groups using a one-way ANOVA, followed by a post-hoc test ($\alpha = 0.05$). e) Glucagon distribution in response to Stmn2-KD (red bars) and OE (green bars) with values expressed as average glucagon fluorescence intensity \pm SEM (n=6), compared among groups and cellular regions using a two-way ANOVA, followed by a post-hoc test ($\alpha = 0.05$). * $p < 0.05$. ** $p < 0.01$, *** $p < 0.001$, **** $p < 0.0001$.

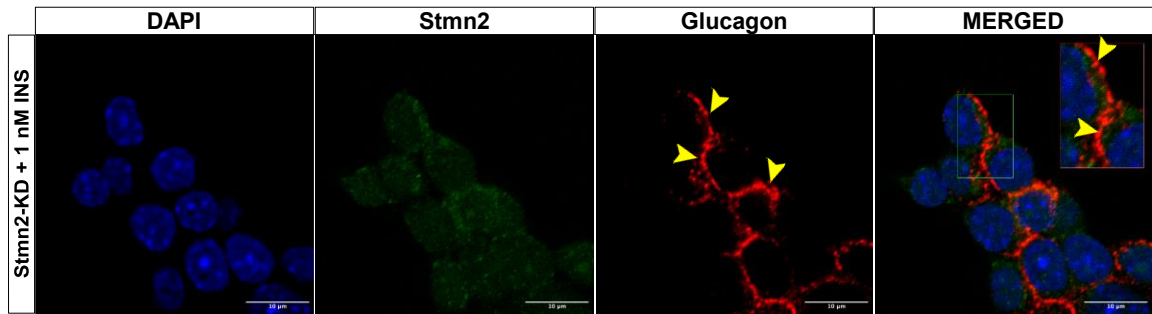
3.7.1 Insulin directs lysosomal trafficking of glucagon in a Stmn2-dependent manner

In this fixed-cell imaging experiment, Stmn2 was overexpressed or silenced, and cells were treated with 1 nM insulin for 24 h. The distribution of glucagon was quantified using previously defined cellular regions. GFP-alone transfection was the negative control for Stmn2-GFP (OE) and Stmn2 siRNAs (KD). Glucagon distribution in the fluorescence images showed a majority of glucagon in the intracellular region in the control and the Stmn2-OE model, while glucagon remained mainly in the periphery in the Stmn2-KD model upon treatment with 1 nM insulin, as shown in **Figure 18 a), b) and c)**. Quantitatively, plot profile analysis (**Figure 18 e)** showed that insulin treatment significantly shifted the distribution of glucagon from the periphery to the intracellular region ($p < 0.0001$), where glucagon fluorescence intensity was 57% higher in the intracellular region compared to the cell periphery. This glucagon distribution pattern did not change upon Stmn2-GFP (OE). However, insulin treatment did not appear to override the effects of Stmn2-KD, as glucagon fluorescence intensity in the cell periphery was significantly ($p < 0.0001$) higher compared to the intracellular region by approximately 2.7 folds, a pattern consistent from the previous experiment in the absence of insulin (**Figure 17 e)**.

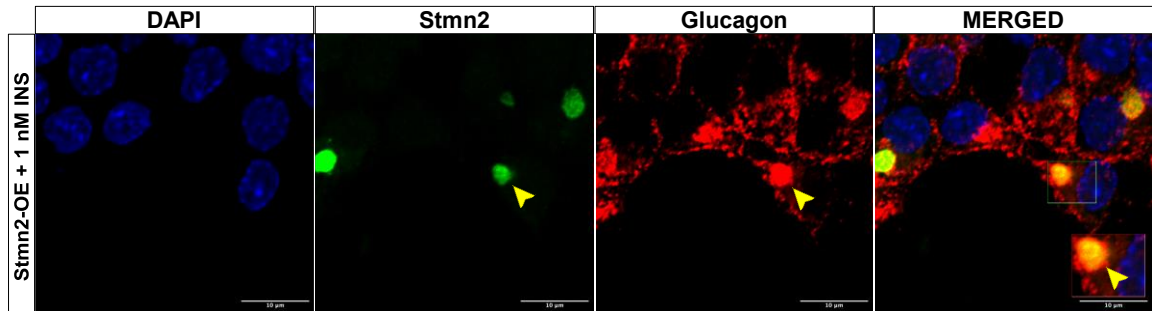
a)



b)



c)



d)

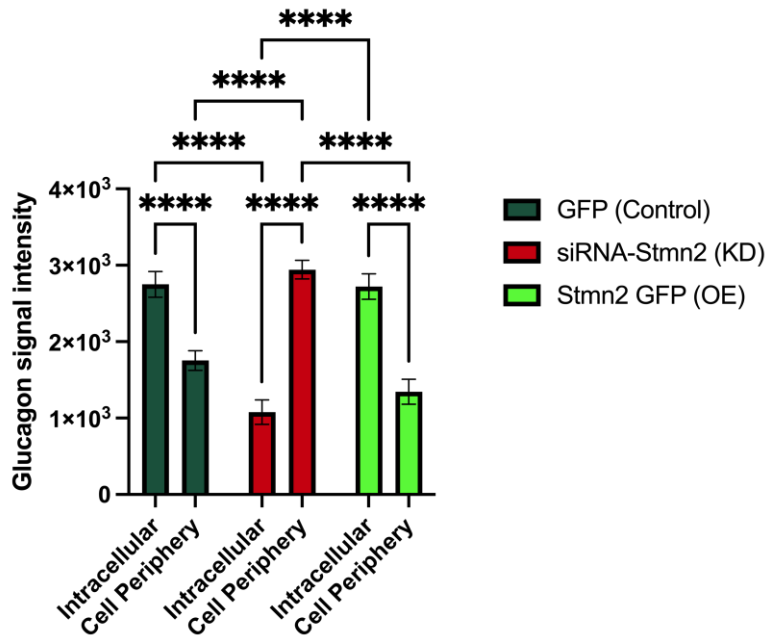
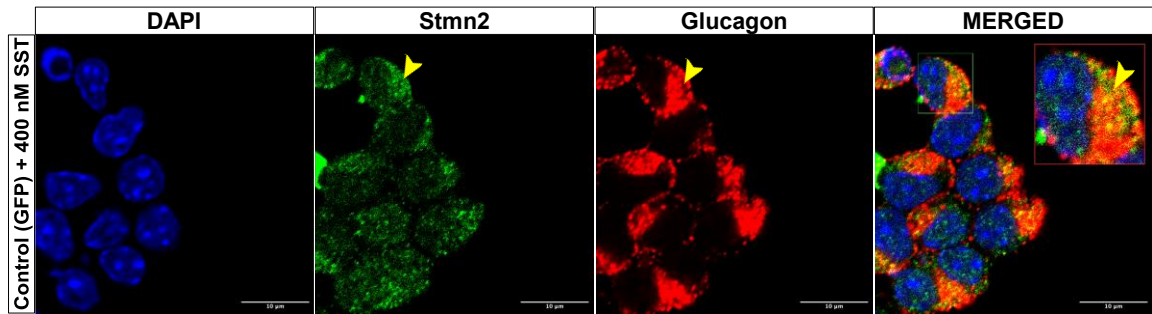


Figure 18. Fixed-cell immunostaining showing glucagon distribution changes in the presence of 1 nM insulin in cells with Stmn2-GFP (OE) and Stmn2 siRNAs(KD). Cells were transfected, recovered in 25 mM glucose media overnight, and treated with 1 nM insulin for 24 hours. Cells were then immunostained using primary antibodies against Stmn2 and glucagon. a) Cells transfected with just GFP and treated with 1 nM insulin resulted in Stmn2 (green) and glucagon (red) redistributing intracellularly. b) The Stmn2-KD model diminished Stmn2 fluorescence and resulted in glucagon in the periphery, even after 1 nM insulin treatment. c) The Stmn2-OE model increased Stmn2 fluorescence intensity and colocalized strongly with glucagon in the intracellular region after 1 nM insulin treatment. d) Glucagon distribution in response to Stmn2-KD (red bars) and OE (green bars) with values expressed as average glucagon fluorescence intensity \pm SEM (n=6), compared among groups and cellular regions using a two-way ANOVA, followed by a post-hoc test ($\alpha = 0.05$). ****p<0.0001.

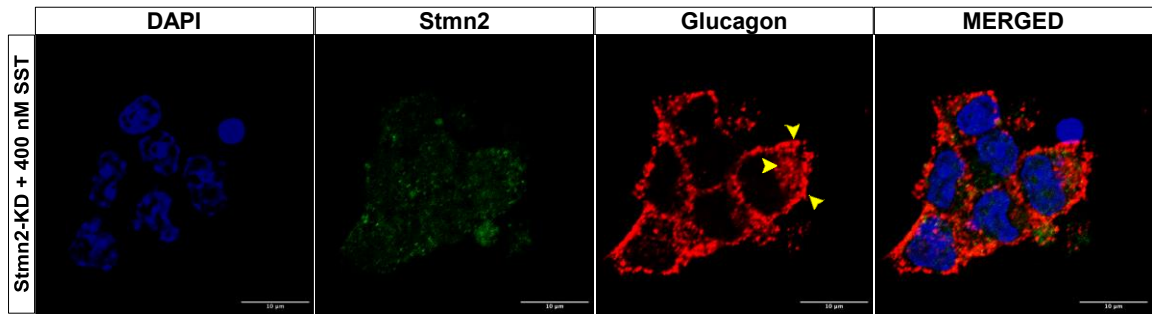
3.7.2 Somatostatin directs lysosomal trafficking of glucagon in a Stmn2-dependent manner

In this fixed-cell imaging experiment, Stmn2 was overexpressed or silenced, and cells were treated with 400 nM somatostatin for 24 h. The distribution of glucagon was quantified using previously defined cellular regions. GFP-alone transfection was the negative control for Stmn2-GFP (OE) and Stmn2 siRNAs (KD). Glucagon distribution in the fluorescence images also showed a majority of glucagon in the intracellular region in the control and the Stmn2-OE model, while glucagon remained mainly in the periphery in the Stmn2-KD model upon treatment with 400 nM somatostatin, as shown in **Figure 19 a), b) and c)**. Quantitatively, plot profile analysis (**Figure 18 e)** showed that somatostatin treatment significantly shifted the distribution of glucagon from the periphery to the intracellular region ($p < 0.01$), where glucagon fluorescence intensity was 37% higher in the intracellular region compared to the cell periphery. Stmn2-GFP(OE) also showed glucagon redistribution intracellularly ($p < 0.0001$) in response to somatostatin and a significant reduction ($p < 0.01$) in glucagon fluorescence intensity in the periphery compared to the control by approximately 42%. Somatostatin treatment did not appear to override the effects of Stmn2-KD, as glucagon fluorescence intensity in the cell periphery was significantly ($p < 0.0001$) higher compared to the intracellular region by approximately 2.7 folds, a pattern consistent from the previous experiments in the absence and presence of insulin.

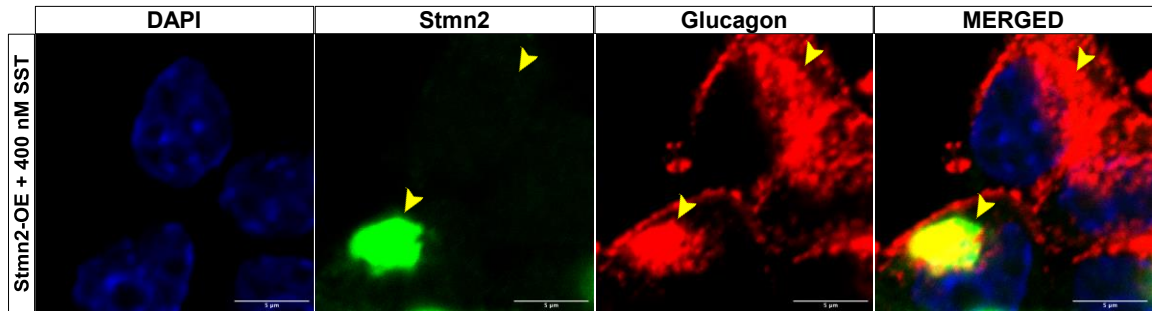
a)



b)



c)



d)

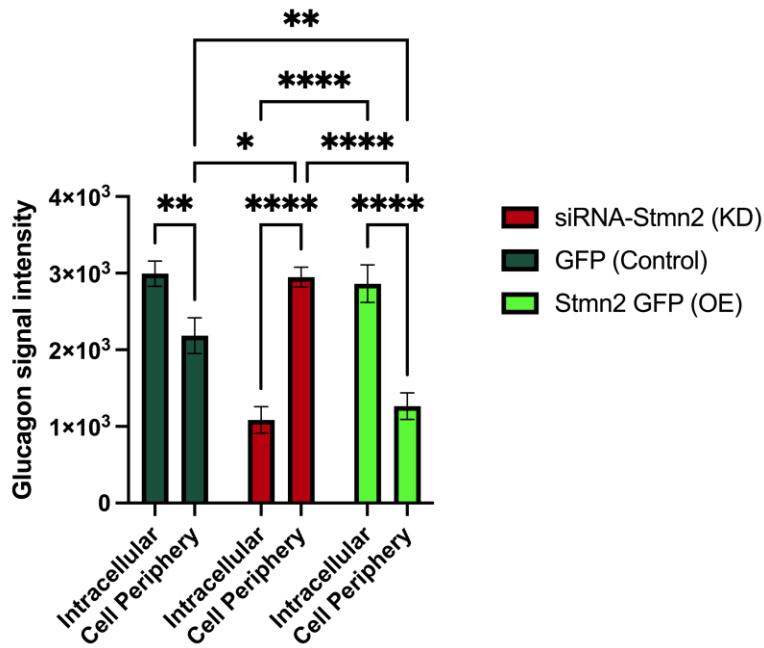
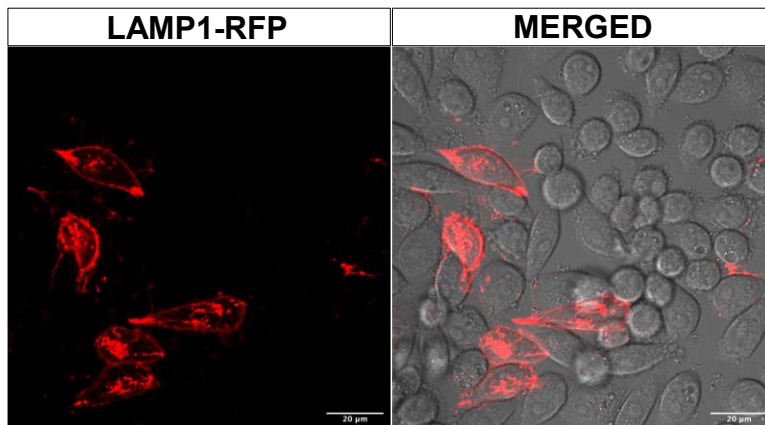


Figure 19. Fixed-cell immunostaining showing glucagon distribution changes in the presence of 400 nM somatostatin in cells with Stmn2-GFP (OE) and Stmn2 siRNAs(KD). Cells were transfected, recovered overnight in 25 mM glucose media, and treated with 400 nM somatostatin for 24 hours. Cells were then immunostained using primary antibodies against Stmn2 and glucagon. a) Cells transfected with just GFP and treated with 400 nM somatostatin resulted in Stmn2 (green) and glucagon (red) distributing mostly in the intracellular region. b) The Stmn2-KD model diminished Stmn2 fluorescence intensity, and most glucagon remained in the periphery, even after 400 nM somatostatin treatment. c) The Stmn2-OE model increased Stmn2 fluorescence intensity while colocalizing strongly with glucagon in the intracellular region after 400 nM somatostatin treatment. d) Glucagon distribution in response to Stmn2-KD (red bars) and OE (green bars) with values expressed as average glucagon fluorescence intensity \pm SEM (n=6) and compared among groups and cellular regions using a two-way ANOVA, followed by a post-hoc test ($\alpha = 0.05$). *p<0.05. **p<0.01, ****p<0.0001.

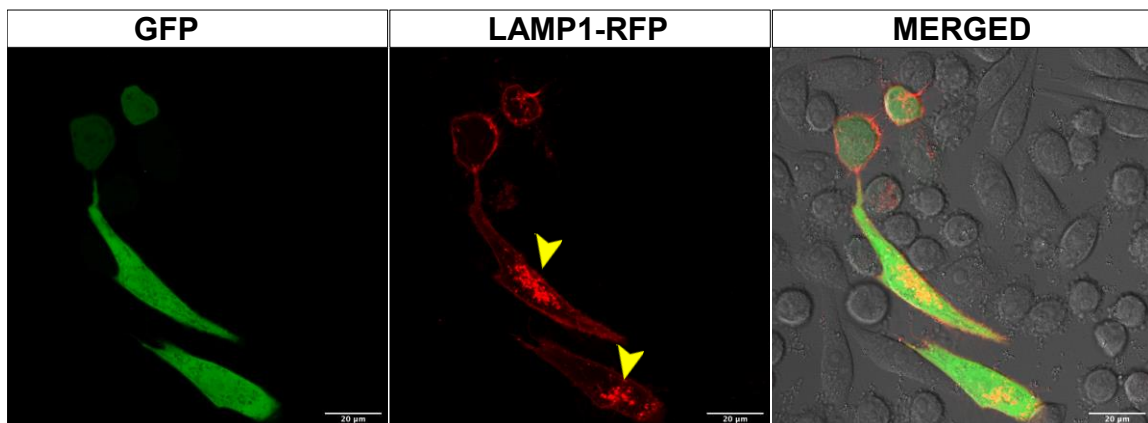
3.8 A novel human alpha-like cell line expresses Stmn2-GFP and LAMP1-RFP similarly to mouse pancreatic α TC1-6 cells

The experiments in this body of work have shown that the fluorescent reporters Stmn2-GFP and LAMP1-RFP allowed for live visualization of the spatial dynamics of lysosomal trafficking in response to paracrine factors. Since all my experiments have been conducted in a mouse cell line, I sought to replicate some of my findings in a novel human pancreatic alpha-like cell line. In **Figure 20 a**), transfection of LAMP1-RFP alone human alpha-like cell line showed a typical LAMP1 distribution, in which lysosomes primarily distributed in the intracellular region with some in the cell periphery. Upon co-transfection of GFP, LAMP1-RFP showed an unchanged pattern (**Figure 20 b**). However, upon co-transfection with Stmn2-GFP, LAMP1-RFP showed very strong colocalization in the intracellular region (**Figure 20 c**) with some RFP fluorescence in the cell periphery.

a)



b)



c)

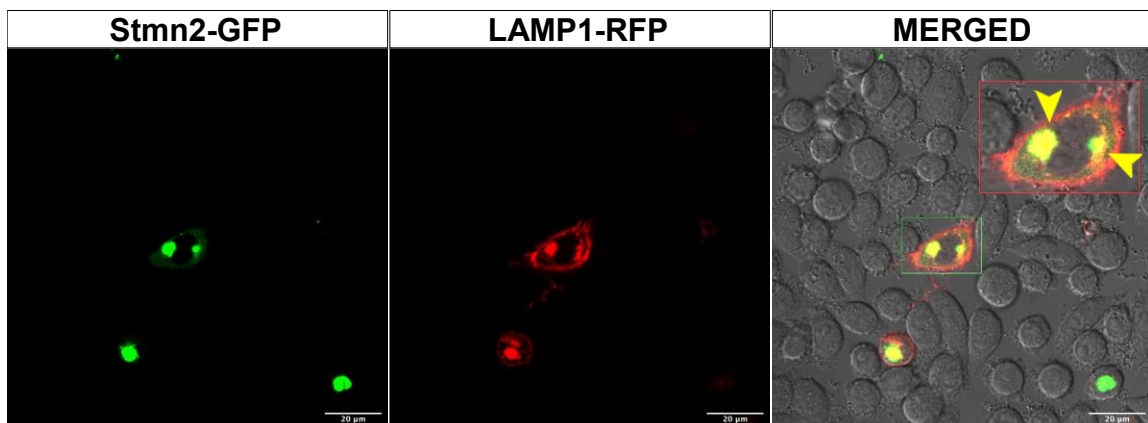


Figure 20. Human pancreatic alpha-like cells express LAMP1-RFP and Stmn2-GFP in patterns similar to α TC1-6 cells. Cells (n=1) were transfected similarly to α TC1-6 cells and imaged 24 hours post-transfection. a) Human alpha-like cells transfected with only LAMP1-RFP,

display fluorescence in the intracellular region and cell periphery the typical LAMP1 distribution pattern. b) LAMP1-RFP co-transfected with GFP-alone as a negative control for Stmn2-overexpression (OE) displays the same LAMP1-RFP distribution pattern as in a). c) LAMP1-RFP co-transfected with Stmn2-GFP(OE) shows strong co-localization in the intracellular region, while LAMP1-RFP alone is detected in the cell periphery.

Chapter 4

4 Discussions and Future Direction

Diabetes mellitus is a condition characterized by dysregulated glycemia resulting from excess glucagon secretion and insulin deficiency. Current disease management involves exogenous insulin administration (T1DM), drugs enhancing insulin secretion or sensitivity (T2DM), and closely monitoring blood glucose levels. However, there is no cure for diabetes mellitus to date, and the dysfunctions of islet cell types other than the β cell contributing to the disease progression have been heavily overlooked. To better understand the development and control of hyperglycemia, glucagon-secreting alpha cells need to be studied intricately, as glucagon is the major glucose counterregulatory hormone. Understanding the regulation of glucagon secretion could open new doors for therapeutics that target excess glucagon secretion, thus better controlling hyperglycemia. In the work described in this thesis, I sought to characterize *Stmn2* as a regulator of glucagon trafficking through the lysosomal network during paracrine regulation in α TC1-6 cells. In doing so, my work may lead to a therapeutic target that increases glucagon trafficked towards the lysosomes to reduce excess glucagon secretion and, in turn, alleviate hyperglucagonemia and in turn hyperglycemia of diabetes.

The main objectives were 1. To investigate paracrine regulation of glucagon secretion in relation to *Stmn2* and cellular compartment markers in α TC1-6 cells by immunofluorescence microscopy; 2. To determine how *Stmn2* affects lysosomal biogenesis in α TC1-6 cells using immunofluorescence microscopy and qPCR; and 3. To determine if paracrine factors inhibit glucagon secretion by *Stmn2*-dependent lysosomal trafficking using live-cell imaging.

4.1 Measurement of overall glucagon levels masked treatment effects due to heterogeneity in cell circadian phase, secretion capacity and inhibition

My results showed inconsistent glucagon secretion responses to different glucose concentrations and insulin and GABA after a 24-hour accumulation period. While K^+ -stimulated secretion was more consistent and prominent over a 15-minute accumulation period, there was no response to insulin and GABA. There are many potential reasons for this discrepancy. The unique dynamics of glucagon secretion may not be well captured at a singular time point, and the heterogeneity of cell accessibility to paracrine treatment and the different cellular phases of individual cells may result in differences in their secretion capacities that were masked when glucagon levels were measured at the population level^{89,90}. In addition, differences in transfection efficiency and cell viability across *Stmn2*-OE and KD samples may have also contributed to the inconsistency of overall secreted glucagon levels, which have contradicted my hypothesis and my immunofluorescence data showcasing glucagon at the cell membrane and potentially ready for exocytosis in the *Stmn2*-KD model and glucagon in lysosomes and potentially not available for exocytosis in the *Stmn2*-OE model. A study that compared the dynamics of glucagon secretion in alpha cells and insulin secretion in β cells of isolated human islets found that glucagon secretion responds to changes in glucose concentration and not the absolute glucose levels, unlike insulin⁹⁰. Glucagon's autocrine signalling capacity and its more dominant electrophysiological properties allow its secretion to be much more robust and transient, which is needed in a hypoglycemic emergency^{38,90}. As a result, glucagon secretion in a constant glucose concentration in response to a 24-hour treatment in my secretion experiments may have resulted in a heterogeneity of cells of those transiently inhibited and those that have desensitized to the treatment over the incubation time. In addition, the surface available for the cell-to-cell and cell-to-environment interactions differs depending on the growth of a subpopulation and the location of cells within the clustered population⁹¹. Specifically, cells near the center of a clustered population have more of their surface in contact with neighboring cells, leaving less surface available for access to treatment than those in the periphery and those growing more independently. Heterogeneity also exists in the cellular phase the individual cells

are in at the time of media collection, which impacts their secreting capacity. A study conducted temporal transcriptional profiling of rodent islets and found individual β cells to display distinct phases of either cell growth and repair or maximal insulin synthesis and secretion, regulated by circadian clock genes^{89,92}. Interestingly, these oscillating phases of either cell growth and repair or secretion are found in human pancreatic islets and dispersed human islet cells, suggesting self-sustaining circadian rhythms even in individual cultured cells⁹³. Given that heterogeneity lies in accessibility to treatment, transfection efficiency, cell viability, and the cellular phase that alters their sensitivity to treatment and secretion capacity, measuring overall secreted glucagon levels was confounded by many variables and may not be able to capture the true secretory response to our treatment. A study concerning cellular heterogeneity stated, “Ensemble-averaged measurements can mask information contained in heterogeneity, and decompositions of heterogeneity may be tested for functionally important information.”⁷⁴. As a result, we shifted focus to immunofluorescence microscopy to visualize, identify and analyze individual cells with the dominant phenotype, understanding that heterogeneity exists. In addition, immunofluorescence microscopy allowed us to eliminate some heterogeneity or confounding variables in measuring regulated glucagon trafficking. Specifically, we excluded highly confluent and clustered cells with potentially unequal access to treatment, cells of the minor phenotype, and unsuccessfully transfected cells in our transfection experiments. Lastly, microscopy allowed us to visualize the spatial localization of glucagon in specific cellular compartments, revealing information about glucagon trafficking and possibly exocytosis at the single-cell level.

4.2 Paracrine factors affect glucagon trafficking to lysosomes via Stmn2

Studies have performed colocalization analysis on LAMP1 and glucagon as a measure of glucagon crinophagy in α TC9 cells using the Pearson Correlation Coefficient, validated by western blot⁶². I developed another type of colocalization analysis that quantified two proteins' colocalized signal intensity and intracellular distribution, thereby revealing information on trafficking between associated cytoplasmic compartments⁸⁵. Specifically, my results showed that paracrine treatment of insulin and GABA or somatostatin alone increased the colocalization intensity of glucagon and LAMP1 in the intracellular region. These results suggested that the inhibitory effects of insulin/GABA or somatostatin on glucagon secretion may operate through lysosomes⁶². Interestingly, paracrine factors also reduced the amount of colocalized glucagon and Stmn2 in the cell periphery and increased the amount of colocalized glucagon and Syntxin1A in the intracellular region, potentially suggesting that glucagon at the cell periphery along with exocytotic proteins were trafficked in the retrograde direction by Stmn2 along the secretory pathway. By using previously defined cellular regions and colocalizing glucagon and multiple cellular markers, I showed that the paracrine factors insulin/GABA and somatostatin induced glucagon crinophagy. Nevertheless, it was important to determine that Stmn2 is, in fact, involved in the lysosomal network and has a direct influence on paracrine-induced crinophagy. I therefore examined glucagon and lysosome distribution in response to insulin/GABA or somatostatin after Stmn2-OE or siRNA-mediated Stmn2 KD.

Stmn2 overexpression redistributed glucagon intracellularly, and the pattern remained unchanged upon treatment with insulin and somatostatin. This intracellular redistribution by overexpressing Stmn2 was similar to the control treated with insulin or somatostatin, suggesting a potential overlap of functions between Stmn2 and paracrine factors in trafficking glucagon towards the lysosomes. This association was further validated in the Stmn2 knockdown model in which glucagon remained exclusively in the cell periphery with none in the intracellular region. In addition, insulin and somatostatin treatment had no effect on glucagon trafficking to lysosomes after Stmn2 knockdown, suggesting Stmn2 as a regulator in the paracrine redistribution of glucagon towards the lysosomes.

Without *Stmn2*, glucagon remained in the cell periphery for exocytosis without degradation, which may mimic excess glucagon secretion or hyperglucagonemia in diabetes. Most importantly, our glucagon distribution data also aligned with our lab's previous work that showed *Stmn2*-OE abolished K^+ -stimulated glucagon secretion and *Stmn2*-KD increasing basal glucagon secretion in α TC1-6 cells⁶⁹. I found the exact same distribution pattern when I used live-cell imaging to track lysosomal dynamics with LAMP1-RFP in the GFP-transfected, *Stmn2*-overexpressed and knockdown models, such that both insulin and somatostatin redistributed lysosomes intracellularly in the control, but lost the redistribution capacity after *Stmn2* knockdown, suggesting a clear role for *Stmn2* in directing glucagon towards the lysosomes as a function of paracrine inhibition of glucagon secretion. Interestingly, impaired lysosomal functions have also been shown to contribute to β cell failure through stress-induced nascent granule degradation (SINGD), which results in insufficient insulin secretion in T2D⁹⁴. The loss of lysosomal redistribution capacity after *Stmn2* knockdown may indicate a change in functionality or impaired overall function that results in insufficient glucagon degradation and excess secretion.

4.3 Alpha cell membrane protrusions similar to filopodia and neuronal axon

My live-cell imaging showed some α TC1-6 cells displayed neuron-like protrusions, mostly in cells located in the periphery of clusters or in individual cells. These pancreatic endocrine cell protrusions have been found to be important structures for overall islet assembly in Zebrafish (*Danio rerio*) islets, such that these protrusions may be analogous to epithelial filopodia as exploratory structures in mediating cell recognition and adhesion^{95,96}. Filopodia are membrane protrusions, typically regulated by cytoskeletal mechanisms, which have also been found to be important in neuronal development and differentiation^{96,97}. In Zebrafish islets, when cellular signalling pathways through PI3K and $G\alpha$ and $G\beta\gamma$ components of the G-protein-coupled-receptor (GPCR) involving cell morphology development, motility and cytoskeleton regulation were disrupted, protrusions of pancreatic endocrine cells became minimal and islet cell aggregation

reduced. Nevertheless, we found that once our α TC1-6 cells began to aggregate and started to grow in large clusters, these protrusions typically disappeared, potentially mimicking a later stage in islet development where exploratory cell recognition and adhesions are no longer needed. Why such protrusions were not as common in human pancreatic alpha-like cells remains to be investigated and requires further characterization of the phenotype. Most interestingly, upon transfecting α TC1-6 cells with LAMP1-RFP, I could visualize some peripheral lysosomes clustering in these membrane protrusion regions. These peripheral lysosomes clustered in those regions may possess unique functions such as cellular content clearance to mediate inter-cell recognition during islet development⁹⁶⁻⁹⁹. In neurons, the spatial location of lysosomes is associated with different functionalities, which suggests endocrine cells like alpha cells may also have similar capacities as they highly resemble neurons in their physiology, functions, gene expressions and pathways¹⁰⁰⁻¹⁰³.

4.4 Stmn2 levels alter lysosomal distribution

Upon manipulating *Stmn2* levels using siRNAs and *Stmn2*-GFP, my results showed that the lysosomal abundance and distribution pattern were visibly altered. In the *Stmn2*-knockdown models, most of the lysosomes marked by LAMP1-RFP distributed in the elongated membrane protrusions and near the cell membrane. In contrast, *Stmn2* overexpression models caused LAMP1-RFP to colocalize very strongly with the *Stmn2*-GFP in the intracellular region adjacent to the nucleus at an increased intensity. Most importantly, this strong colocalization between *Stmn2*-GFP and LAMP1-RFP was found in both our mouse-derived α TC1-6 cells and the human pancreatic alpha-like cells, further validating the association between *Stmn2* and lysosomes across models and leading clinical significance to the association. As mentioned, the different patterns in lysosomal distribution may reflect differences in functionality of those lysosomes, commonly seen in neurons, which pancreatic endocrine cells share many similarities with. Specifically, neuronal activity has been shown to induce lysosomal exocytosis by lysosomes fusing with the plasma membrane to release contents specifically in the dendrites and axons, which are morphologically almost identical to the membrane

protrusions we observed in our α TC1-6 cells¹⁰⁴. In addition, lysosomes near the cell periphery have also been found to have reduced acidity (higher pH), reduced RILP density thus reduced RILP recruitment, and impaired proteolytic activity, which supports the heterogeneity in lysosomal distribution and the versatility of lysosomal functions^{100,105}. As a result, lysosomes near the membrane protrusions or the cell periphery found in our *Stmn2*-KD model may be lysosomes with either impaired degradative functions due to reduced acidity or lysosomes bound to fuse with the plasma membrane to release contents such as glucagon. These results were also aligned with our lab's previous work showing evidence of lysosomal exocytosis of glucagon in α TC1-6 cells. Specifically, treating cells with the lysosomal inhibitor, bafilomycin A1, reduced K^+ -stimulated glucagon exocytosis, further suggesting that glucagon can exocytose through the lysosomal compartment near the plasma membrane⁸². Previous work from our lab and my results both supported that *Stmn2*-KD models may mimic diabetes in which degradative lysosomal function is impaired and peripheral secretory lysosomes result in excess secretion of glucagon, which contributes to hyperglucagonemia. On the other hand, *Stmn2*-OE models not only showed strong colocalization between *Stmn2*-GFP and LAMP1-RFP in the intracellular region, where acidity is the highest and most optimal for proteolytic activity but *Stmn2*-OE was also found to upregulate genes involved in autophagy and lysosomal biogenesis and redistribute glucagon towards the intracellular region, validating *Stmn2*'s role in trafficking glucagon to the lysosomal network.

4.5 Stmn2 induces nuclear translocation of TFEB

Autophagy is a general catabolic process which directs cellular materials to the degradative lysosomes to meet energy demand under starvation¹⁰⁶. Nevertheless, nutrient-sensing by the mTORC1 is key in regulating autophagy^{62,107}. Specifically, mTORC1 is activated under nutrient-rich conditions, which inhibits autophagy. On the other hand, mTORC1 is inhibited during starvation, which increases autophagy. Downstream of mTORC1 is a well-characterized key player in lysosomal biogenesis and autophagy, known as transcription factor EB (TFEB)^{108,109}. TFEB is regulated by phosphorylation at its serine residues, typically inactive in the cytoplasm, and localizes to the nucleus for downstream activation of autophagy genes when dephosphorylated¹⁰⁸. The master regulator of TFEB phosphorylation occurs at the lysosomal membrane by mTORC1¹⁰⁸. Under starvation, mTORC1 becomes inactive, leaving the lysosomal membrane to phosphorylate TFEB¹¹⁰. At the same time, mucolipin 1 (MCOLN1), an ion channel that releases lysosomal Ca^{2+} , activates calcineurin phosphatase, which dephosphorylates TFEB into its activation status during starvation or cellular clearance⁸⁸. In addition to meeting metabolic demands, activation of TFEB for downstream mitophagy and autophagy has also been shown to be a key player in maintaining β -cell function during metabolic stress¹⁰⁹.

My results showed that Stmn2 overexpression induced the nuclear translocation of TFEB and the upregulation of MCOLN1 transcripts, suggesting an increased release of lysosomal Ca^{2+} and increased activation of TFEB. In addition, our live-cell imaging experiments showed distinctively increased LAMP1 signal intensity in the intracellular region, perhaps through the redistribution of lysosomes spatially or an actual increase in the number of lysosomes, which had been previously found in models of TFEB overexpression¹¹¹. Studies have also found that by inhibiting the lysosomal nutrient sensor mTORC1, which typically inactivates TFEB, colocalization between LAMP1 and glucagon in α TC9 cells increases while glucagon secretion decreases⁶². This suggests that TFEB, in its activated state, plays a part in the nutrient-sensing mechanism, which regulates glucagon secretion by redistributing glucagon to degradative lysosomes. In addition, given that Stmn2 overexpression increases activation of TFEB, Stmn2, in turn,

must also redistribute glucagon towards the lysosomes and reduce glucagon secretion, which was validated in our glucagon distribution and colocalization experiments. Another transcription factor, TFE3 has been shown more recently to also play a major role in the nutrient-sensing and ER stress pathway in upregulating autophagy-related genes¹¹². TFE3 function is TFEB-independent; however, both TFE3 and TFEB are required for maximal induction of lysosomal biogenesis under starvation^{112,113}. As a result, TFE3, another potential master autophagy regulator, should be investigated in our Stmn2-OE model to complete our understanding of the extent of lysosomal biogenesis in regulating glucagon levels.

4.6 Novel proposed mechanism of insulin and somatostatin resistance of α cells in diabetes

According to the findings I have described in my thesis, I propose that Stmn2 found in the secretory granules of α cells is involved in mediating retrograde trafficking of fused secretory granules and lysosomes near the plasma membrane through changing microtubule dynamics during paracrine-induced glucagon crinophagy. Upon Stmn2-mediated retrograde trafficking of the fused granular-lysosomal compartment, acidity within the compartment increases and becomes optimal for glucagon degradation, as shown in **Figure 21**. Lysosomal biogenesis may be increased by Stmn2 via nuclear translocation of TFEB. Therefore, a possible mechanism for normal paracrine regulation of glucagon secretion may include Stmn2-mediated lysosomal trafficking and biogenesis. Downregulated Stmn2 in diabetes results in insufficient retrograde trafficking, causing the granule-lysosome compartment to remain at the periphery with insufficient acidification for optimal proteolytic activity. Due to their localization, these compartments result in glucagon secretion into the extracellular space, exacerbating hyperglucagonemia. In addition, disrupting the paracrine inhibition of glucagon secretion through the Stmn2-mediated lysosomal pathway may be a novel mechanism in which insulin and somatostatin resistance of α cells develop in diabetes.

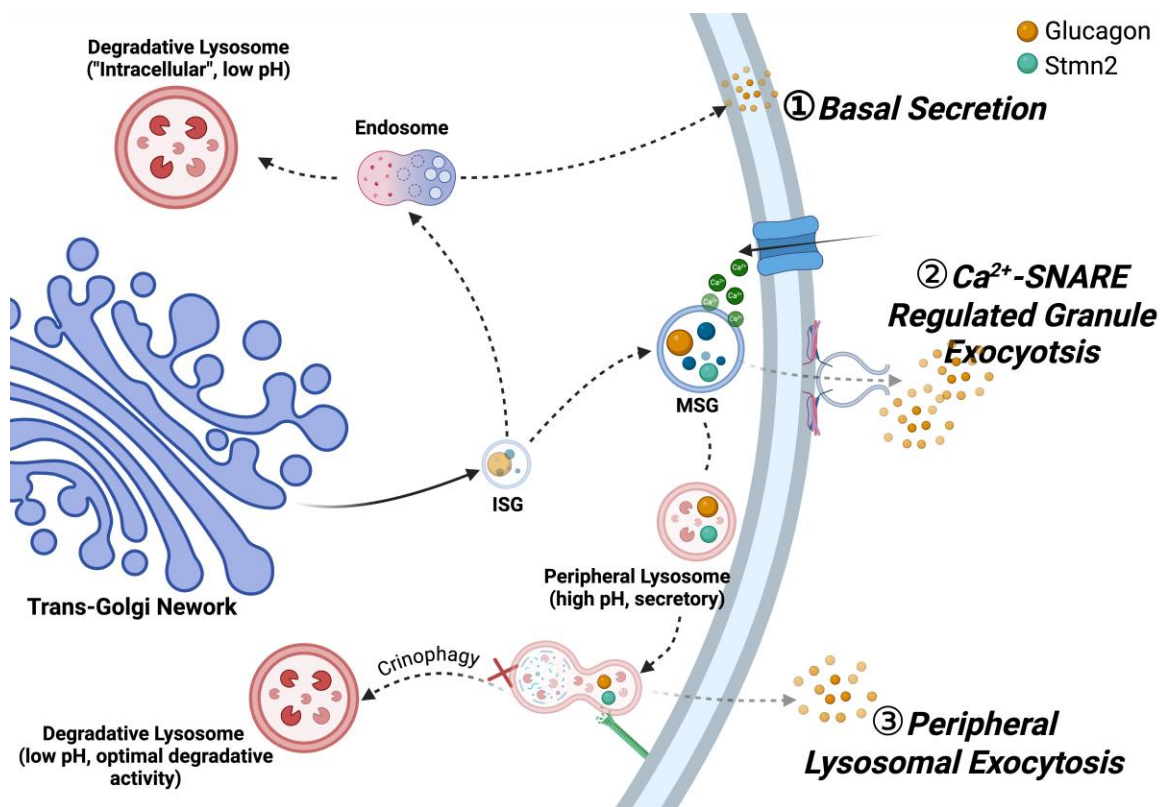


Figure 21. Types of glucagon secretion and the proposed mechanism of Stmn2-mediated crinophagy in α cells. 1) Basal glucagon secretion starts with small vesicles budding off the immature secretory granule (ISG) from the Trans-Golgi Network (TGN), fusing with endosomes destined for degradative lysosomes or the plasma membrane for constitutive basal secretion. 2) Ca^{2+} -SNARE regulated glucagon secretion starts with pro-glucagon within the ISG undergoing post-translational processing to become mature glucagon in the mature secretory granule (MSG), which then in the presence of Ca^{2+} influx binds to exocytotic proteins at the plasma membrane to form SNARE complex for exocytosis. 3) Peripheral lysosomal exocytosis can occur via impaired crinophagy, such that upon fusing of MSG with lysosomes at the plasma membrane, Stmn2 within the MSG is required to modulate microtubule dynamics to move fused granular-lysosomal compartment in the retrograde direction. This movement allows for the buildup of acidity within the compartment for optimal proteolytic activity. In the absence of Stmn2, retrograde trafficking is lost, and the compartment loses proteolytic capacity and secretes its content, also known as “lysosomal exocytosis.” Created with BioRender.com.

4.7 Future directions

I demonstrated that *Stmn2* could be a key regulator of the lysosomal network in α TC1-6 cells, responsible for trafficking glucagon towards degradative lysosomes in normal physiological regulation by paracrine factors.

The inconsistencies across glucagon secretion experiments, potentially due to heterogeneity in cellular phases, a long accumulation period, and the instantaneous response of lysosomes to paracrine factors shown in live-cell imaging, suggest a much faster cellular response to paracrine inhibition. Future secretion experiments should consider collecting media at much shorter intervals over time and synchronizing cellular phase before treatment, as done by other researchers with MIN6 cells^{114,115}. Secretion can also be measured using a neuropeptide Y (NPY) fluorescent reporter and total internal reflection microscopy (TIRF)^{116,117}.

In addition, most of the experiments were conducted using the mouse α TC1-6 clonal cells. Although the cell line has been highly used to study islet biology, it has potential deviations from islets in rodents, and the extrapolation of the results in a mouse cell line to human physiology also needs to be confirmed. As a result, future studies should consider implementing more models; specifically, the novel human alpha-like cell line may be an attractive model upon better characterization. Findings from this work should be replicated in the human alpha-like cell line.

Cellular regions were defined using lysosomal and exocytotic protein markers, and proteins of interest were manually categorized based on their location relative to their nucleus. As the plot profiles were generated manually, there could be bias in choosing the regions of interest, which can be avoided in future upon automation of the process or development of a protein distribution quantification method with immunofluorescence images. In addition, colocalization analysis indicates only the localization of two proteins but not that they are bound or interacting, so future studies can consider analyzing protein-protein interactions upon finding colocalization with immunofluorescence¹¹⁸.

4.8 Concluding remarks

This study provides insight into the intracellular trafficking of Stmn2 and glucagon in relation to lysosomes and exocytotic proteins in normal physiological regulation by paracrine factors. With Stmn2 functioning at the transcriptional level in the lysosomal network, Stmn2-knockdown showing a loss of sensitivity to paracrine-induced glucagon and lysosome redistribution and a strong colocalization between Stmn2 with intracellular lysosomes upon overexpression in both mouse and human cells, I showed that paracrine factors mediate inhibit glucagon secretion through Stmn2-mediated lysosomal trafficking and biogenesis. I showed that the loss of Stmn2 function induced excess glucagon secretion via impairing lysosomal trafficking, potentially mimicking what could contribute to hyperglucagonemia of diabetes, making it a potential therapeutic target.

Despite the advancements in the insulin-centered glycemic management of diabetes, understanding the importance of paracrine interplay and an increased emphasis on glucagon-secreting alpha cells can potentially further optimize glycemic management or even alleviate disease progression. Investigating the intracellular trafficking of glucagon in mouse and human alpha-like cells represents a step towards finding therapeutics to optimize lysosomal function and reduce abnormal excess glucagon secretion, alleviating hyperglucagonemia of diabetes.

References or Bibliography

1. Sapra A, Bhandari P. Diabetes. In: StatPearls [Internet]. Treasure Island (FL): StatPearls Publishing; 2024 [cited 2024 Mar 5]. Available from: <http://www.ncbi.nlm.nih.gov/books/NBK551501/>
2. Unger RH, Orci L. The essential role of glucagon in the pathogenesis of diabetes mellitus. *Lancet Lond Engl*. 1975 Jan 4;1(7897):14–6.
3. Unger RH, Cherrington AD. Glucagonocentric restructuring of diabetes: a pathophysiologic and therapeutic makeover. *J Clin Invest*. 2012 Jan 1;122(1):4.
4. Lee Y, Wang MY, Du XQ, Charron MJ, Unger RH. Glucagon Receptor Knockout Prevents Insulin-Deficient Type 1 Diabetes in Mice. *Diabetes*. 2011 Jan 21;60(2):391–7.
5. Conarello SL, Jiang G, Mu J, Li Z, Woods J, Zycband E, et al. Glucagon receptor knockout mice are resistant to diet-induced obesity and streptozotocin-mediated beta cell loss and hyperglycaemia. *Diabetologia*. 2007 Jan;50(1):142–50.
6. Holst JJ, Holland W, Gromada J, Lee Y, Unger RH, Yan H, et al. Insulin and Glucagon: Partners for Life. *Endocrinology*. 2017 Jan 31;158(4):696–701.
7. Hartig SM, Cox AR. Paracrine signaling in islet function and survival. *J Mol Med Berl Ger*. 2020 Apr;98(4):451–67.
8. Da Silva Xavier G. The Cells of the Islets of Langerhans. *J Clin Med*. 2018 Mar 12;7(3):54.
9. Dunphy JL, Taylor RG, Fuller PJ. Tissue distribution of rat glucagon receptor and GLP-1 receptor gene expression. *Mol Cell Endocrinol*. 1998 Jun 25;141(1–2):179–86.
10. Glucagon Receptor Signaling and Glucagon Resistance - PMC [Internet]. [cited 2024 Jun 6]. Available from: <https://www.ncbi.nlm.nih.gov/pmc/articles/PMC6651628/>
11. Rix I, Nexøe-Larsen C, Bergmann NC, Lund A, Knop FK. Glucagon Physiology. In: Feingold KR, Anawalt B, Blackman MR, Boyce A, Chrousos G, Corpas E, et al., editors. *Endotext* [Internet]. South Dartmouth (MA): MDText.com, Inc.; 2000 [cited 2023 Nov 19]. Available from: <http://www.ncbi.nlm.nih.gov/books/NBK279127/>
12. Wewer Albrechtsen NJ, Kuhre RE, Pedersen J, Knop FK, Holst JJ. The biology of glucagon and the consequences of hyperglucagonemia. *Biomark Med*. 2016 Nov;10(11):1141–51.
13. Godoy-Matos AF. The role of glucagon on type 2 diabetes at a glance. *Diabetol Metab Syndr*. 2014 Aug 24;6(1):91.

14. Kawamori D, Kulkarni RN. Insulin modulation of glucagon secretion: the role of insulin and other factors in the regulation of glucagon secretion. *Islets*. 2009;1(3):276–9.
15. Steenberg VR, Jensen SM, Pedersen J, Madsen AN, Windeløv JA, Holst B, et al. Acute disruption of glucagon secretion or action does not improve glucose tolerance in an insulin-deficient mouse model of diabetes. *Diabetologia*. 2016 Feb;59(2):363–70.
16. Gelling RW, Du XQ, Dichmann DS, Romer J, Huang H, Cui L, et al. Lower blood glucose, hyperglucagonemia, and pancreatic alpha cell hyperplasia in glucagon receptor knockout mice. *Proc Natl Acad Sci U S A*. 2003 Feb 4;100(3):1438–43.
17. Webb GC, Akbar MS, Zhao C, Swift HH, Steiner DF. Glucagon replacement via micro-osmotic pump corrects hypoglycemia and alpha-cell hyperplasia in prohormone convertase 2 knockout mice. *Diabetes*. 2002 Feb;51(2):398–405.
18. Parker JC, Andrews KM, Allen MR, Stock JL, McNeish JD. Glycemic control in mice with targeted disruption of the glucagon receptor gene. *Biochem Biophys Res Commun*. 2002 Jan 18;290(2):839–43.
19. Dean ED. A Primary Role for α -Cells as Amino Acid Sensors. *Diabetes*. 2020 Apr;69(4):542–9.
20. Dean ED, Li M, Prasad N, Wisniewski SN, Von Deylen A, Spaeth J, et al. Interrupted Glucagon Signaling Reveals Hepatic- α -Cell Axis and Role for L-Glutamine in α -Cell Proliferation. *Cell Metab*. 2017 Jun 6;25(6):1362-1373.e5.
21. Caicedo A. PARACRINE AND AUTOCRINE INTERACTIONS IN THE HUMAN ISLET: MORE THAN MEETS THE EYE. *Semin Cell Dev Biol*. 2013 Jan;24(1):11–21.
22. Asadi F, Dhanvantari S. Pathways of Glucagon Secretion and Trafficking in the Pancreatic Alpha Cell: Novel Pathways, Proteins, and Targets for Hyperglucagonemia. *Front Endocrinol [Internet]*. 2021 [cited 2022 Sep 16];12. Available from: <https://www.frontiersin.org/articles/10.3389/fendo.2021.726368>
23. Strowski MZ, Parmar RM, Blake AD, Schaeffer JM. Somatostatin inhibits insulin and glucagon secretion via two receptors subtypes: an in vitro study of pancreatic islets from somatostatin receptor 2 knockout mice. *Endocrinology*. 2000 Jan;141(1):111–7.
24. Elliott AD, Ustione A, Piston DW. Somatostatin and insulin mediate glucose-inhibited glucagon secretion in the pancreatic α -cell by lowering cAMP. *Am J Physiol-Endocrinol Metab*. 2015 Jan 15;308(2):E130–43.

25. Cabrera O, Berman DM, Kenyon NS, Ricordi C, Berggren PO, Caicedo A. The unique cytoarchitecture of human pancreatic islets has implications for islet cell function. *Proc Natl Acad Sci*. 2006 Feb 14;103(7):2334–9.
26. Muratore M, Santos C, Rorsman P. The vascular architecture of the pancreatic islets: A homage to August Krogh. *Comp Biochem Physiol A Mol Integr Physiol*. 2021 Feb 1;252:110846.
27. Bosco D, Armanet M, Morel P, Niclauss N, Sgroi A, Muller YD, et al. Unique Arrangement of α - and β -Cells in Human Islets of Langerhans. *Diabetes*. 2010 May 1;59(5):1202–10.
28. Brereton MF, Vergari E, Zhang Q, Clark A. Alpha-, Delta- and PP-cells: Are They the Architectural Cornerstones of Islet Structure and Co-ordination? *J Histochem Cytochem Off J Histochem Soc*. 2015 Aug;63(8):575–91.
29. Bru-Tari E, Oropeza D, Herrera PL. Cell Heterogeneity and Paracrine Interactions in Human Islet Function: A Perspective Focused in β -Cell Regeneration Strategies. *Front Endocrinol [Internet]*. 2021 Feb 3 [cited 2024 Mar 26];11. Available from: <https://www.frontiersin.org/journals/endocrinology/articles/10.3389/fendo.2020.619150/full>
30. Rorsman P, Ashcroft FM. Pancreatic β -Cell Electrical Activity and Insulin Secretion: Of Mice and Men. *Physiol Rev*. 2018 Jan 1;98(1):117–214.
31. Jansson L, Hellerström C. Glucose-induced changes in pancreatic islet blood flow mediated by central nervous system. *Am J Physiol*. 1986 Dec;251(6 Pt 1):E644–647.
32. Ballian N, Brunicardi FC. Islet vasculature as a regulator of endocrine pancreas function. *World J Surg*. 2007 Apr;31(4):705–14.
33. Richards OC, Raines SM, Attie AD. The role of blood vessels, endothelial cells, and vascular pericytes in insulin secretion and peripheral insulin action. *Endocr Rev*. 2010 Jun;31(3):343–63.
34. Tamayo A, Gonçalves LM, Rodriguez-Diaz R, Pereira E, Canales M, Caicedo A, et al. Pericyte Control of Blood Flow in Intraocular Islet Grafts Impacts Glucose Homeostasis in Mice. *Diabetes*. 2022 Aug;71(8):1679–93.
35. Akesson B, Mosén H, Panagiotidis G, Lundquist I. Interaction of the islet nitric oxide system with L-arginine-induced secretion of insulin and glucagon in mice. *Br J Pharmacol*. 1996 Oct;119(4):758–64.
36. Arvan P, Halban PA. Sorting Ourselves Out: Seeking Consensus on Trafficking in the Beta-Cell. *Traffic*. 2004;5(1):53–61.
37. Armour SL, Stanley JE, Cantley J, Dean ED, Knudsen JG. Metabolic regulation of glucagon secretion. *J Endocrinol [Internet]*. 2023 Sep 1 [cited 2024 Mar 5];259(1).

Available from: <https://joe.bioscientifica.com/view/journals/joe/259/1/JOE-23-0081.xml>

38. Gao R, Acreman S, Ma J, Abdulkader F, Wendt A, Zhang Q. α -cell electrophysiology and the regulation of glucagon secretion. 2023 Aug 1 [cited 2024 Jun 6]; Available from: <https://joe.bioscientifica.com/view/journals/joe/258/2/JOE-22-0295.xml>
39. Andersson SA, Pedersen MG, Vikman J, Eliasson L. Glucose-dependent docking and SNARE protein-mediated exocytosis in mouse pancreatic alpha-cell. *Pflüg Arch - Eur J Physiol*. 2011 Sep 1;462(3):443–54.
40. Omar-Hmeadi M, Lund PE, Gandasi NR, Tengholm A, Barg S. Paracrine control of α -cell glucagon exocytosis is compromised in human type-2 diabetes. *Nat Commun*. 2020 Apr 20;11(1):1896.
41. α Cell Function and Gene Expression Are Compromised in Type 1 Diabetes - PubMed [Internet]. [cited 2024 Jun 13]. Available from: <https://pubmed.ncbi.nlm.nih.gov/29514095/>
42. Glucagon Release - an overview | ScienceDirect Topics [Internet]. [cited 2024 Mar 30]. Available from: <https://www.sciencedirect.com/topics/medicine-and-dentistry/glucagon-release>
43. Leung YM, Ahmed I, Sheu L, Gao X, Hara M, Tsushima RG, et al. Insulin regulates islet alpha-cell function by reducing KATP channel sensitivity to adenosine 5'-triphosphate inhibition. *Endocrinology*. 2006 May;147(5):2155–62.
44. Xu E, Kumar M, Zhang Y, Ju W, Obata T, Zhang N, et al. Intra-islet insulin suppresses glucagon release via GABA-GABAA receptor system. *Cell Metab*. 2006 Jan 1;3(1):47–58.
45. Vergari E, Knudsen JG, Ramracheya R, Salehi A, Zhang Q, Adam J, et al. Insulin inhibits glucagon release by SGLT2-induced stimulation of somatostatin secretion. *Nat Commun*. 2019 Jan 11;10(1):139.
46. Tsuchiyama N, Takamura T, Ando H, Sakurai M, Shimizu A, Kato K ichiro, et al. Possible role of alpha-cell insulin resistance in exaggerated glucagon responses to arginine in type 2 diabetes. *Diabetes Care*. 2007 Oct;30(10):2583–7.
47. Zmazek J, Grubelnik V, Markovič R, Marhl M. Role of cAMP in Double Switch of Glucagon Secretion. *Cells*. 2021 Apr 14;10(4):896.
48. Gromada J, Høy M, Buschard K, Salehi A, Rorsman P. Somatostatin inhibits exocytosis in rat pancreatic α -cells by Gi2-dependent activation of calcineurin and depriving of secretory granules. *J Physiol*. 2001 Sep 1;535(Pt 2):519–32.

49. Grube D, Bohn R. The microanatomy of human islets of Langerhans, with special reference to somatostatin (D-) cells. *Arch Histol Jpn Nihon Soshikigaku Kiroku*. 1983 Jun;46(3):327–53.
50. Arrojo e Drigo R, Jacob S, García-Prieto CF, Zheng X, Fukuda M, Nhu HTT, et al. Structural basis for delta cell paracrine regulation in pancreatic islets. *Nat Commun*. 2019 Aug 16;10(1):3700.
51. Zhang Q, Ramracheya R, Lahmann C, Tarasov A, Bengtsson M, Braha O, et al. Role of KATP Channels in Glucose-Regulated Glucagon Secretion and Impaired Counterregulation in Type 2 Diabetes. *Cell Metab*. 2013 Dec 3;18(6):871–82.
52. Barg S, Galvanovskis J, Göpel SO, Rorsman P, Eliasson L. Tight coupling between electrical activity and exocytosis in mouse glucagon-secreting alpha-cells. *Diabetes*. 2000 Sep 1;49(9):1500–10.
53. Tooze SA. Biogenesis of secretory granules in the trans-Golgi network of neuroendocrine and endocrine cells. *Biochim Biophys Acta*. 1998 Aug 14;1404(1–2):231–44.
54. The sorting of proglucagon to secretory granules is mediated by carboxypeptidase E and intrinsic sorting signals in: *Journal of Endocrinology* Volume 217 Issue 2 (2013) [Internet]. [cited 2024 Jun 7]. Available from: <https://joe.bioscientifica.com/view/journals/joe/217/2/229.xml>
55. Dey A, Lipkind GM, Rouillé Y, Norrbom C, Stein J, Zhang C, et al. Significance of prohormone convertase 2, PC2, mediated initial cleavage at the proglucagon interdomain site, Lys70-Arg71, to generate glucagon. *Endocrinology*. 2005 Feb;146(2):713–27.
56. Furuta M, Zhou A, Webb G, Carroll R, Ravazzola M, Orci L, et al. Severe defect in proglucagon processing in islet A-cells of prohormone convertase 2 null mice. *J Biol Chem*. 2001 Jul 20;276(29):27197–202.
57. Guizzetti L, McGirr R, Dhanvantari S. Two Dipolar α -Helices within Hormone-encoding Regions of Proglucagon Are Sorting Signals to the Regulated Secretory Pathway *. *J Biol Chem*. 2014 May 23;289(21):14968–80.
58. Carboxypeptidase E, a prohormone sorting receptor, is anchored to secretory granules via a C-terminal transmembrane insertion - PubMed [Internet]. [cited 2024 Jun 7]. Available from: <https://pubmed.ncbi.nlm.nih.gov/11772002/>
59. Kuliawat R, Arvan P. Distinct molecular mechanisms for protein sorting within immature secretory granules of pancreatic beta-cells. *J Cell Biol*. 1994 Jul;126(1):77–86.
60. Waguri S, Sato N, Watanabe T, Ishidoh K, Kominami E, Sato K, et al. Cysteine proteinases in GH4C1 cells, a rat pituitary tumor cell line, are secreted by the

- constitutive and regulated secretory pathways. *Eur J Cell Biol.* 1995 Aug;67(4):308–18.
61. Zhou Y, Liu Z, Zhang S, Zhuang R, Liu H, Liu X, et al. RILP Restricts Insulin Secretion Through Mediating Lysosomal Degradation of Proinsulin. *Diabetes.* 2019 Oct 17;69(1):67–82.
 62. Rajak S, Xie S, Tewari A, Raza S, Wu Y, Bay BH, et al. MTORC1 inhibition drives crinophagic degradation of glucagon. *Mol Metab.* 2021 Nov;53:101286.
 63. Csizmadia T, Juhász G. Crinophagy mechanisms and its potential role in human health and disease. *Prog Mol Biol Transl Sci.* 2020;172:239–55.
 64. Szenci G, Csizmadia T, Juhász G. The role of crinophagy in quality control of the regulated secretory pathway. *J Cell Sci.* 2023 Apr 24;136(8):jcs260741.
 65. Pasquier A, Vivot K, Erbs E, Spiegelhalter C, Zhang Z, Aubert V, et al. Lysosomal degradation of newly formed insulin granules contributes to β cell failure in diabetes. *Nat Commun.* 2019 Jul 25;10(1):3312.
 66. Yang Z, Klionsky DJ. An Overview of the Molecular Mechanism of Autophagy. *Curr Top Microbiol Immunol.* 2009;335:1–32.
 67. Komatsu M, Ueno T, Waguri S, Uchiyama Y, Kominami E, Tanaka K. Constitutive autophagy: vital role in clearance of unfavorable proteins in neurons. *Cell Death Differ.* 2007 May;14(5):887–94.
 68. Kuma A, Hatano M, Matsui M, Yamamoto A, Nakaya H, Yoshimori T, et al. The role of autophagy during the early neonatal starvation period. *Nature.* 2004 Dec 23;432(7020):1032–6.
 69. Asadi F, Dhanvantari S. Stathmin-2 Mediates Glucagon Secretion From Pancreatic α -Cells. *Front Endocrinol.* 2020;11:29.
 70. Asadi F, Dhanvantari S. Plasticity in the Glucagon Interactome Reveals Novel Proteins That Regulate Glucagon Secretion in α -TC1-6 Cells. *Front Endocrinol [Internet].* 2019 [cited 2022 Sep 16];9. Available from: <https://www.frontiersin.org/articles/10.3389/fendo.2018.00792>
 71. Bramswig NC, Everett LJ, Schug J, Dorrell C, Liu C, Luo Y, et al. Epigenomic plasticity enables human pancreatic α to β cell reprogramming. *J Clin Invest.* 2013 Mar;123(3):1275–84.
 72. Single-cell transcriptomes identify human islet cell signatures and reveal cell-type-specific expression changes in type 2 diabetes - PubMed [Internet]. [cited 2024 Mar 23]. Available from: <https://pubmed.ncbi.nlm.nih.gov/27864352/>

73. Riederer BM, Pellier V, Antonsson B, Di Paolo G, Stimpson SA, Lütjens R, et al. Regulation of microtubule dynamics by the neuronal growth-associated protein SCG10. *Proc Natl Acad Sci U S A*. 1997;94(2):741–5.
74. Di Paolo G, Lutjens R, Osen-Sand A, Sobel A, Catsicas S, Grenningloh G. Differential distribution of stathmin and SCG10 in developing neurons in culture. *J Neurosci Res*. 1997 Dec 15;50(6):1000–9.
75. Krus KL, Strickland A, Yamada Y, Devault L, Schmidt RE, Bloom AJ, et al. Loss of Stathmin-2, a hallmark of TDP-43-associated ALS, causes motor neuropathy. *Cell Rep*. 2022 Jun 28;39(13):111001.
76. Liu Y, Yan D, Yang L, Chen X, Hu C, Chen M. Stathmin 2 is a potential treatment target for TDP-43 proteinopathy in amyotrophic lateral sclerosis. *Transl Neurodegener*. 2024 Apr 11;13(1):20.
77. Mahapatra NR, Taupenot L, Courel M, Mahata SK, O'Connor DT. The trans-Golgi proteins SCLIP and SCG10 interact with chromogranin A to regulate neuroendocrine secretion. *Biochemistry*. 2008 Jul 8;47(27):7167–78.
78. Ho KH, Yang X, Osipovich AB, Cabrera O, Hayashi ML, Magnuson MA, et al. Glucose Regulates Microtubule Disassembly and the Dose of Insulin Secretion via Tau Phosphorylation. *Diabetes*. 2020 Sep;69(9):1936–47.
79. Zhu X, Hu R, Brissova M, Stein RW, Powers AC, Gu G, et al. Microtubules Negatively Regulate Insulin Secretion in Pancreatic β Cells. *Dev Cell*. 2015 Sep 28;34(6):656–68.
80. Hoboth P, Müller A, Ivanova A, Mziaut H, Dehghany J, Sönmez A, et al. Aged insulin granules display reduced microtubule-dependent mobility and are disposed within actin-positive multigranular bodies. *Proc Natl Acad Sci U S A*. 2015 Feb 17;112(7):E667-676.
81. Omar-Hmeadi M, Idevall-Hagren O. Insulin granule biogenesis and exocytosis. *Cell Mol Life Sci CMLS*. 2020 Nov 4;78(5):1957–70.
82. Asadi F, Dhanvantari S. Misrouting of glucagon and stathmin-2 towards lysosomal system of α -cells in glucagon hypersecretion of diabetes. *Islets*. 14(1):40–57.
83. Sherer NM, Lehmann MJ, Jimenez-Soto LF, Ingmundson A, Horner SM, Cicchetti G, et al. Visualization of retroviral replication in living cells reveals budding into multivesicular bodies. *Traffic Cph Den*. 2003 Nov;4(11):785–801.
84. Cheng XT, Xie YX, Zhou B, Huang N, Farfel-Becker T, Sheng ZH. Characterization of LAMP1-labeled nondegradative lysosomal and endocytic compartments in neurons. *J Cell Biol*. 2018 Sep 3;217(9):3127–39.

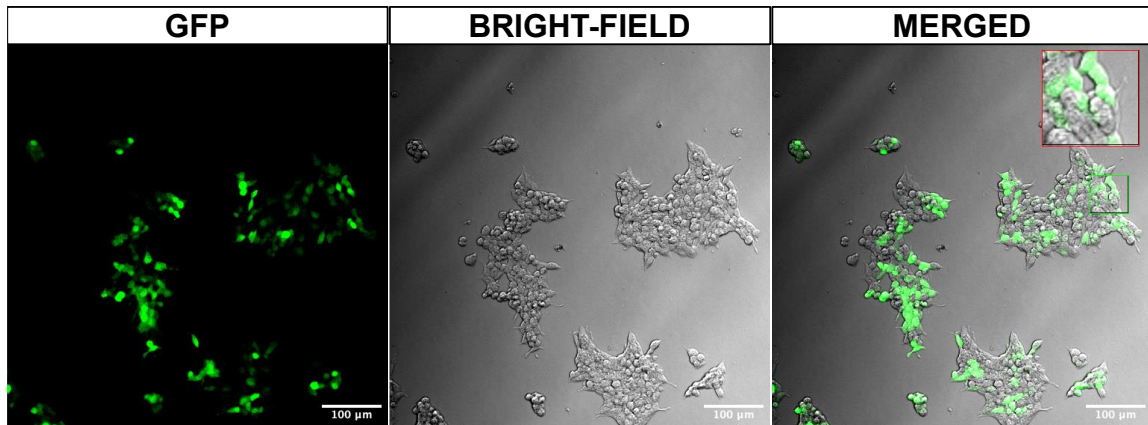
85. do Couto NF, Queiroz-Oliveira T, Horta MF, Castro-Gomes T, Andrade LO. Measuring Intracellular Vesicle Density and Dispersion Using Fluorescence Microscopy and ImageJ/FIJI. *Bio-Protoc.* 2020 Aug 5;10(15):e3703.
86. Wessel AW, Hanson EP. A Method for the Quantitative Analysis of Stimulation-Induced Nuclear Translocation of the p65 Subunit of NF- κ B from Patient-Derived Dermal Fibroblasts. *Methods Mol Biol Clifton NJ.* 2015;1280:413–26.
87. Piro S, Mascali LG, Urbano F, Filippello A, Malaguarnera R, Calanna S, et al. Chronic Exposure to GLP-1 Increases GLP-1 Synthesis and Release in a Pancreatic Alpha Cell Line (α -TC1): Evidence of a Direct Effect of GLP-1 on Pancreatic Alpha Cells. *PLOS ONE.* 2014 Feb 28;9(2):e90093.
88. Medina DL, Di Paola S, Peluso I, Armani A, De Stefani D, Venditti R, et al. Lysosomal calcium signalling regulates autophagy through calcineurin and TFEB. *Nat Cell Biol.* 2015 Mar;17(3):288–99.
89. Seshadri N, Doucette CA. Circadian Regulation of the Pancreatic Beta Cell. *Endocrinology.* 2021 Sep 1;162(9):bqab089.
90. Panzer JK, Caicedo A. Targeting the Pancreatic α -Cell to Prevent Hypoglycemia in Type 1 Diabetes. *Diabetes.* 2021 Dec;70(12):2721–32.
91. Kapałczyńska M, Kolenda T, Przybyła W, Zajączkowska M, Teresiak A, Filas V, et al. 2D and 3D cell cultures – a comparison of different types of cancer cell cultures. *Arch Med Sci AMS.* 2018 Jun;14(4):910–9.
92. An intrinsic circadian clock of the pancreas is required for normal insulin release and glucose homeostasis in mice - PMC [Internet]. [cited 2024 May 23]. Available from: <https://www.ncbi.nlm.nih.gov/pmc/articles/PMC2995870/>
93. Pulimeno P, Mannic T, Sage D, Giovannoni L, Salmon P, Lemeille S, et al. Autonomous and self-sustained circadian oscillators displayed in human islet cells. *Diabetologia.* 2013 Mar;56(3):497–507.
94. Pasquier A, Vivot K, Erbs E, Spiegelhalter C, Zhang Z, Aubert V, et al. Lysosomal degradation of newly formed insulin granules contributes to β cell failure in diabetes. *Nat Commun.* 2019 Jul 25;10(1):3312.
95. Mattila PK, Lappalainen P. Filopodia: molecular architecture and cellular functions. *Nat Rev Mol Cell Biol.* 2008 Jun;9(6):446–54.
96. Freudenblum J, Iglesias JA, Hermann M, Walsen T, Wilfinger A, Meyer D, et al. In vivo imaging of emerging endocrine cells reveals a requirement for PI3K-regulated motility in pancreatic islet morphogenesis. *Dev Camb Engl.* 2018 Feb 1;145(3):dev158477.

97. Wit CB, Hiesinger PR. Neuronal filopodia: From stochastic dynamics to robustness of brain morphogenesis. *Semin Cell Dev Biol.* 2023 Jan 15;133:10–9.
98. Cabukusta B, Neefjes J. Mechanisms of lysosomal positioning and movement. *Traffic Cph Den.* 2018 Oct;19(10):761–9.
99. Settembre C, Fraldi A, Medina DL, Ballabio A. Signals for the lysosome: a control center for cellular clearance and energy metabolism. *Nat Rev Mol Cell Biol.* 2013 May;14(5):283–96.
100. Ferguson SM. Neuronal Lysosomes. *Neurosci Lett.* 2019 Apr 1;697:1–9.
101. Lysosomal subcellular distribution in neurons: Are there synaptic lysosomes? - Cunha - 2021 - Alzheimer's & Dementia - Wiley Online Library [Internet]. [cited 2024 Jun 5]. Available from: <https://alz-journals.onlinelibrary.wiley.com/doi/abs/10.1002/alz.053844>
102. Endocrine Cell - an overview | ScienceDirect Topics [Internet]. [cited 2024 Jun 5]. Available from: <https://www.sciencedirect.com/topics/biochemistry-genetics-and-molecular-biology/endocrine-cell>
103. β -Cell evolution: How the pancreas borrowed from the brain - Arntfield - 2011 - BioEssays - Wiley Online Library [Internet]. [cited 2024 Jun 5]. Available from: <https://onlinelibrary.wiley.com/doi/10.1002/bies.201100015>
104. Iyata K, Yuzaki M. Destroy the old to build the new: Activity-dependent lysosomal exocytosis in neurons. *Neurosci Res.* 2021 Jun;167:38–46.
105. Johnson DE, Ostrowski P, Jaumouillé V, Grinstein S. The position of lysosomes within the cell determines their luminal pH. *J Cell Biol.* 2016 Mar 14;212(6):677–92.
106. Settembre C, Di Malta C, Polito VA, Arencibia MG, Vetrini F, Erdin S, et al. TFEB Links Autophagy to Lysosomal Biogenesis. *Science.* 2011 Jun 17;332(6036):1429–33.
107. Rabanal-Ruiz Y, Otten EG, Korolchuk VI. mTORC1 as the main gateway to autophagy. *Essays Biochem.* 2017 Dec 12;61(6):565–84.
108. Napolitano G, Ballabio A. TFEB at a glance. *J Cell Sci.* 2016 Jul 1;129(13):2475–81.
109. Park K, Lim H, Kim J, Hwang Y, Lee YS, Bae SH, et al. Lysosomal Ca²⁺-mediated TFEB activation modulates mitophagy and functional adaptation of pancreatic β -cells to metabolic stress. *Nat Commun.* 2022 Mar 14;13(1):1300.
110. Sancak Y, Bar-Peled L, Zoncu R, Markhard AL, Nada S, Sabatini DM. Ragulator-Rag complex targets mTORC1 to the lysosomal surface and is necessary for its activation by amino acids. *Cell.* 2010 Apr 16;141(2):290–303.

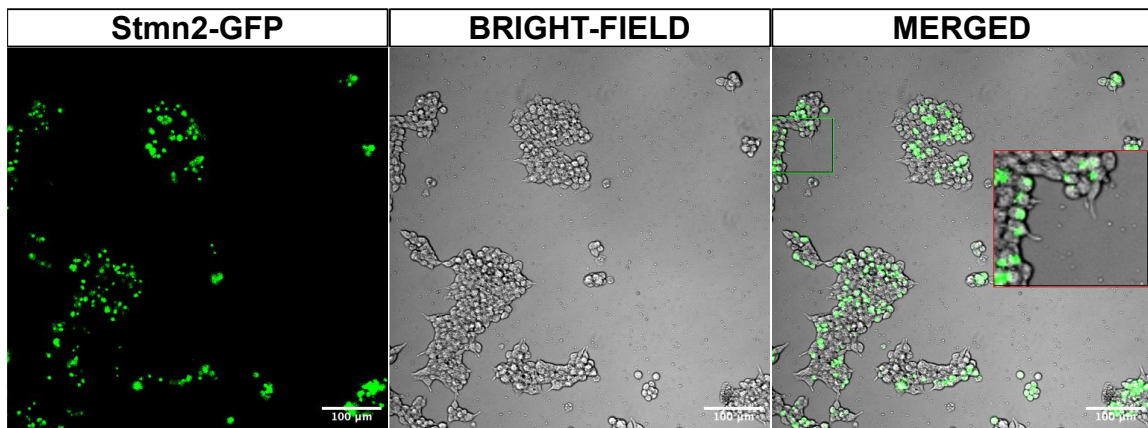
111. Sardiello M, Palmieri M, di Ronza A, Medina DL, Valenza M, Gennarino VA, et al. A gene network regulating lysosomal biogenesis and function. *Science*. 2009 Jul 24;325(5939):473–7.
112. Raben N, Puertollano R. TFEB AND TFE3, LINKING LYSOSOMES TO CELLULAR ADAPTATION TO STRESS. *Annu Rev Cell Dev Biol*. 2016 Oct 6;32:255–78.
113. Martina JA, Diab HI, Lishu L, Jeong-A L, Patange S, Raben N, et al. The nutrient-responsive transcription factor TFE3 promotes autophagy, lysosomal biogenesis, and clearance of cellular debris. *Sci Signal*. 2014 Jan 21;7(309):ra9.
114. Greco JA, Oosterman JE, Belsham DD. Differential effects of omega-3 fatty acid docosahexaenoic acid and palmitate on the circadian transcriptional profile of clock genes in immortalized hypothalamic neurons. *Am J Physiol Regul Integr Comp Physiol*. 2014 Oct 15;307(8):R1049-1060.
115. Seshadri N, Jonasson ME, Hunt KL, Xiang B, Cooper S, Wheeler MB, et al. Uncoupling protein 2 regulates daily rhythms of insulin secretion capacity in MIN6 cells and isolated islets from male mice. *Mol Metab*. 2017 Apr 27;6(7):760–9.
116. Fish KN. Total Internal Reflection Fluorescence (TIRF) Microscopy. *Curr Protoc Cytom Editor Board J Paul Robinson Manag Ed A1*. 2009 Oct;0 12:Unit12.18.
117. Makhmutova M, Liang T, Gaisano H, Caicedo A, Almacá J. Confocal Imaging of Neuropeptide Y-pHluorin: A Technique to Visualize Insulin Granule Exocytosis in Intact Murine and Human Islets. *J Vis Exp JoVE*. 2017 Sep 13;(127):56089.
118. Dianati E, Plante I. Analysis of Protein-protein Interactions and Co-localization Between Components of Gap, Tight, and Adherens Junctions in Murine Mammary Glands. *J Vis Exp JoVE*. 2017 May 30;(123):55772.

Appendices

a)



b)

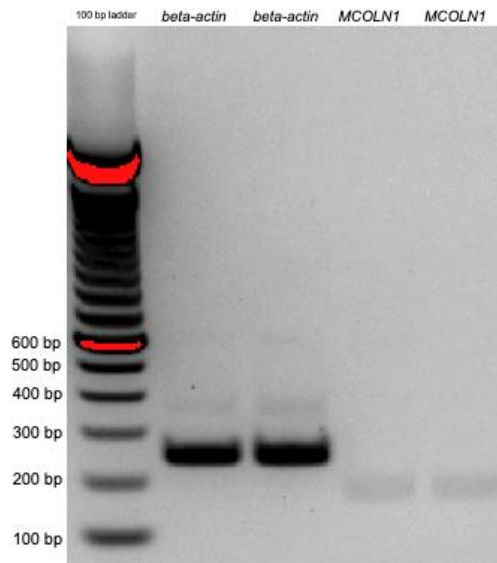


Appendix Figure 1. 40 nM GFP-alone and Stmn2-GFP localization and efficiency in α TC1-6 cells. Cells were transfected with 40 nM plasmids overnight and imaged the following day at 20x magnification using Galvano laser. a) GFP-transfected cells showing relatively high transfection efficiency and diffusion of GFP fluorescence signal (green) across the entirety of individual cells. b) Stmn2-GFP-transfected cells showing relatively high transfection efficiency and localization of fluorescence signal (green) in the intracellular region.

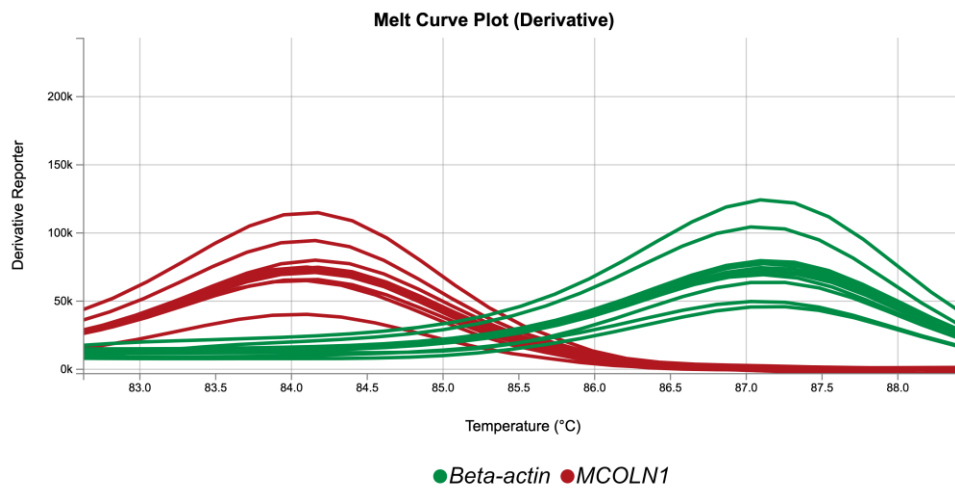
Appendix Table 1. α TC1-6 cell viability assay post-transfection (n=1).

Transfection	GFP-alone	Stmn2-GFP (OE)	siRNA-Stmn2 (KD)
# of cells	8.91 x 10 ⁵ cells/ mL	9.03 x 10 ⁵ cells/ mL	1.04 x 10 ⁶ cells/ mL
% of live & dead cells	59 % live, 41% dead	59% live, 41% dead	47 % live, 53 % dead
Co-Transfection	GFP + LAMP1-RFP	Stmn2-GFP + LAMP1-RFP	siRNA-Stmn2 + LAMP1-RFP
# of cells	1.05 x 10 ⁶ cells/ mL	8.74 x 10 ⁵ cells/ mL	1.09 x 10 ⁶ cells/ mL
% of live & dead cells	54% live, 46% dead	58% live, 42% dead	36% live, 64% dead

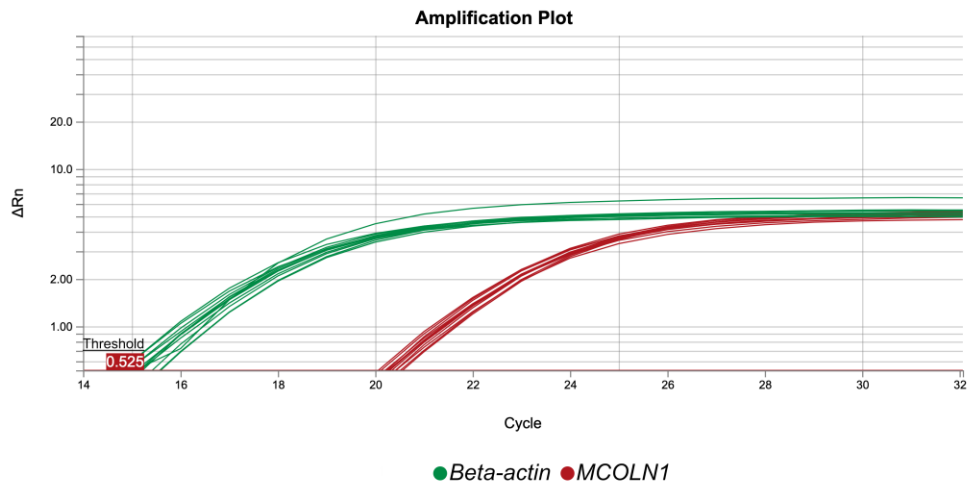
a)



b)



c)

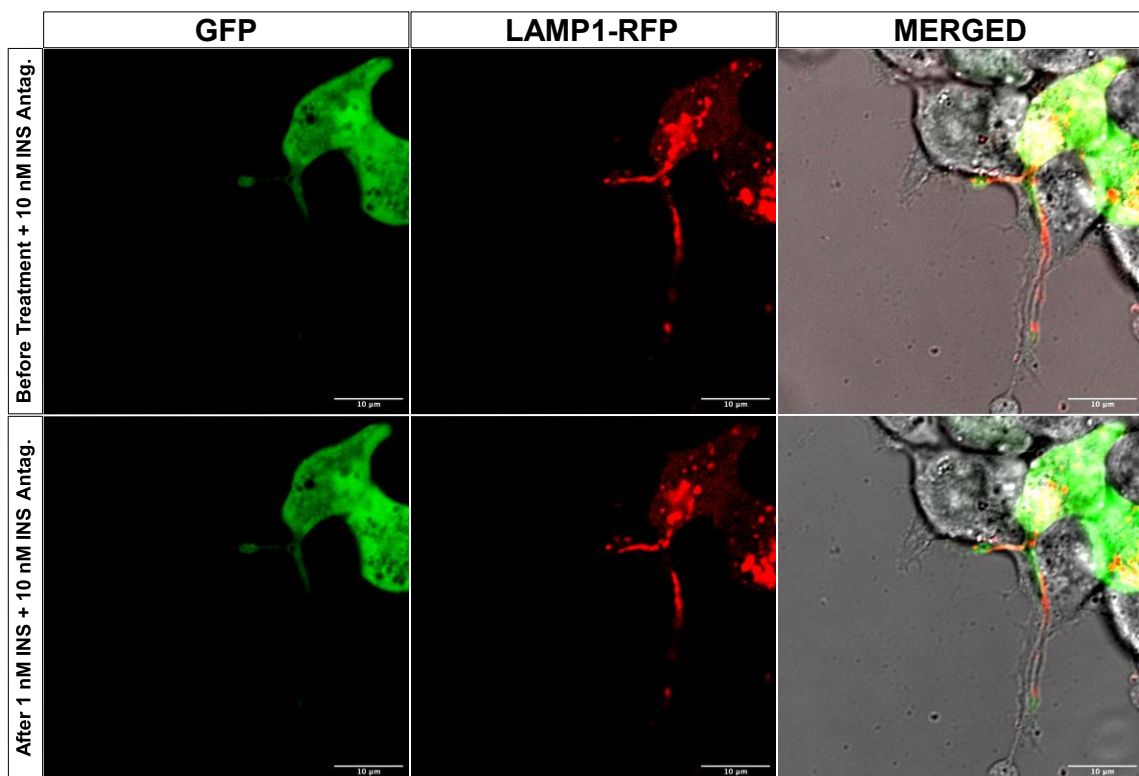


Appendix Figure 2. MCOLN1 and beta-actin amplicons post-qPCR, and their specificity, purity and size in α TC1-6 cells cultured in regular 25 mM glucose growth media. a)

Amplicons showing primer specificity for beta-actin (housekeeper protein) and MCOLN1 (Gene of interest) on a 2% agarose gel. Primers for beta-actin were expected to yield 253 bps product, and primers for MCOLN1 were expected to yield a product length of 187 bps (n=2). b) Melt curve analysis post-qPCR, displaying two specific amplicons produced and their associated melting temperature (n=6). c) Amplification plot post-qPCR, displaying two specific amplicons produced and their typical associated C_q values (n=6).

Appendix Table 2. Raw MCOLN1 and beta-actin C_q values after Stmn2-OE and KD in α TC1-6 cells cultured in regular growth media. Relative gene expression was calculated through the $2^{\Delta\Delta CT}$ method with assumed primer efficiency. Fold change was compared to the control normalized to housekeeper protein with \pm SEM (n=6).

	Beta Actin C _q	MCOLN1 C _q	Δ CT	$\Delta\Delta$ CT	$2^{\Delta\Delta$ CT		Fold Change	SEM
GFP (Control) ①	15.53	21.06	5.53	0.77	1.70	Control	1.08	\pm 0.20
GFP (Control) ②	16.55	20.95	4.40	-0.37	0.78			
GFP (Control) ③	14.46	20.01	5.55	0.78	1.72			
GFP (Control) ④	16.17	20.59	4.42	-0.35	0.79			
GFP (Control) ⑤	16.40	20.84	4.44	-0.32	0.80			
GFP (Control) ⑥	16.35	20.61	4.26	-0.51	0.70			
Stmn2-GFP (OE) ①	14.82	20.52	5.69	0.93	1.90	Treated	1.56	\pm 0.38
Stmn2-GFP (OE) ②	14.74	21.23	6.50	1.73	3.32			
Stmn2-GFP (OE) ③	15.11	19.75	4.65	-0.12	0.92			
Stmn2-GFP (OE) ④	15.97	20.56	4.59	-0.18	0.88			
Stmn2-GFP (OE) ⑤	15.60	20.35	4.75	-0.02	0.99			
Stmn2-GFP (OE) ⑥	15.68	20.87	5.19	0.42	1.34			
Scramble siRNA (Control) ①	16.10	20.11	4.01	-1.04	0.49	Control	1.07	\pm 0.17
Scramble siRNA (Control) ②	15.12	20.04	4.92	-0.13	0.91			
Scramble siRNA (Control) ③	15.32	21.01	5.69	0.64	1.56			
Scramble siRNA (Control) ④	15.09	20.71	5.62	0.56	1.48			
Scramble siRNA (Control) ⑤	15.09	20.39	5.30	0.24	1.18			
Scramble siRNA (Control) ⑥	15.69	20.47	4.78	-0.27	0.83			
siRNA-Stmn2 (KD) ①	17.99	21.03	3.04	-2.01	0.25	Treated	0.59	\pm 0.18
siRNA-Stmn2 (KD) ②	16.00	20.60	4.60	-0.45	0.73			
siRNA-Stmn2 (KD) ③	14.92	20.41	5.50	0.44	1.36			
siRNA-Stmn2 (KD) ④	18.08	20.66	2.57	-2.48	0.18			
siRNA-Stmn2 (KD) ⑤	16.00	20.42	4.42	-0.63	0.64			
siRNA-Stmn2 (KD) ⑥	16.93	20.58	3.66	-1.40	0.38			



Appendix Figure 3. Live imaging of LAMP1-RFP treated with 10 nM insulin receptor antagonist in response to 1 nM insulin. Cells (n=1) were transfected with 40 nM plasmids overnight, and live images were captured 24 hours post-transfection. Images were captured in the same cell before, during, and five minutes after treatment with 1 nM insulin. Co-transfection of LAMP1-RFP with GFP-alone showed no change in the LAMP1-RFP intensity and redistribution upon 1 nM insulin treatment.

Curriculum Vitae

Name: Nelson Chang

Post-secondary Education and Degrees: *University of Western Ontario*
London, Ontario, Canada
2018-2022 Bachelor of Medical Sciences

University of Toronto
Toronto, Ontario, Canada
2023 Visiting Graduate Student

University of Western Ontario
London, Ontario, Canada
2022-2024 Master of Sciences

Honours and Awards: *NSERC Canadian Islet Research Training Network Scholarship*
\$26,000
2022-2024

Lawson Health Research Institute Internal Research Fund
\$13,000
2023-2024

Pathology and Laboratory Medicine Research Day Best Basic Science Poster Presentation
Apr 2024

Vanderbilt Diabetes Research Day Best Poster Presentation
May 2024

Related Work Experience *Graduate Teaching Assistant (Interdisciplinary Medical Sciences)*
University of Western Ontario, London, Ontario, Canada
2022-2024

Publications:

Bonyadi Behrouz, Ardavan; **Chang, Nelson**; Luo, Jasmine; Olteanu, Daniel; and Smith, Naomi, "A Wicked Problem: The Implementation of Clinical Guidelines Application to Optimize Patient Care (UHN OpenLab)" (2021). Medical Sciences 4300A: Addressing Healthcare Misconceptions Using Scientific Inquiry. 5.
https://ir.lib.uwo.ca/schulichcel_medsci4300A/5

Emma J L Walker, Mark Pampuch, **Nelson Chang**, Ryan R Cochrane, Bogumil J Karas, Design and assembly of the 117-kb *Phaeodactylum tricornutum* chloroplast genome, *Plant Physiology*, 2023;, kiad670, <https://doi.org/10.1093/plphys/kiad670>

Presentations:

Chang N, Madahey H, Dhanvantari S 2023 Paracrine factors regulate intracellular trafficking of glucagon in pancreatic alpha cells. Islet Study Group annual meeting, Vancouver BC, Canada, June 2023

Chang N, Madahey H, Dhanvantari S 2023 Paracrine factors regulate intracellular trafficking of glucagon in pancreatic alpha cells. Diabetes Canada annual meeting, Montreal QC, Canada, October 2023

Chang N, Madahey H, Dhanvantari S 2023 Paracrine factors regulate intracellular trafficking of glucagon in pancreatic alpha cells. Canadian Islet Research Training Network National Meeting, Montreal QC, Canada, October 2023

Chang N, Madahey H, Wilmarenthe M, Schornack A, Dean D, Dhanvantari S 2024 Paracrine factors regulate glucagon secretion through the Stmn2-mediated lysosomal network. Vanderbilt Diabetes Research Day, Nashville, TN, United States of America, May 2024